University of Karlsruhe (TH)
Chair of Statistics, Econometrics and
Mathematical Finance
(Professor Rachev)

Diploma Thesis

SMILE MODELING IN THE LIBOR MARKET MODEL

submitted by:

Markus Meister
Seckbacher Landstraße 45
60389 Frankfurt am Main
Markus.Meister@gmx.de

supervised by:

Dr. Christian Fries
(Dresdner Bank, Risk Control)
Dr. Christian Menn
(University of Karlsruhe)

Frankfurt am Main, August 20, 2004

Contents

List of Figures

List of Tables

Abbreviations and Notation

$A(t)$	the asset or stock price at time t
a	the mean of the logarithm of the jump size ($\ln[J]$)
b	the $n \times m$ matrix of the coefficients b_{ik}
$b_{ik}(t)$	the percentage volatility of the forward rate $L_i(t)$ coming from factor k as part of the total volatility
$\mathrm{Bl}(K,L,v)$	$= L\Phi\left(\frac{\ln[L/K]+\frac{1}{2}v^2}{v}\right) - K\Phi\left(\frac{\ln[L/K]-\frac{1}{2}v^2}{v}\right)$
J	the jump size of the forward rate
K	the strike of an option
$L(t,T,T+\delta)$	forward rate at time t for the expiry(T)-maturity($T+\delta$) pair
$L_i(t)$	$L(t,T_i,T_{i+1})$
$LN(a,b)$	the lognormal distribution with parameters a and b for the underlying normal distribution $N(a,b)$
M	the standardized moneyness of an option $M = \frac{\ln\left[\frac{K}{L_i(t)}\right]}{\sigma_i\sqrt{T_i-t}}$
m	the expected percentage change of the forward rate because of one jump
$N(a,b)$	the Gaussian normal distribution with mean a and variance b
N_T	the number of jump events up to time T
NP	the notional of an option
$O(x^k)$	the residual error is smaller in absolute value than some constant times x^k if x is close enough to 0
$p_{i,j}$	the probability of scenario j for forward rate $L_i(t)$
$P(t,T+\delta)$	the price of a discount bond at time t with maturity $T+\delta$
$\mathrm{Payoff}(\mathrm{Product})_t$	the (expected) payoff of a derivative at time t

$S_{r,s}(t)$	the equilibrium swap rate at time t for a swap with the first reset date in T_r and the last payment in T_s
s	the volatility of the logarithm of the jump size ($\ln[J]$)
X_i	the variable in the displaced diffusion approach that is lognormally distributed
V	the variance of the forward rate
w	the Brownian motion of the variance in the stochastic volatility models
$z_{(k)}$	the Brownian motion of factor k
z_i	the Brownian motion of the forward rate $L_i(t)$ with $\mathrm{d}z_i = \sum_{k=1}^{m} b_{ik}(t)\mathrm{d}z_{(k)}$
$z_{r,s}$	the Brownian motion of the swap rate $S_{r,s}(t)$ with $\mathrm{d}z_{r,s} = \sum_{k=1}^{m} \frac{\sigma_{r,s,k}(t)}{\sigma_{r,s}(t)}\mathrm{d}z_{(k)}$
α	the offset of the forward rate in the displaced diffusion approach
β	the skew parameter in the stochastic volatility models
γ	the parameter for the forward rate in the constant elasticity of variance approach
δ	the time distance between T_i and T_{i+1} and therefore the tenor of a forward rate
ε	the volatility of variance
κ	the reversion speed to the reversion level of the variance
λ	the Poisson arrival rate of a jump process
$\mu_i(t)$	the drift of the forward rate $L_i(t)$
ρ	the correlation matrix of the forward rates
$\rho_{i,j}(t)$	the correlation between the forward rates $L_i(t)$ and $L_j(t)$
$\rho_{i,V}(t)$	the correlation between the forward rate $L_i(t)$ and the variance $V(t)$
ρ_∞	the parameter determining the correlation between the first and the last forward rate
$\sigma_i(t)$	the volatility of the logarithm of the forward rate $L_i(t)$
$\sigma_{ik}(t)$	the volatility of the logarithm of the forward rate $L_i(t)$ coming from factor k
$\sigma_i(t;L_i(t))$	the local volatility of the forward rate $L_i(t)$
$\sigma_{r,s}(t)$	the volatility of the logarithm of the swap rate $S_{r,s}(t)$

$\sigma_{r,s,k}(t)$	the volatility of the logarithm of the swap rate $S_{r,s}(t)$ coming from factor k
$\hat{\sigma}$	the volatility σ implied from market prices of options
$\tilde{\sigma}$	the level adjusted volatility in the DD approach: $\tilde{\sigma}_i = \sigma_i \frac{L_i(0)+\alpha_i}{L_i(0)}$
$\phi(x)$	the density of the standardized normal distribution at point x
$\Phi(x)$	the cumulated standardized normal distribution for x
$\omega_i(t)$	the time-dependent weighting factor of forward rate $L_i(t)$ when expressing the swap rate as a linear combination of forward rates
$\mathbf{1}_{i \geq h}$	the indicator function with value 1 for $i \geq h$ and value 0 for $i < h$
ATM	at the money
CEV	constant elasticity of variance
CDF	cumulated distribution function
DD	displaced diffusion
DE	double exponential distribution
ECB	European Central Bank
FRA	forward rate agreement
GK	Glasserman/Kou
GM	Glasserman/Merener
i.i.d.	independent identically distributed
JLZ	Jarrow/Li/Zhao
LCEV	limited constant elasticity of variance
MoL	mixture of lognormals
MPP	marked point process
OTC	over the counter
PDF	partial distribution function
SV	stochastic volatility

Part I

The LIBOR Market Model and the Volatility Smile

Chapter 1

Introduction

There are many different models for valuing interest rate derivatives. They differ among each other depending on the modeled interest rate (e.g. short, forward or swap rate), the distribution of the future unknown rates (e.g. normal or lognormal), the number of driving factors (one or more dimensions), the appropriate involved techniques (trees or Monte Carlo simulations) and different possible extensions.

One of the most discussed models recently is the market model presented in [BGM97], [MSS97] and [Jam97]. The development of this model has two main consequences. First, for the first time an interest rate model can value caplets or swaptions consistently with the long-used formulæ of Black. Second, this model can easily be extended to a larger number of factors. These two features, combined with the fact that this model usually needs slow Monte Carlo simulations for pricing non plain-vanilla options, lead to using this model mainly as a benchmark model. This usage as a benchmark additionally enforces the need for consistent pricing of all existing options in the market.

Two main lines of actual research exist. On the one hand, more and more complex derivatives are coming up in the market. As they usually depend heavily upon the correlation matrix and/or the term structure of volatility and/or a large number of

forward rates, many new efficient techniques are needed, e.g. for implementing exercise boundaries, computing deltas ...[1]

On the other hand, there is still a big pricing issue left with the underlying plain-vanilla instruments. The original model is calibrated with these instruments but only with the at-the-money (= ATM) options. The market price of options in or out of the money is almost always very different from the price actually computed in the ATM-calibrated model. This behavior is not only troublesome for these plain-vanilla instruments but also for more complex derivatives such as Bermudan swaptions.

This thesis concentrates on the latter line of research and gives an overview of many possible ways of incorporating this volatility smile. It tries to focus on the implementation and calibration of these models and to give an overview of the advantages and shortcomings of each model. The main goal will be to fit the whole term-structure of all forward rates with one model rather than pricing only one single volatility smile, i.e. the smile of caplets on one forward rate with different strikes, as close as possible. Special attention is drawn to the model implied future volatility smiles since these model immanent prices have a strong influence on exotic derivative prices and are not controllable but determined by the chosen model.

Chapter 2 starts with introducing the LIBOR market model and the involved techniques for calibrating the model and pricing derivatives. In Chapter 3 the volatility smile is examined and the desired features of possible extensions are discussed. The second part of this thesis discussing possible basic models and elaborating the advantages but even more the shortcomings of each is divided into four chapters. In Chapter 4 the local volatility models are introduced, Chapter 5 presents uncertain volatility models, in Chapter 6 stochastic volatility models are discussed and Chapter 7 gives an overview of models with jump processes. The third part compares these basic models and basing on the findings suggests advanced, combined models. In Chapter 8 the model implied future volatility skew is compared and building on these findings combined models are proposed. In Chapter 9 these

[1] See e.g. [Pit03a].

advanced models are tested trying to reach the goal of fitting the whole term-structure of volatility smiles. Chapter 10 finally summarizes and gives an outlook of still existing problems and suggestions for future research.

The comparison rather than the mathematical derivation of these models is the main goal of this thesis. Mathematical concepts are therefore explained ”on demand” during the text or deferred to Appendix A.

Chapter 2

The LIBOR Market Model

In this chapter the basics of the market models established by [BGM97], [MSS97] and [Jam97] shall be introduced first. The focus of this thesis will be on the LIBOR market model which models the evolution of forward rates of fixed step size as a multi-factorial Ito diffusion. After describing the input quantities of the model (yield curve, volatility, correlation), at the end of the chapter different techniques for pricing interest rate derivatives will be presented and a summary of differences to other models will be given.[1]

2.1 Yield Curve

In every model as a first step one has to build up the yield curve from plain vanilla instruments without optionality. In the market there are different instruments available: cash (= spot) rates, forward rate agreements (FRAs), futures and swap rates. Depending on the currency, the most liquid ones are chosen to span the curve. Usually, for US-$ short term interest rates one to three cash rates (1 day, 1 month and 3 months LIBOR) and 16 to 28 Euro-Dollar futures are used, i.e. starting with the front future the three-months LIBOR futures for 4 up to 7 years. 4 to 9 swap

[1] For a more comprehensive overview over deriving the LIBOR market model and pricing derivatives see [Mei04].

rates (5, 7, 10, 12, 15, 20, 25, 30 and 50 years) span the long-term part of the yield curve.[2]

As the reset dates of the Euro-Dollar futures are fixed they usually do not coincide with the fixed step size of the LIBOR market model, where one assumes that – depending on the currency – every 3 or 6 months in the future one forward rate resets. Therefore, the discount factors are used to compute all needed forward LIBOR rates $L(t,T,T+\delta)$ at time t for any reset date T and tenor δ:

$$L(t,T,T+\delta) = \left(\frac{P(t,T)}{P(t,T+\delta)} - 1\right)/\delta \tag{2.1}$$

where $P(t,T)$ is the price of a discount bond at time t with maturity T.

Since one not only wants to price derivatives with reset dates that coincide with the reset dates chosen in the model but also other non-standardized derivatives that are usually traded "over the counter" (= OTC), a "bridging-technique" for interpolating the required forward rates is used.[3] For ease of presentation in the following this problem is neglected. When in the model these forward rates are evolved over time one can see the first big advantage of the LIBOR market model: these forward rates are actually market observables.[4]

2.2 Volatility

For evolving these forward rates, that have been defined in the previous section, over time one has to determine two parts. The first part is the uncertainty, i.e. the random up or down moves with a specified volatility. This part is independent of

[2] How many of those instruments are actually chosen mainly depends on the liquidity of these derivatives. The number of forward rates that have to be evolved in the LIBOR market model over time is chosen independently of this.

[3] See [BM01], p. 264-266.

[4] Although the forward rate in the LIBOR market model is not exactly the same as the Euro-Dollar future rate, OTC forward rate agreements that have exactly the same specification as the forward rate in the model can be traded. With models using spot or instantaneous forward rates this is not possible.

the chosen probability measure.[5] The second part is the deterministic drift of the forward rate depending on the chosen measure. For each forward rate there exists one special measure for which the drift equals 0. This measure then is called the (respective) forward or terminal measure.

With the assumption that the forward rates follow a lognormal evolution over time, we can write for the forward rate $L_i(t) = L(t, T_i, T_{i+1})$ the

Forward Rate Evolution:

$$\mathrm{d}L_i(t) \;=\; L_i(t)\mu_i(t)\mathrm{d}t + L_i(t)\sum_{k=1}^{m}\sigma_{ik}(t)\mathrm{d}z_{(k)} \tag{2.2}$$

where

$\mu_i(t)$ = the drift of the forward LIBOR rate $L_i(t)$ under the chosen measure,

m = the number of factors/dimensions of the model,[6]

$\sigma_{ik}(t)$ = the volatility of the logarithm of the forward rate $L_i(t)$ coming from factor k,

$\mathrm{d}z_{(k)}$ = the Brownian increment of factor k.[7]

With simplifying

$$\sigma_i^2(t) \;=\; \sum_{k=1}^{m}\sigma_{ik}^2(t) \quad \text{and} \quad b_{ik}(t) \;=\; \frac{\sigma_{ik}(t)}{\sigma_i(t)} \tag{2.3}$$

equation (2.2) can be written as[8]

$$\frac{\mathrm{d}L_i(t)}{L_i(t)} \;=\; \mu_i(t)\mathrm{d}t + \sigma_i(t)\sum_{k=1}^{m}b_{ik}(t)\mathrm{d}z_{(k)} \;=\; \mu_i(t)\mathrm{d}t + \sigma_i(t)\mathrm{d}z_i \tag{2.4}$$

[5] For a concise definition and explanation of these concepts see [Reb00], p. 447-490.

[6] The number of forward rates n can be larger than m, the number of factors.

[7] When talking about the volatility of a forward rate one – strictly speaking – refers to the volatility of the logarithm of the forward rate.

[8] See [Reb02], p. 71.

with

$$\begin{aligned} dz_i &= \sum_{k=1}^{m} b_{ik}(t)dz_{(k)}, \\ b(t) &= \text{the } n \times m \text{ matrix of the coefficients } b_{ik}(t) \end{aligned}$$

where it can easily be seen that the covariance of different forward rates can be separated into the volatility of each forward rate and the correlation matrix $\rho(t)$. As will be shown in the following sections the volatility $\sigma_i(t)$ is calibrated as time-dependent and the correlation matrix is restricted to be totally time-homogeneous ($\rho_{i+k,j+k}(t+k\delta) = \rho_{i,j}(t)$ for all $k = 0,1,...$) for reducing the degrees of freedom:

$$\rho(t) = b(t)b(t)^T \tag{2.5}$$

with $\rho_{i,j}(t)$ denotes the instantaneous correlation between the forward rates $L_i(t)$ and $L_j(t)$.

As a first step the volatility for each forward rate has to be computed. This is done by taking the market observable price of an ATM caplet with this specific forward rate as underlying and solving for the implicit volatility in Black's formula, introduced in his seminal article.[9]

2.2.1 Black's Formula for Caplets

The payoff of a caplet at time T_{i+1} is given by:[10]

$$\text{Payoff(Caplet)}_{T_{i+1}} = NP[L_i(T_i) - K]^+\delta \tag{2.6}$$

where

$$\begin{aligned} K &= \text{strike}, \\ NP &= \text{notional}. \end{aligned}$$

[9] See [Bla76], p. 177.
[10] See [Reb02], p. 32f.

The underlying assumption in Black's formula is the lognormal distribution of the forward rate. This leads to:

$$\ln[L_i(T_i)] \sim N\left(\ln[L_i(t)] - \frac{1}{2}\sigma_i^2(T_i - t), \sigma_i^2(T_i - t)\right) \tag{2.7}$$

where

$$\begin{aligned} N(a,b) &= \text{the Gaussian normal distribution with mean } a \\ &\quad \text{and variance } b, \\ \sigma_i &= \text{the annualized volatility of the logarithm of the} \\ &\quad \text{forward rate } L_i(t). \end{aligned}$$

From this distribution together with equation (2.6) follows

Black's Caplet Pricing Formula: ⌝

$$\text{Caplet}(0, T_i, \delta, NP, K, \sigma_i) = NP\,\delta P(0, T_{i+1})\text{Bl}(K, L_i(0), v) \tag{2.8}$$

where

$$\begin{aligned} \text{Bl}(K, L_i(0), v) &= L_i(0)\Phi(h_1) - K\Phi(h_2), \\ \Phi(x) &= \text{the cumulated normal distribution for } x, \\ h_1 &= \frac{\ln[L_i(0)/K] + \frac{1}{2}v^2}{v}, \\ h_2 &= h_1 - v, \\ v &= \sigma_i\sqrt{T_i}. \end{aligned}$$

⌟

With this formula and market prices for caplets one can then compute the market implied annualized volatility of the logarithm of the forward rate $\hat{\sigma}_i$. For brevity reasons this parameter is usually just called volatility of the forward rate.

2.2.2 Term Structure of Volatility

Having computed the volatility for each forward rate $L_i(0)$ cumulated over the lifetime of the rate (T_i) the next step is to determine how this volatility $\hat{\sigma}_i$ can be distributed over this time. One extreme would be to say that one rate keeps the same volatility throughout its lifetime, i.e. a time-constant volatility. This clearly contradicts evidence from historical market data where it can be seen that a similar shape for the term structure of the volatility of forward rates almost always prevails in the markets. The other extreme is a totally time-homogeneous term structure of volatility, i.e. the volatility of a forward rate purely depends on the time to maturity:[11]

$$\sigma_{i+k}(k\delta) \;=\; \sigma_i(0) \quad \text{for all} \;\; k = 0,1,\ldots \tag{2.9}$$

In this case, all new volatilities with increasing maturity can be bootstrapped via:[12]

$$\begin{aligned} \sigma_i(0) &= \sqrt{\frac{\hat{\sigma}_i^2 T_i}{\delta} - \sum_{k=1}^{i-1} \sigma_k^2(0)} \\ &= \sqrt{\frac{\hat{\sigma}_i^2 T_i - \hat{\sigma}_{i-1}^2 T_{i-1}}{\delta}}. \end{aligned} \tag{2.10}$$

For always having positive values for $\sigma_i(0)$ one sees clearly the necessary requirement in equation (2.10): $\hat{\sigma}_i^2 T_i$ must be a monotonous increasing function of i. Unfortunately this precondition is not generally fulfilled and even if, the results obtained with this technique are not always very stable. Therefore, one imposes additional structure on the volatility of the forward rate:[13]

$$\sigma_i(t) \;=\; f(T_i - t) \;=\; [a + b(T_i - t)]\, \mathrm{e}^{-c(T_i - t)} + d. \tag{2.11}$$

[11] See [BM01], p. 195.
[12] See [Reb02], p. 149.
[13] See [Reb99], p. 307.

This function generates exact time-homogeneity and ensures non-negativity of volatilities. It is flexible enough to be fitted not only to the usual humped shape but also to a monotonous decreasing volatility structure that prevails sometimes in the markets.

This proposed function, however, is not sufficient to fit all implied caplet volatilities exactly and can be extended by two additional steps leading to:[14]

$$\sigma_i(t) \;=\; f(T_i - t)\, g(t)\, h(T_i). \tag{2.12}$$

In an optional first step $g(t)$ is determined to reflect time-dependent movements in the level of volatility. To avoid modeling noise another structure is imposed on this function. Usually it is modeled as a sum of a small number of sine waves multiplied with an exponentially decaying factor.

To ensure the exact recovery of market prices of ATM caplets as a second step $h(T_i)$ is computed:[15]

$$h(T_i) \;=\; 1+\delta_i \;=\; \sqrt{\frac{\hat{\sigma}_i^2 T_i}{\int_0^{T_i} f(T_i-u)^2 g(u)^2 \mathrm{d}u}}. \tag{2.13}$$

Ideally the resulting δ_i should be very small.

With this functional form and these one or two additional steps the volatility of each forward rate has been distributed over time to ensure non-negativity, approximate time-homogeneity and exact replication of market prices of caplets.

2.3 Correlation Matrix

Having found a pricing formula for caplets and having determined the term-structure of volatilities, for pricing swaptions one also needs the correlation ma-

[14] See [Reb02], p. 165f.
[15] See [Reb02], p. 387.

trix ρ between the forward rates from equation (2.5). These correlations are the so-called instantaneous correlations. The terminal correlations between the forward rates that can be estimated from historical market data are different as they not only depend upon the instantaneous correlations but also upon the term-structure of volatilities. This effect can be approximated via:[16]

$$\text{Corr}(L_j(T_i), L_k(T_i)) \approx \rho_{j,k}(t) \frac{\int_0^{T_i} \sigma_j(t)\sigma_k(t)\mathrm{d}t}{\sqrt{\int_0^{T_i} \sigma_j^2(t)\mathrm{d}t}\sqrt{\int_0^{T_i} \sigma_k^2(t)\mathrm{d}t}} \tag{2.14}$$

with

$$\begin{aligned} \rho_{j,k}(t) &= \text{the instantaneous correlation between the forward rates } L_j(t) \text{ and } L_k(t), \\ \text{Corr}(L_j(T_i), L_k(T_i)) &= \text{the terminal correlation between the forward rates } L_j(t) \text{ and } L_k(t) \text{ for the evolution of the term-structure of interest rates up to time } T_i.[17] \end{aligned}$$

However, this is only an approximation and additionally the terminal correlations depend upon the chosen measure. Another way for using historical market data to determine the correlation matrix is to estimate the instantaneous correlation directly. Choosing a step size of one day is sufficiently small for being measure invariant.

Generally, there are three ways of determining this instantaneous correlation matrix. First, one could use historical terminal correlations and then use (2.14) to determine the instantaneous correlations. Second, one could estimate the instantaneous correlation directly. Third, actual market prices of European swaptions can be used. Especially considering the problems with the measure-dependent terminal correlations, illiquid swaption prices, bid-ask spreads and the heavy influence a little price change would have on the "implied" correlations, the second approach seems preferable.

[16] See [BM01], p. 219.

[17] While the instantaneous correlations were set to be time-constant, the terminal correlation between two forward rates is not, as it also depends upon the time-varying volatilities.

2.3.1 Black's Formula for Swaptions

When deciding for the second approach, however, one needs first an analytic formula for efficiently pricing swaptions for avoiding the computational expensive step of a simulation. Starting with the payoff of a swaption

$$\text{Payoff}\left(\text{Swaption}\right)_{T_r} \;=\; NP\left[S_{r,s}(T_r)-K\right]^{+}\frac{\delta}{P(0,T_r)}\sum_{i=r}^{s-1}P(0,T_i+1) \qquad (2.15)$$

and the assumption that the swap rate is lognormally distributed[18]

$$\ln\left[S_{r,s}(T_r)\right] \;\sim\; N\left(\ln\left[S_{r,s}(t)\right]-\frac{1}{2}\sigma_{r,s}^2(T_r-t),\sigma_{r,s}^2(T_r-t)\right) \qquad (2.16)$$

where

$$\begin{aligned} S_{r,s}(t) &= \text{the equilibrium swap rate, i.e. the swap rate leading to a swap value of 0, from the first reset date in } T_r \text{ to the last payment of the underlying swap in } T_s, \\ \sigma_{r,s} &= \text{the annualized volatility of the logarithm of the swap rate } S_{r,s}(t), \end{aligned}$$

one gets

Black's Swaption Pricing Formula: ¬

$$\text{Swaption}\left(0,T_r,T_s,NP,K,\sigma_{r,s}\right) \;=\; \text{Bl}\left(K,S_{r,s}\left(0\right),v\right)\delta NP\sum_{i=r}^{s-1}P(0,T_{i+1}) \qquad (2.17)$$

where

$$\begin{aligned} \text{Bl}\left(K,S_{r,s}(0),v\right) &= S_{r,s}(0)\Phi\left(h_1\right)-K\Phi\left(h_2\right), \\ h_1 &= \frac{\ln\left[S_{r,s}(0)/K\right]+\frac{1}{2}v^2}{v}, \\ h_2 &= h_1-v \end{aligned}$$

[18] See [Reb02], p. 35f.

and

$$v \;=\; \sigma_{r,s}\sqrt{T_r}.$$

⌟

As for caplets the above formula and market data can be used to calculated the market implied volatility of the swap rate $\hat{\sigma}_{r,s}$.

2.3.2 A Closed Form Approximation for Swaptions

Although the swap rates in the forward rate based model are not exactly lognormally distributed, their distribution is very close to the lognormal one, so that Black's formula for swaptions (2.17) can be used.[19] Using the presentation of a swap rate as a linear combination of forward rates

$$S_{r,s}(t) \;=\; \sum_{i=r}^{s-1} \omega_i(t) L_i(t) \tag{2.18}$$

where

$$\omega_i(t) \;=\; \frac{P(t,T_{i+1})}{\sum_{j=r}^{s-1} P(t,T_{j+1})}, \tag{2.19}$$

the volatility of swap rates can be computed by differentiating both sides of the equation:[20]

$$\begin{aligned} \mathrm{d}S_{r,s}(t) &= \sum_{i=r}^{s-1} [\omega_i(t)\mathrm{d}L_i(t) + L_i(t)\mathrm{d}\,\omega_i(t)] + (\ldots)\mathrm{d}t \\ &= \sum_{h=r}^{s-1} \mathrm{d}L_h(t) \sum_{i=r}^{s-1} \left[\omega_h(t)\delta_{h,i} + L_i(t)\frac{\partial\,\omega_i(t)}{\partial L_h(t)}\right] + (\ldots)\mathrm{d}t \end{aligned} \tag{2.20}$$

[19] See [BM01], p. 229.
[20] See [BM01], p. 246-249.

where

$$\begin{aligned}
\delta_{i,i} &= 1, \\
\delta_{i,h} &= 0, \text{ for } i \neq h, \\
\frac{\partial \omega_i(t)}{\partial L_h(t)} &= \frac{\omega_i(t)\delta}{1+\delta L_h(t)} \left[\frac{\sum_{k=h}^{s-1} \prod_{j=r}^{k} \frac{1}{1+\delta L_j(t)}}{\sum_{l=r}^{s-1} \prod_{m=r}^{l} \frac{1}{1+\delta L_m(t)}} - \mathbf{1}_{i \geq h} \right] \\
&= \frac{\omega_i(t)\delta P(t,T_{h+1})}{P(t,T_h)} \left[\frac{\sum_{k=h}^{s-1} P(t,T_{k+1})}{\sum_{l=r}^{s-1} P(t,T_{l+1})} - \mathbf{1}_{i \geq h} \right]. \qquad (2.21)
\end{aligned}$$

One fixes:

$$\overline{\omega}_h(t) = \omega_h(t) + \sum_{i=r}^{s-1} L_i(t) \frac{\partial \omega_i(t)}{\partial L_h(t)}. \qquad (2.22)$$

For ease of computation the coefficients $\overline{\omega}_i(t)$ are frozen at time $t = 0$. Equations (2.20) and (2.22) then lead to:

$$\mathrm{d}S_{r,s}(t) \approx \sum_{i=r}^{s-1} \overline{\omega}_i(0) \mathrm{d}L_i(t) + (\ldots)\mathrm{d}t. \qquad (2.23)$$

The quadratic variation of that equals:

$$\mathrm{d}S_{r,s}(t)\mathrm{d}S_{r,s}(t) \approx \sum_{i=r}^{s-1} \sum_{j=r}^{s-1} \overline{\omega}_i(0)\overline{\omega}_j(0) L_i(t) L_j(t) \rho_{i,j}(t) \sigma_i(t) \sigma_j(t) \mathrm{d}t.$$

As a second approximation the forward rates are frozen at time $t = 0$ leading to a percentage quadratic variation:

$$\begin{aligned}
\left(\frac{\mathrm{d}S_{r,s}(t)}{S_{r,s}(t)} \right) \left(\frac{\mathrm{d}S_{r,s}(t)}{S_{r,s}(t)} \right) &= \mathrm{d}\ln S_{r,s}(t) \mathrm{d}\ln S_{r,s}(t) \\
&\approx \sum_{i=r}^{s-1} \sum_{j=r}^{s-1} \frac{\overline{\omega}_i(0)\overline{\omega}_j(0) L_i(0) L_j(0)}{S_{r,s}^2(0)} \rho_{i,j}(t) \sigma_i(t) \sigma_j(t) \mathrm{d}t.
\end{aligned}$$

The variance for Black's formula for swaptions can be computed as the integral over the percentage quadratic variation during the life-time of the option:

$$\sigma_{r,s}^2 \approx \sum_{i=r}^{s-1}\sum_{j=r}^{s-1} \frac{\overline{\omega}_i(0)\overline{\omega}_j(0)L_i(0)L_j(0)\rho_{i,j}(t)}{S_{r,s}^2(0)} \int_0^{T_r} \sigma_i(t)\sigma_j(t)\mathrm{d}t. \tag{2.24}$$

The result of equation (2.24) can then be used in (2.17) for pricing swaptions and is called Hull and White's formula. This obtained fast pricing method for swaptions is essential for computing the correlation matrix efficiently.

2.3.3 Determining the Correlation Matrix

Independent of having a correlation matrix from historical market data or from current swaption market prices it is usually preferable to smooth this matrix and present the data with a small number of parameters. The following one factor parametrization could be seen as a minimalist approach:

$$\rho_{i,j} = \mathrm{e}^{-c|T_i - T_j|} \tag{2.25}$$

with c being a small positive number.

Generally, when trying to fit a parametric estimate to a correlation matrix, this parametric form should be able to incorporate these three empirical observations:[21]

1. The correlation between the first and the other forward rates is a convex function of distance.
2. The correlation between the first and the last forward rate is positive.
3. The correlation between two forward rates with the same distance is an increasing function of maturity.

[21] See [Reb02], p. 183f, 190.

The last condition, especially, is violated by many approaches, for example the one factor form in (2.25).

One parametric approach, fulfilling all three conditions, although needing only two parameters, is: [22]

$$\rho_{i,j} = \exp\left[\frac{|j-i|}{n-1}\left(\ln\rho_\infty - d\frac{i^2+j^2+ij-3ni-3nj+3i+3j+2n^2-n-4}{(n-2)(n-3)}\right)\right] \tag{2.26}$$

where

$$i,j = 1,...,n,$$
$$0 < d < -\ln\rho_\infty.$$

With this formula the two parameters (ρ_∞, d) can be estimated iteratively so that they fit the historic correlation matrix or prices of swaptions and maybe even other correlation sensitive derivatives as closely as possible. The parameter ρ_∞ can be interpreted as the positive correlation between the first and the last forward rate; d determines the difference between $\rho_{1,2}$ and $\rho_{n-1,n}$. For the usual case where $\rho_{n-1,n} > \rho_{1,2}$, i.e. the correlation between two adjacent forward rates is increasing with maturity, d takes positive values.[23]

2.3.4 Factor Reduction Techniques

For efficient valuation of derivatives the correlation matrix has to be reduced to a smaller number of factors as with the number of factors the number of random numbers that have to be drawn increases and thereby slows down the simulation of the forward rates. Another reason for keeping the number of factors rather small is trying to explain these factors with usual market movements. The first factor is interpreted as a shift of the yield curve (= simultaneous up or down movement of the forward rates), the second factor as a tilt of the curve (= the forward rates close to the reset date and the forward rates far away from the reset date move in opposite directions) and the third factor as a butterfly movement, where forward rates

[22] See [SC00], p. 8.

[23] For more different parametric forms for the correlation matrix and a comparison of them, see [BM04], p. 14-18.

close to and far away from the reset date move stronger in the same direction than forward rates in between. These factors can easily be understood and increasing their number far beyond this is usually avoided.

One possible technique for reducing to a number of factors m smaller than the number of forward rates n shall be presented here.[24] From equation (2.3) follows:

$$\sum_{k=1}^{m} b_{ik}^2 = 1. \tag{2.27}$$

The following parametrization can be chosen to ensure that this condition is fulfilled:[25]

$$\begin{aligned} b_{ik} &= \cos\theta_{ik} \prod_{j=1}^{k-1} \sin\theta_{ij} \quad \text{for } k = 1, ..., m-1, \\ b_{im} &= \prod_{j=1}^{m-1} \sin\theta_{ij}. \end{aligned} \tag{2.28}$$

As a first step these $(m-1)n$ different θ_{ij} are chosen arbitrarily. Inserting these values as a second step in equation (2.28) one can compute the b_{jk}. As a third step the correlation matrix is determined by:

$$\rho_{jk} = \sum_{i=1}^{m} b_{ji} b_{ki}. \tag{2.29}$$

In the fourth step, this correlation matrix is compared to the original matrix with the help of a penalty function:

$$\chi^2 = \sum_{j=1}^{n} \sum_{k=1}^{m} \left(\rho_{jk}^{original} - \sum_{i=1}^{m} b_{ji} b_{ki} \right)^2. \tag{2.30}$$

[24] Another possibility is the so-called Principle-Component-Analysis. See [Fri04], p. 148f. The problem of all possible factor reduction techniques is that they have, especially when reducing to a very small number of factors, a heavy impact on the correlation matrix changing thereby the evolution of the term-structure of interest rates and option prices.

[25] See [Reb02], p. 259.

This penalty function can then be minimized by iterating steps 2-4 with non-linear optimization techniques.

2.4 Deriving the Drift

For pricing other non plain-vanilla options one has to resort to Monte Carlo techniques, where all forward rates are rolled out simultaneously. When deriving Black's formula for a caplet on the forward rate $L_i(t)$ the zero bond $P(t,T_{i+1})$ was used as a numeraire to discount the payoffs of the caplet. With this numeraire in the connected probability measure, the so-called forward or terminal measure, the evolution of the interest rate $L_i(t)$ over time is drift-free and hence a martingale. For different forward rates, however, one needs different numeraires for canceling out the drift. To price derivatives depending on more forward rates one needs these forward rates in one single measure. Therefore, for all (or at least for all but one) forward rates the measure has to be changed and the drift of each forward rate has to be determined.

A systematic way of changing drifts shall be presented here. When changing from one numeraire to another this formula can be used, sometimes referred to as a "change-of-numeraire toolkit":[26]

$$\mu_X^U = \mu_X^S - \left[X, \frac{S}{U}\right]_t \tag{2.31}$$

where

$$\begin{aligned} \mu_X^U, \mu_X^S &= \text{the percentage drift terms of } X \text{ under the measure associated} \\ &\quad \text{to the numeraires } U \text{ and } S, \\ X &= \text{the process for which the drift shall be determined} \end{aligned}$$

[26] See [BM01], p. 28-32.

and

$$[X,Y]_t \;=\; \text{the quadratic covariance between the two Ito diffusions } X \text{ and } Y\text{, notated in the so called "Vaillant brackets" where } [X,Y]_t = \sigma_X(t)\,\sigma_Y(t)\,\rho_{XY}(t).^{27}$$

The spot measure, i.e. the measure with a discretely rebalanced bank account

$$B_d(t) \;=\; P(t,T_{\beta(t)-1}+\delta)\prod_{k=0}^{\beta(t)-1}(1+\delta L_k(T_k)) \tag{2.32}$$

as numeraire, is usually used to simulate the development of forward rates with Monte Carlo.

Therefore, one sets:

$$\begin{aligned} X &= L_i(t),\\ S &= P(t,T_i+\delta),\\ U &= B_d(t),\\ \beta(t) &= m, \quad \text{if } T_{m-1}<t<T_m \end{aligned}$$

resulting in:

$$\mu_i^d(t) \;=\; \mu_{L_i}^{B_d(t)}(t) \;=\; \mu_i^i(t) - \left[L_i(t),\frac{P(t,T_i+\delta)}{B_d(t)}\right]_t. \tag{2.33}$$

As $P(t,T_{i+1})$ is the numeraire of the associated measure for $L_i(t)$, this leads to $\mu_i^i = 0$ and:

$$P(t,T_i+\delta) \;=\; P(t,T_{\beta(t)-1}+\delta)\prod_{j=\beta(t)}^{i}\frac{1}{1+\delta L_j(t)}. \tag{2.34}$$

[27] See [Reb02], p. 182.

Inserting equations (2.34) and (2.32) in (2.33) one gets:[28]

$$\begin{aligned}
\mu_i^d(t) &= -\left[L_i(t), \frac{\prod_{j=\beta(t)}^{i} \frac{1}{1+\delta L_j(t)}}{\prod_{k=0}^{\beta(t)-1}(1+\delta L_k(T_k))}\right]_t \\
&= \sum_{j=\beta(t)}^{i} \left[L_i(t), 1+\delta L_j(t)\right]_t + \sum_{k=0}^{\beta(t)-1} \left[L_i(t), 1+\delta L_k(T_k)\right]_t \\
&= \sum_{j=\beta(t)}^{i} \frac{\delta L_j(t)}{1+\delta L_j(t)} \left[L_i(t), L_j(t)\right]_t + \sum_{k=0}^{\beta(t)-1} \frac{\delta L_k(t)}{1+\delta L_k(t)} \overbrace{\left[L_i(t), L_k(T_k)\right]_t}^{=0} \\
&= \sigma_i(t) \sum_{j=\beta(t)}^{i} \frac{\delta L_j(t) \rho_{i,j}(t) \sigma_j(t)}{1+\delta L_j(t)}. \qquad (2.35)
\end{aligned}$$

Hence, the dynamics of a forward rate under the spot measure is given by:[29]

$$\frac{\mathrm{d}L_i(t)}{L_i(t)} = \sigma_i(t) \sum_{j=\beta(t)}^{i} \frac{\delta L_j(t) \rho_{i,j}(t) \sigma_j(t)}{1+\delta L_j(t)} \mathrm{d}t + \sigma_i(t) \mathrm{d}z_i. \qquad (2.36)$$

With the same technique the process of one forward rate can also be expressed in any other measure, e.g. the terminal measure of another forward rate.[30]

Having calibrated the yield curve to the underlying FRAs and swaps, the volatility to the caplets and the correlation matrix to the swaptions or to historical data, one can implement Monte Carlo simulations to evolve the forward rates over time for pricing more exotic derivatives.

[28] The Vaillant brackets have the following properties:
$[X, YZ] = [X,Y] + [X,Z]$ and $[X,Y] = -\left[X, \frac{1}{Y}\right]$.
[29] See [BM01], p. 203.
[30] See [Mei04], p. 14f.

2.5 Monte Carlo Simulation

The LIBOR market model is Markovian only w. r. t. the full dimensional process, i.e. the forward rate $L_i(t+\delta)$ is a function of all forward rates $(L_1(t), L_2(t), ..., L_n(t))$. Therefore, one has to price options with Monte Carlo simulations, the usual "tool of last resort".

These Monte Carlo methods consist of iterating the modeled process, pricing the derivative on this path (PV_i) and determining the price of a derivative as the average of all paths. Due to the law of large numbers this converges to the correct price. The estimate PV_{est} and its standard deviation $s(PV_{est})$ are given by:[31]

$$\begin{aligned} PV_{est} &= \frac{1}{n}\sum_{i=1}^{n} PV_i, \\ s(PV_{est}) &= \sqrt{\frac{1}{n-1}\sum_{i=1}^{n}(PV_i - PV_{est})^2}. \end{aligned}$$

This leads to:

$$PV_{est} \sim N\left(PV, \frac{s^2(PV_{est})}{n}\right). \tag{2.37}$$

There are two shortcomings of valuing derivatives with Monte Carlo simulations. First, the convergence is rather slow, i.e. even with 10,000 pathes the pricing error can be more than 10 basis points. Second, when valuing the same derivative under the same market conditions (yield curve, volatility) different prices can be computed, i.e. valuations are not repeatable if one does not use the same random number generator with the same seed. Due to these two reasons Monte Carlo techniques are generally avoided although for path dependent derivatives they are straightforward to implement.

For using Monte Carlo techniques efficiently the step sizes have to be discretized. This can be done by an Euler scheme applied to the logarithm of the forward rate

[31] See [Jac02], p. 20.

as shown for the one-factor case:[32]

$$\ln[L_i(t+\Delta t)] \;=\; \ln[L_i(t)] + \left(\mu_i(t) - \frac{1}{2}\sigma_i(t)\right)\Delta t + \sigma_i(t)\Delta z_i \tag{2.38}$$

with

$$\begin{aligned} \Delta z_i &= x_i\sqrt{\Delta t}, \\ x_i &= \text{a } N(0,1) \text{ distributed random number.} \end{aligned} \tag{2.39}$$

For $\Delta t \to 0$ this is the exact solution, but in applications in practice due to time constraints Δt is usually chosen to be equivalent to the tenor δ of the forward rate that shall be simulated. This does not cause any problems with volatility but with the drift $\mu_i(t)$ because it is dependent upon the actual level of forward rates that are not computed between the step sizes. One possible mechanism reducing this problem is the so-called "predictor-corrector" approximation.[33] The real drift is approximated by the average of the drift at the beginning and at the end of the step. As the drift at the end of the step is dependent upon the forward rates at that time it cannot be computed exactly. It is approximated applying an Euler step by using the initial drift to determine the forward rates at the end of the step.

Since calculating the drift term takes most of the time, a possibility for speeding up this simulation of the forward rates significantly is an approximation where not the forward rates themselves but some other variables from which you can compute the forward rates are evolved over time.[34] With an appropriate choice of these variables they are drift-free under the terminal measure of the last forward rate that is rolled out. The only difficulty is that the volatility of each forward rate is state-dependent. Caplet and swaption prices, however, can still be approximated efficiently from these variables and volatilities.

[32] See [Fri04], p. 77-80.
[33] See [Reb02], p. 123-131.
[34] See [Mey03], p. 170-177.

2.6 Differences to Spot and Forward Rate Models

The LIBOR market model was deviated in 1997 from the HJM framework. Due to its success and very special characteristics it is usually seen as distinct from the original HJM framework. Its main differences to this framework are:[35]

1. It is the only model for the evolution of the term structure of interest rates that embraces Black's formulæ for caps or swaptions.
2. Different from most models with a lognormal distribution of interest rates the forward rates do not explode, i.e. go to infinity, in this discretized setting.
3. The market model is easily extendable to a larger number of forward rates.
4. When calibrating the LIBOR market model traders have a large number of degrees of freedom. This facilitates efficient methods for calibrating and testing market data.

After this introduction to the basics of the LIBOR market model, in the next chapter the problems with the volatility smile will be discussed.

[35] See [Mei04], p. 37-43.

Chapter 3

The Volatility Smile

When deriving Black's formula for caplets in Section 2.2.1 one assumed the exact lognormal distribution of the forward rates. With this assumption for all strike levels the same volatility σ_i can be used. When computing the implied Black volatilities of market prices with equation (2.8), however, one almost always gets for every strike – keeping the other parameters fixed – a different volatility. Furthermore, when determining the implied distribution from market prices, this distribution is not very close to the lognormal distribution. These observations clearly contradict the underlying conditions to derive Black's formula.

Usually, these findings are summarized by plotting the implied volatility as a function of the strike ($\hat{\sigma}_i(K)$). The result is the so-called "volatility smile". To account for the fact that this smile does not have its minimum for ATM options one also uses the expression "volatility skew".

Models that will be presented in the following chapters try to fit smiles existing in the market in very different ways. Especially models with only one parameter are often not able to reproduce all features of the market implied volatility smile. For the rest of the thesis I will use the expression "symmetric volatility smile" for the case a model only is able to generate volatility smiles with the minimum for ATM options and the expression "volatility smirk" for the case a model implies the minimum volatility for $K \to 0$ or $K \to \infty$. Finally, the expression "smile surface"

depicts the surface spanned by the volatility smiles of caplets and/or swaptions with different maturities and/or tenors.

For depicting these volatility smiles it is preferable to express these graphs as a function of the standardized moneyness M instead of the strike K since M accounts for different expiries and volatilities:

$$M = \frac{\ln\left[\frac{K}{L_i(0)}\right]}{\hat{\sigma}_i(L_i(0))\sqrt{T_i}}. \tag{3.1}$$

Due to the assumed lognormal distribution (and $\hat{\sigma}_i(K)$ being the volatility of the logarithm of the forward rate $L_i(t)$) the logarithm $\ln\left[\frac{K}{L_i(0)}\right]$ rather than the ratio $\frac{K-L_i(0)}{L_i(0)}$ suggested in [Tom95] is chosen.

Another advantage of this way of presenting moneyness is the fact that – as will be seen later in this thesis – some local volatility models, jump processes with a lognormal distribution of the jump size and a mean of 0, stochastic volatility processes and uncertain volatility models lead to a totally symmetric volatility smile w. r. t. the moneyness M, i.e. for the implied volatility $\hat{\sigma}$ as a function of M:

$$\hat{\sigma}(M) = \hat{\sigma}(-M).$$

3.1 Reasons for the Smile

Generally, there exist two possible concepts for explaining the volatility smile:

1. The underlying dynamics of the forward rates are different from a lognormal distribution of the forward rates with deterministic and only time-dependent volatilities.

2. The underlying dynamics of the forward rates are well enough described by the assumptions in Black's model but additional effects influence the price of options.

The first concept immediately leads to changing the proposed dynamics of the forward rates from (2.2). There exist several possibilities for doing so derived from some very strong assumptions in Black's model:

1. Having a lognormal distribution the volatility of the logarithm of the forward rate is independent of the level of the forward rate. This leads to the volatility of the forward rate being proportional to the level of the forward rate.

2. The volatility in Black's model is assumed to be deterministic.

3. In Black's model one assumes a continuous development of the underlying.

With weakening one or more of these assumptions one can change the dynamics of the forward rates immediately leading to a volatility smile.

The second concept does not lead to a rejection of the proposed dynamics in Black's model but tries to explain why market prices of caplets and swaptions do not imply a lognormal distribution but different dynamics. One possible reason for that is supply and demand of caplets with different strikes. For example in the stock market especially out of the money puts are a logical crash protection. Since investors are stocks – at least on average – long, the demand for out of the money puts is bigger than for other options. Investment banks trying to benefit from that fact supply these puts hedging themselves. However, due to transaction costs – even if market participants were certain about the lognormal dynamics of the underlying stock – investors would be charged a premium for those puts leading, when using these market prices for calculating the implied volatilities, to a volatility smile. Similarly, for interest rate derivatives the different level of supply and demand of options with different strikes can cause a volatility smile.

Another possible reason for volatility smiles are estimation biases as shown in [Hen03]. Starting from the fact that both the market price of an option and the other input parameters except the strike are typically contaminated by measurement errors, tick sizes, bid-ask spreads and non-synchronous observations the author shows that computing the implied volatility out of these data is very error-prone leading to extremely wide confidence intervals for options in or out of the

money. The further away from ATM options are the wider these confidence intervals are as there small price differences already lead to big volatility differences.[1] The bias that leads to higher implied volatilities in or out of the money than for options at the money comes from arbitrage conditions. As prices that violate arbitrage restrictions are not quoted and usually the lower absence-of-arbitrage bound is violated, quoted prices and, therefore, implied volatilities have an upwards bias.[2] This bias exists even if the distribution would be really lognormal.

Certainly both concepts have an influence on option prices. The scope of this thesis will be to determine what forward rate processes would imply option prices as observed in the market.

3.2 Sample Data

The market data has been supplied by Dresdner Kleinwort Wasserstein for US-$ and € as of August 6th, 2003. The data consists of the yield curve and swaption data in the form of a so called ”volatility cube” for different expiries, tenors and strikes.

From the existing ”volatility cube” (expiry $\times$ tenor $\times$ strike) missing data points are interpolated with cubic spline methods. As differences between the grid points in expiries, tenors and strikes are reasonably small, only a little loss of accuracy results, especially considering bid-ask spreads of 2 up to 4 kappas (= volatility points).

Usually in the markets there is a huge gap between caplet volatilities and swaptions volatilities. Since explaining this difference is beyond the scope of this thesis the forward tenor δ is set to one year and available market data for swaptions for different expiries and tenors are used as if $\delta = 1$. The used data in this thesis therefore has more the characteristics of possible market data rather than real market data.

[1] See [Hen03], p. 4.
[2] See [Hen03], p. 19-22.

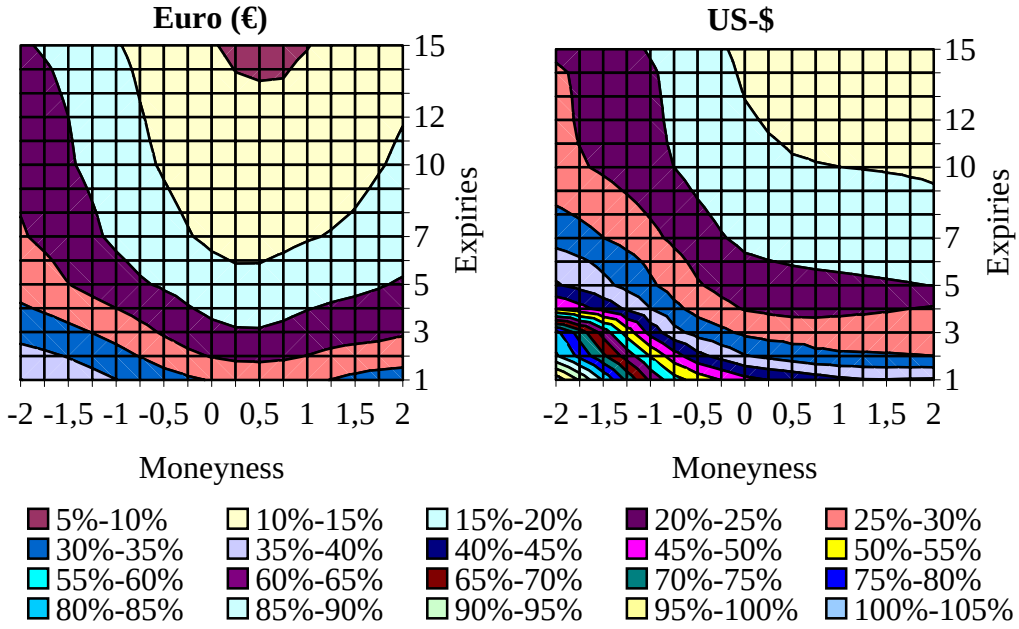

Figure 3.1: *Contour lines of the caplet volatility surface for € and US-$.*

When comparing the caplet volatility surfaces of the two currencies in Figure 3.1 one can see huge differences in the level and the shape of the volatility smile. In the € market the volatility smiles for caplets – as can be seen in Figure 3.2 – are quite pronounced even for very long expiries. In the US-$ market, however, volatilities are much higher for short expiries but flatten out for longer expiries quite rapidly. Figure B.1 on page XIII shows that for some expiries the minimum implied volatility is for caplets with the highest moneyness.

Since the volatility skews in the € market are more demanding for a model to replicate than the volatility smirks at US-$, during the text part of this thesis the graphs presented are (until otherwise stated) for € data while US-$ graphs are deferred due to space reasons to Appendix B.

For swaptions close to expiry with different tenors the volatility smile flattens out quite quickly in both markets (see Figures 3.3 and B.2).

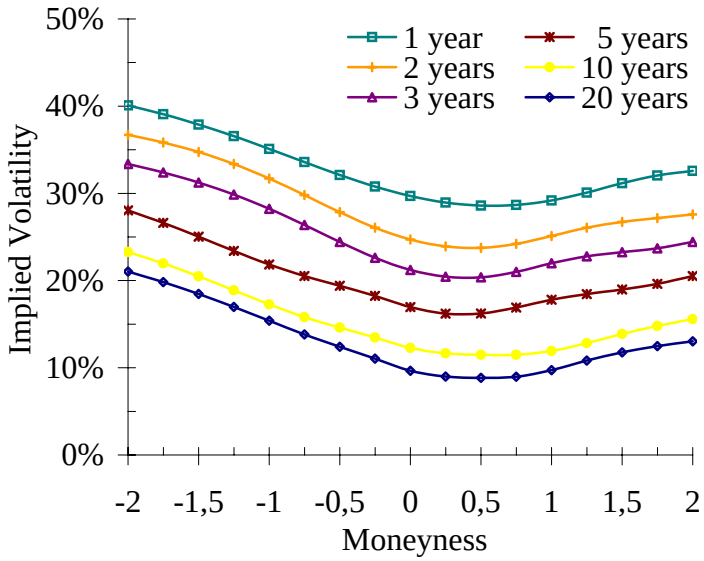

Figure 3.2: *Caplet volatility smiles for different expiries.*

Finally, a comparison between the implied distributions of a future forward rate and of a flat volatility smile is given in Figure 3.4.[3]

In the following chapters the focus of this thesis will be on testing the available models to evaluate if they are capable of fitting the entire volatility surface at all rather than testing how good the actual fit to a single volatility smile is. The reason for this aim is the fact that having two or more free parameters with most models it is not a problem to fit a single volatility smile but when pricing exotic options, e.g. Bermudan swaptions, their value depends on numerous forward rates, volatilities and their joint evolution over time. The difference between the later proposed models will be more in this joint evolution as the same caplet pricing formula can imply – depending on the underlying model – very different joint dynamics of the forward rates. This issue will be discussed deeper in Chapter 8.

[3] See also Appendix A.1.

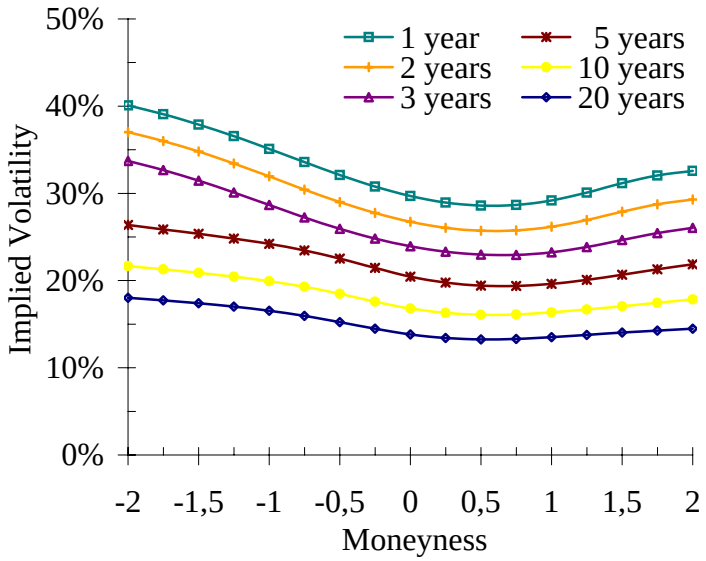

Figure 3.3: *Swaption volatility smiles for 1 year expiry and different tenors.*

3.3 Requirements for a Good Model

When trying to find a tractable interest rate model that fits market data best, several aspects have to be considered:

1. For fast calibration efficient formulæ for caplets and swaptions should be available.

2. The model shall be used to price all possible interest rate derivatives. Therefore, besides efficient[4] formulæ for plain-vanilla options one also needs a way to simulate the evolution of the term structure of interest rates. These simulations can be done by different methods with the Monte Carlo technique being the most flexible considering correlations.

3. The model shall allow to price options with all possible expiries, tenors and strikes simultaneously without the need for re-calibration.

4. For many applications like the pricing of exotic options the exact replication of the hedging instruments like ATM caplets and swaptions is essential.

[4] That can be analytic, numeric or even very good approximative formulæ.

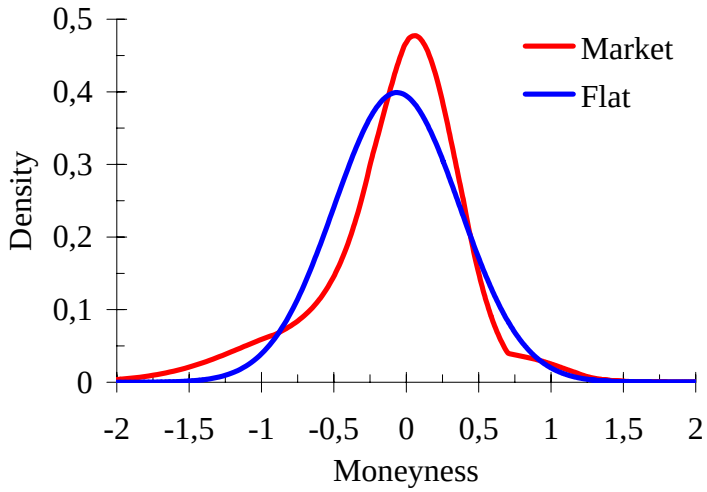

Figure 3.4: *Comparison of the densities of a future forward rate between market data and a flat volatility smile with the same ATM implied volatility for a €-caplet that expires in 1 year.*

While this holds true for all interest rate models, additional requirements for the smile modeling are:

1. The parameters used for fitting the volatility smile should be meaningful and stable. Their number has to be carefully chosen to ensure both a good fit to the volatility smiles in the market and to avoid overfitting.

2. The simultaneous pricing of all derivatives mentioned in point 3 of the general requirements is essential as some models – as can be seen in the following chapters – can only fit one single (= for a chosen expiry-tenor pair) volatility smile at a time.

3. The volatility smile implied by the model should be self-similar, i.e. independent of the future level of interest rates the volatility smile at future times shall have a similar shape.

Certainly, one will not be able to find a model that fulfills all these requirements 100%, but these are the different aims when trying to find a good model. For a benchmark model the actual speed of calibration is not that important.

3.4 Calibration Techniques

There are different ways to measure the calibration quality of different models and their closed form solutions to actual market data. In this thesis, until otherwise stated, due to comparability the methodology is the same for all models. The fit is measured by the least squares method, i.e. one tries to minimize the sum of the squares of the differences between market and model prices. Unlike other papers about these models, the price differences as opposed to the volatility differences are chosen due to three reasons:

1. The volatility differences for ATM options are more important than for other options. Instead of using different weights for different strikes the price differences are chosen as the vega has maximum size at the money.

2. The calibration is faster. While this is not an issue for all models, for those models where complex computations – especially numerical integrations – are involved this can speed up the calibration process significantly as an additional step with Newton iterations can be avoided.

3. The price errors are the errors that really determine the success of a model in real trading. Therefore, it is important that the loss function when calibrating a model is the same as when evaluating the model.[5]

Other possibilities might be to fit as close as possible the PDF or CDF that is implied by market prices. Especially with the PDF, however, a good fit to this distribution might result in model prices that are totally different.

To ensure consistent calibration criteria the models are usually calibrated throughout the thesis at options with the following set of standardized moneynesses:

$$\{M_j\} = \{0, \pm 0.25, \pm 0.5, \pm 0.75, \pm 1, \pm 1.5, \pm 2\}. \tag{3.2}$$

[5] See [CJ02], p. 19f.

3.5 Overview over Different Basic Models

After collecting the different requirements for the models, three assumptions of the underlying Black model can be weakened to generate a better fit to the market implied distribution of interest rates.[6]

1. The diffusion part of the evolution of interest rates is no longer assumed to be lognormal. The basic idea is to assume a normal or square-root distribution of forward rates but more general extensions can also be implemented. All these extensions have in common that they can be written as the volatility of the logarithm of the forward rate being not only dependent upon the time but also upon the level of the forward rate. These models are also called local volatility models and will be presented in Chapter 4.

2. Another assumption that heavily contradicts market observations is deterministic volatility. Non-deterministic volatility can then be modeled again with a Brownian motion (uncorrelated or correlated with the evolution of forward rates), with jump processes or with a jump to one of several possible deterministic volatility scenarios (= uncertain volatility models). Chapter 5 will discuss uncertain volatility models and Chapter 6 will give an overview of stochastic volatility models.

3. In the markets prices are fixed with the distance of at least one second. Continuous or discrete stochastic processes with a underlying lognormal distribution are not consistent with the distribution of interest changes for this minimum step size. Therefore, jump processes, one possible way to deal with this and also with the observation of unusual big movements in the level of interest rates due to new information usually occurring over night, are discussed in Chapter 7.

[6] The assumption of a Brownian motion for the forward rate process can be weakened, too. For instance more general Levy processes or other distributions can substitute the Brownian motion. As these models are far more than an extension to Black's formulæ or the LIBOR market model they are not further discussed in this thesis. For an overview over the applications of Levy processes in finance, see [BNMR01].

An overview of these models and a kind of graphical table of contents is given in Figure 3.5.

These four different possible basic models and their advantages and shortcomings shall be discussed at length in the next part. To improve the comparability between the different models the same structure of discussion is applied to all models. This structure can be divided into three up to five steps:

1. **Rate Evolution:**
   The model is specified by the evolution of the forward or swap rate.

2. **Pricing Formula:**
   For efficient calibration of the model analytic or numeric solutions for caplet or swaption prices have to be available.

3. **Calibration Quality w. r. t. a Fixed Maturity:**
   In this step the quality of calibration to market data for each caplet or maturity separately is assessed.

4. **Term Structure Evolution:**
   For pricing all possible interest rate derivatives in a single model simultaneously the joint evolution of all forward rates over time is needed usually deteriorating the fit of each single volatility smile.

5. **Calibration Quality w. r. t. the Full Term Structure Evolution:**
   The quality of the calibration to the complete market data is the final step in presenting a model.

The steps four and five are left out for example when results in step three already show how poor the fit to the volatility smile of a single expiries already is.

An additional sixth step, the discussion of how each model is able to produce a self-similar volatility smile, is deferred to Section 8.1.

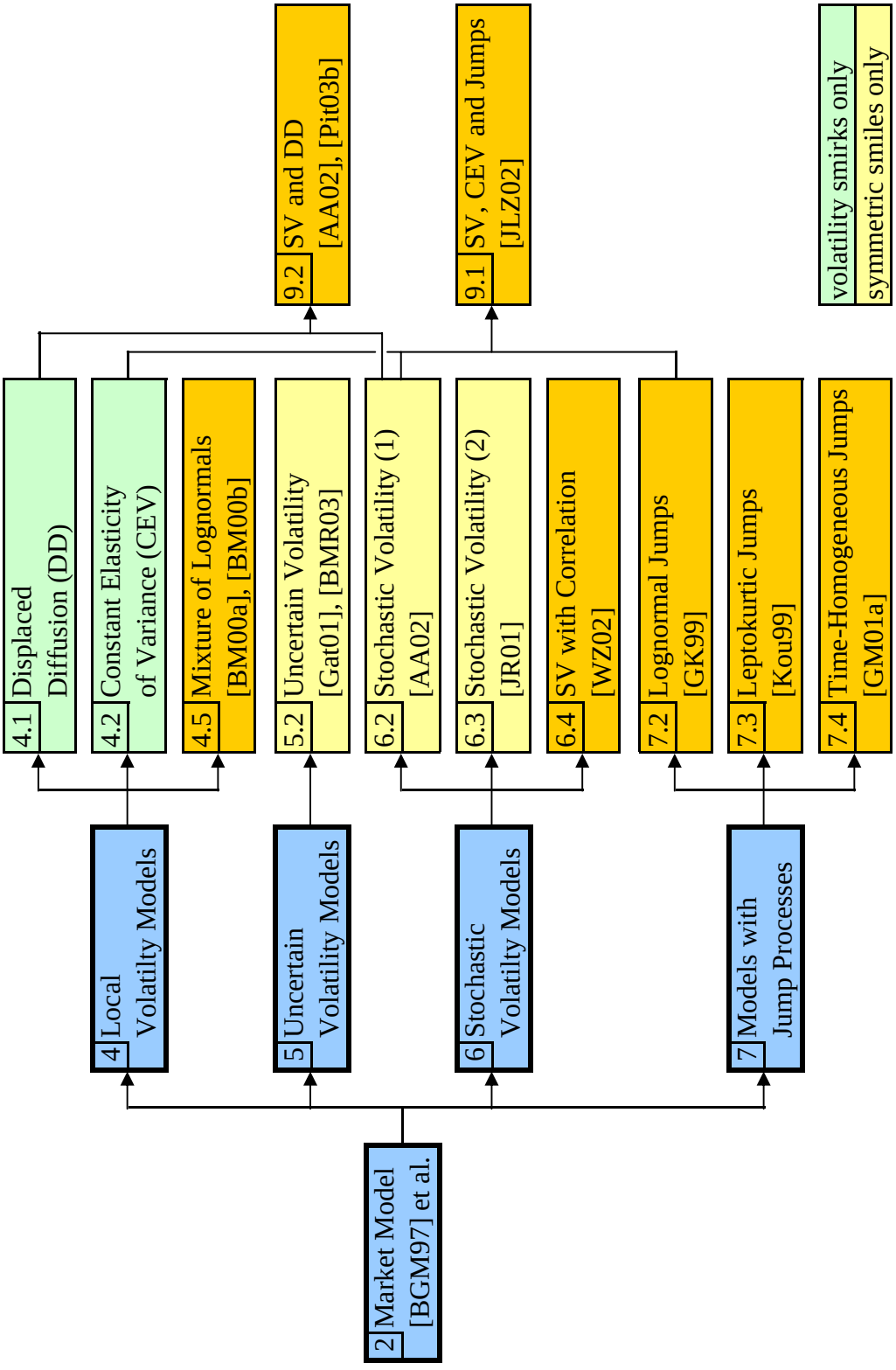

Figure 3.5: *Model Overview*

Part II

Basic Models

Chapter 4

Local Volatility Models

Having defined the LIBOR market model and set up the desired features of an extended model, the four different possible basic models have already been briefly introduced at the end of the previous part. In the chapters of Part II they will be presented and tested. Even if none of those models alone will be able to improve the LIBOR market model such that it fits the whole term structure of volatility smiles, they are essential ”building blocks” for generating more comprehensive and advanced models.

As a first approach for fitting a single caplet or swaption smile, the underlying assumption for Black's formulæ of lognormally distributed interest rates with state-independent volatilities of the logarithm of the forward rates is given up. This leads in the terminal measure to the

General Forward Rate Evolution:

$$\frac{\mathrm{d}L_i(t)}{L_i(t)} = \sigma_i(t;L_i(t))\,\mathrm{d}z_i \tag{4.1}$$

with $\sigma_i(t;L_i(t))$ still being a deterministic function but not only time-dependent but also dependent upon the level of the forward rate.

The articles by [Dup94] and [DK94] showed that under the assumption of having a complete volatility surface for all strikes and all expiries there exists exactly

one diffusion process that leads to the market implied distributions of the forward rates.[1] Dupire could furthermore derive an exact solution for computing this local volatility function from market prices. However, since there are not all caplet prices for every expiry and every strike available and those quoted prices would be too noisy for computing exact local volatility functions, one usually parameterizes these functions.

In the following sections different parametrizations for $\sigma_i(t;L_i(t))$ shall be presented, starting with very basic models like displaced diffusion (DD) or constant elasticity of variance (CEV) and leading to a more advanced model.

4.1 Displaced Diffusion (DD)

At the displaced diffusion approach first presented in [Rub83] one no longer assumes the lognormal distribution of the forward rates but of the variables

$$X_i(t) = L_i(t) + \alpha_i \tag{4.2}$$

with $X_i(t)$ evolving under its associated terminal measure according to:

$$\frac{\mathrm{d}X_i(t)}{X_i(t)} = \sigma_{i,\alpha_i}(t)\mathrm{d}z_i.$$

This has the side effect that exactly the same simulation mechanism for this $X_i(t)$ can be applied as has been in the basic model for the forward rate $L_i(t)$.

Re-substituting $X_i(t)$ with $L_i(t)+\alpha_i$ leads to the process of the forward rate:

$$\frac{\mathrm{d}(L_i(t)+\alpha_i)}{L_i(t)+\alpha_i} = \frac{\mathrm{d}L_i(t)}{L_i(t)+\alpha_i} = \sigma_{i,\alpha_i}(t)\mathrm{d}z_i. \tag{4.3}$$

Therefore, in the notation of the general forward rate evolution proposed at the

[1] See [Gat03], p. 6-12.

beginning of the chapter one can express the

Forward Rate Evolution:

$$\frac{\mathrm{d}L_i(t)}{L_i(t)} = \sigma_{i,DD}(t;L_i(t))\,\mathrm{d}z_i \tag{4.4}$$

with

$$\sigma_{i,DD}(t;L_i(t)) = \frac{L_i(t)+\alpha_i}{L_i(t)}\sigma_{i,\alpha_i}(t). \tag{4.5}$$

The lognormal distribution of $X_i(t)$ can be used straightforward to find an exact and especially easy solution for pricing caplets. This certainly is one of the main reasons for the success of this model. The payoff of the caplet in time T_{i+1} equals:

$$\text{Payoff(Caplet)}_{T_{i+1}} = NP\delta\left[L_i(T_i)-K\right]^+ = NP\delta\left[X_i(T_i)-(K+\alpha_i)\right]^+.$$

Hence, while $\alpha_i > -K$ one can easily determine the

Caplet Pricing Formula:

$$\text{Caplet}(0,T_i,\delta,NP,K,\sigma_{i,\alpha_i};\alpha_i) = NP\delta P(0,T_{i+1})\,\text{Bl}\left(K+\alpha_i,L_i(0)+\alpha_i,\sigma_{i,\alpha_i}\sqrt{T_i}\right) \tag{4.6}$$

where

$$\sigma_{i,\alpha_i} = \sqrt{\frac{\int_0^{T_i}\sigma_{i,\alpha_i}^2(u)\mathrm{d}u}{T_i}}.$$

The implied Black volatility ($\hat{\sigma}_i(K)$) can be calculated numerically by matching these prices:

$$\text{Bl}\left(K,L_i(0),\hat{\sigma}_i(K)\sqrt{T_i}\right) = \text{Bl}\left(K+\alpha_i,L_i(0)+\alpha_i,\sigma_{i,\alpha_i}\sqrt{T_i}\right).$$

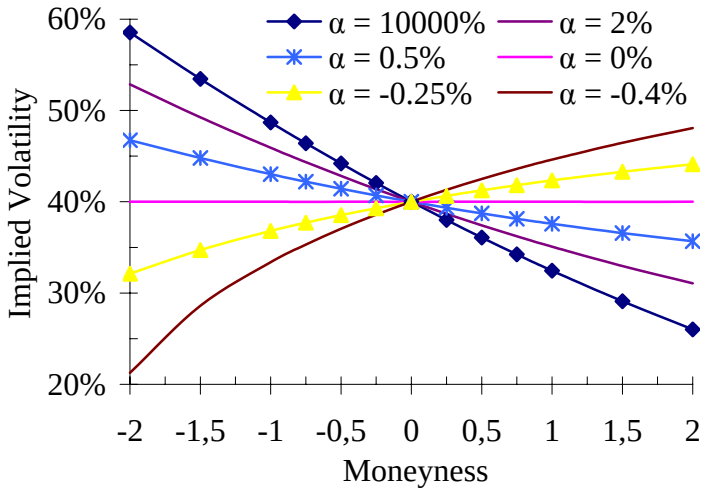

Figure 4.1: *Comparison of implied volatility smiles of the forward rate* $L_1(0) = 1\%$ *for different* α_1 *with the same ATM implied volatility* $\hat{\sigma}_1(0) = 40\%$.

These implied Black volatilities as a function of the diffusion displacement α_i and the moneyness M are compared in Figure 4.1. There it can be seen clearly that for $\alpha_i \to \infty$ arbitrary steep volatility smiles cannot be simulated.

Since $X_i(t)$ is lognormally distributed this variable can take values from $(0,\infty)$ or from $(-\infty,0)$. This leads to:

$$\begin{aligned} L_i(t) &\in (-\alpha_i,\infty) \quad \text{if } L_i(0) < -\alpha_i, \\ L_i(t) &\in (-\infty,-\alpha_i) \quad \text{if } L_i(0) > -\alpha_i. \end{aligned}$$

That means that $\alpha_i > 0$ or $\alpha_i < -L_i(0)$ imply a positive probability for interest rates becoming negative. When calibrating this model to market data usually a positive value for α_i provides the best fit. This unrealistic behavior is the biggest drawback of the displaced diffusion approach.

Calibration Quality w. r. t. a Fixed Maturity

When calibrating the displaced diffusion approach to caplet volatility smiles one can realize in Figure 4.2 two drawbacks of this model. First, the forward rate dependent parameter α_i alone is not sufficient for providing a good fit to the whole

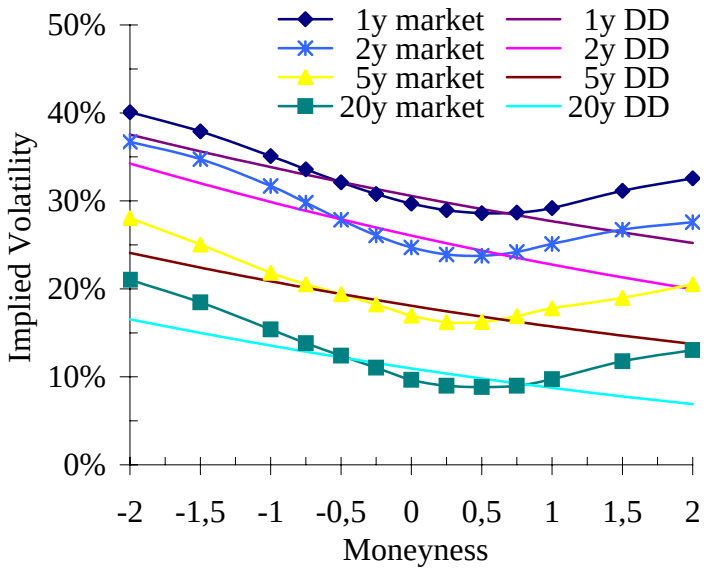

Figure 4.2: *The fit across moneynesses to the market implied caplet volatilities with the displaced diffusion model for different expiries.* $\alpha_1 = 6.6\%$, $\alpha_2 = 13.4\%$, $\alpha_5 = 13.9\%$ *and* $\alpha_{20} = 768\%$.

volatility smile as this parameter leads to an almost straight line for the volatility smile. Second, the calibration results are very unstable since a set of moneynesses different from (3.2) would imply different weights for the in, at and out of the money parts of the volatility for the calibration procedure and therefore lead to different parameters α_i.

4.2 Constant Elasticity of Variance (CEV)

Another very basic model that can generate volatility smirks for caplets is the CEV model. For the LIBOR market model it was developed in [AA97] building on the model in [CR76] for equity derivatives.

In this model the forward rate $L_i(t)$ evolves in the terminal measure according to:

$$\mathrm{d}L_i(t) \;=\; [L_i(t)]^{\gamma_i}\,\sigma_{i,\gamma_i}\,\mathrm{d}z_i \tag{4.7}$$

with $0 \leq \gamma_i \leq 1$.

The lognormal ($\gamma_i = 1$), the square-root ($\gamma_i = \frac{1}{2}$) and the normal ($\gamma_i = 0$) distribution are special cases of this model.

For presenting the local volatility function more clearly a different notation of the

Forward Rate Evolution: ⌝

$$\frac{\mathrm{d}L_i(t)}{L_i(t)} = \sigma_{i,CEV}(t;L_i(t))\mathrm{d}z_i \tag{4.8}$$

with

$$\sigma_{i,CEV}(t;L_i(t)) = [L_i(t)]^{\gamma_i - 1}\sigma_{i,\gamma_i} \tag{4.9}$$

is preferable. ⌟

At the first sight this CEV model seems more appealing than the previously discussed DD model, as it prohibits interest rates from becoming negative (for $\gamma_i > 0$). However, for $0 < \gamma_i < 1$ there is a positive probability of the forward rate $L_i(t)$ attaining 0.[2] For $\gamma_i \geq \frac{1}{2}$ this is an absorbing barrier of the stochastic differential equation. As has been shown in [BS96], however, the process does not have a unique solution for $0 < \gamma_i < \frac{1}{2}$. To ensure a well-behaving process the absorbing boundary condition at 0 is added. Therefore for all $0 < \gamma_i < 1$ there is a positive probability of $L_i(t)$ reaching the "graveyard state" 0. This is a disadvantage of this model, but certainly easier to neglect than possible negative interest rates in the DD model.

The simulation of the evolution of the forward rates in a discretized timeframe is unlike in the basic LIBOR market model or in the displaced diffusion extension no longer exact, that means small time steps have to be used for simulating the forward rates. However, even with extremely small time steps a naive implementation of this process can lead to negative interest rates (and in the following step to an error when trying to compute $L_i(t)^{\gamma_i}$).

[2] See [AA97], p. 8f, 34f.

For example in the case of the square-root process discretized with the Euler scheme:

$$L_i(t+\Delta t) \;=\; L_i(t) + \sqrt{L_i(t)}\sigma_{i,1/2}\Delta z_i \tag{4.10}$$

this problem can be solved by using $\sqrt{|L_i(t)|}$ instead of $\sqrt{L_i(t)}$, but this "mirroring" of the process is not exact. A further improvement of the accuracy of the process can be obtained with the Milstein scheme instead of the Euler scheme:[3]

$$\begin{aligned} L_i(t+\Delta t) &= L_i(t) + \sqrt{L_i(t)}\sigma_{i,1/2}\,\Delta z_i + \frac{1}{4}\sigma_{i,1/2}^2\left((\Delta z_i)^2 - \Delta t\right) \\ &= L_i(t) + \sqrt{L_i(t)}\sigma_{i,1/2}\,x_i\sqrt{\Delta t} + \frac{1}{4}\sigma_{i,1/2}^2\left(x_i^2 - 1\right)\Delta t \end{aligned}$$

with x_i being a $N(0,1)$ distributed random variable.

In this model one can use for all $\gamma \in (0,1)$ an exact

Caplet Pricing Formula:

$$\begin{aligned} &\text{Caplet}\,(0,T_i,\delta,NP,K,\sigma_i;\gamma_i) \\ &\quad= \; NP\,\delta\,P(0,T_{i+1})\left(L_i(0)\left[1-\chi^2(a,b+2,c)\right] - K\chi^2(c,b,a)\right) \end{aligned} \tag{4.11}$$

where

$$a \;=\; \frac{K^{2(1-\gamma_i)}}{(1-\gamma_i)^2\sigma_i^2 T_i}, \qquad b \;=\; \frac{1}{1-\gamma_i}, \qquad c \;=\; \frac{L_i(0)^{2(1-\gamma_i)}}{(1-\gamma_i)^2\sigma_i^2 T_i}.$$

According to [Din89] for the χ^2 distribution there exists a Second Order Wiener Germ approximation:[4]

$$\chi^2(x,\nu,\xi) \;\cong\; \begin{cases} \Phi(\sqrt{S}) & s > 1 \\ \frac{1}{2} & s = 1 \\ \Phi(-\sqrt{S}) & s < 1 \end{cases} \tag{4.12}$$

[3] See [Fri04], p. 79f.
[4] See [PR00], p. 3f.

where

$$\begin{aligned} s &= \frac{\sqrt{1+4x\mu/\nu}-1}{2\mu}, \\ S &= \nu(s-1)^2\left(\frac{1}{2s}+\mu-\frac{h(1-s)}{s}\right)-\ln\left[\frac{1}{s}-\frac{2}{s}\frac{h(1-s)}{1+2\mu s}\right]+\frac{2}{\nu}B(s), \\ h(y) &= \frac{1}{y}\left[\left(\frac{1}{y}-1\right)\ln[1-y]+1\right]-\frac{1}{2} \end{aligned}$$

with

$$\begin{aligned} \mu &= \frac{\xi}{\nu}, \\ B(s) &= -\frac{3(1+4\mu s)}{2(1+2\mu s)^2}+\frac{5(1+3\mu s)^2}{3(1+2\mu s)^3}+\frac{2(1+3\mu s)}{(s-1)(1+2\mu s)^2} \\ &\quad +\frac{3\eta}{(s-1)^2(1+2\mu s)}-\frac{(1+2h(\eta))\,\eta^2}{2(s-1)^2(1+2\mu s)}, \\ \eta &= \frac{1+2\mu s-2h(1-s)-s-2\mu s^2}{1+2\mu s-2h(1-s)}. \end{aligned}$$

Possible volatility smiles from this model are presented in Figure 4.3. There it can be seen that similar to the Figure 4.1 for the DD model only volatility smirks can be generated and that there is a limit for the steepness of the volatility smile created.

The absorption of the forward rate process in 0 is empirically questionable but even more might have undesirable effects on the pricing of exotic options.[5] To avoid this problem the limited CEV (= LCEV) model has been introduced. The positive probability of reaching 0 is avoided by introducing ε which is a small positive fixed number and choosing the local volatility function as:[6]

$$\sigma_{i,LCEV}(t;L_i(t)) = [\max\{\varepsilon,L_i(t)\}]^{\gamma_i-1}\sigma_{i,\gamma_i}. \tag{4.13}$$

This leads to the fact that the caplet pricing formula in equation (4.11) is no longer exactly valid but can still be used as an approximation in the calibration process.

[5] See [BM01], p. 276.
[6] See [AA97], p. 14.

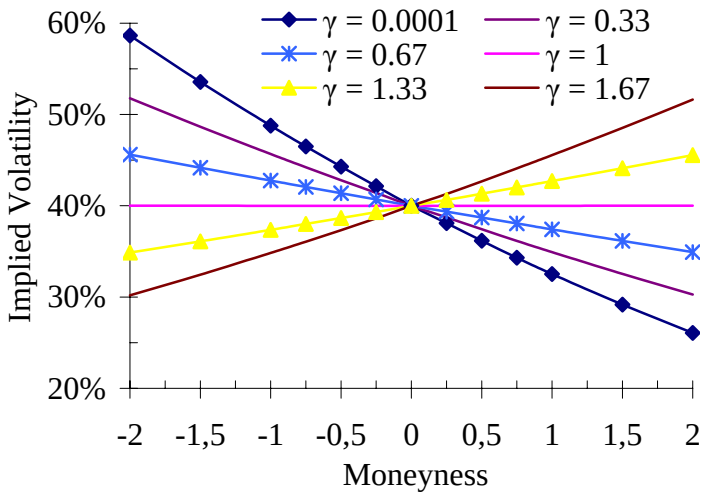

Figure 4.3: *Comparison of implied volatility smiles of the forward rate* $L_1(0) = 1\%$ *for different* γ_1 *with the same ATM implied volatility* $\hat{\sigma}_1(0) = 40\%$.

Calibration Quality w. r. t. a Fixed Maturity

When calibrating this CEV model to market data one can see the same drawbacks of the model as for the DD model. First, the parameter γ_i is not sufficient for providing a good fit for market data. Second, the calibration is very dependent upon the set of moneynesses the model is calibrated to.

4.3 Equivalence of DD and CEV

In the two previous sections the calibration results for the DD and CEV model have been presented. Obviously, both models have similar calibration properties. In fact, as has been shown in [Mar99], these two models are almost equivalent.

Setting in equation (4.2)

$$\alpha_i = \frac{L_i(0)(1-\beta_i)}{\beta_i} \tag{4.14}$$

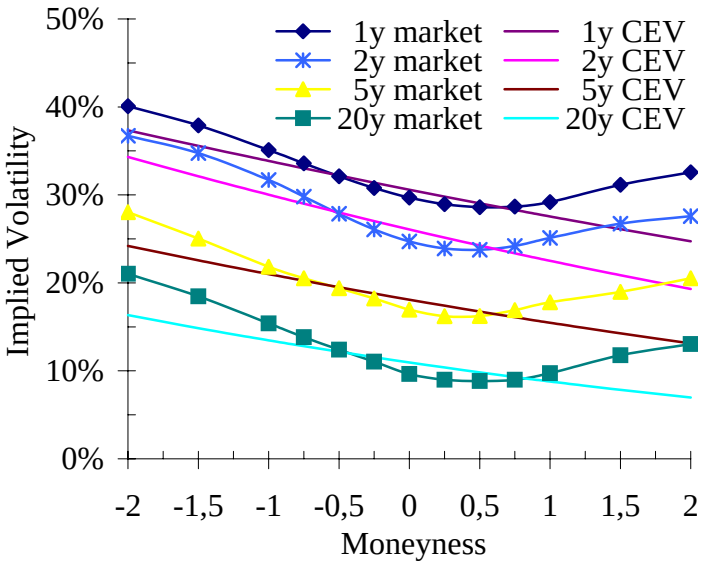

Figure 4.4: *The fit across moneynesses to the market implied caplet volatilities with the constant elasticity of variance model for different expiries.* $\gamma_1 = 0.31$, $\gamma_2 = 0.18$, $\gamma_5 = 0.20$ *and* $\gamma_{20} = 0.03$.

and inserting equation (4.14) in (4.3) gives:

$$\begin{aligned} \mathrm{d}L_i(t) &= \left[L_i(t) + \frac{L_i(0)(1-\beta_i)}{\beta_i}\right]\sigma_{i,\alpha_i}(t)\mathrm{d}z_i \\ &= \left[\beta_i L_i(t) + (1-\beta_i)L_i(0)\right]\frac{\sigma_{i,\alpha_i}(t)}{\beta_i}\mathrm{d}z_i. \end{aligned} \tag{4.15}$$

Hence, one can write for the displaced diffusion model an alternative

Forward Rate Evolution:

$$\frac{\mathrm{d}L_i(t)}{L_i(t)} = \sigma_{i,DD}(t;L_i(t))\mathrm{d}z_i \tag{4.16}$$

with

$$\sigma_{i,DD}(t;L_i(t)) = \left[\beta_i + (1-\beta_i)\frac{L_i(0)}{L_i(t)}\right]\sigma_{i,\beta_i}. \tag{4.17}$$

Using this notation, for $\beta_i = 1$ the forward rates are exactly lognormally dis-

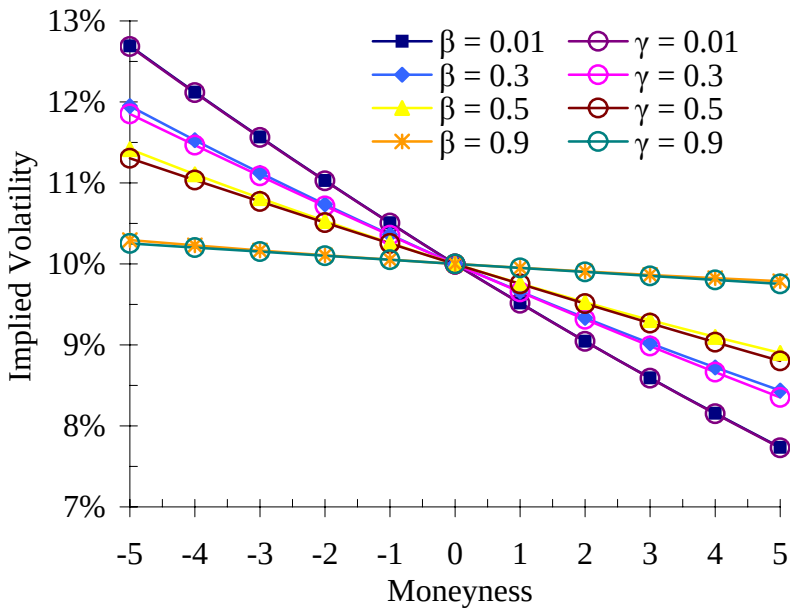

Figure 4.5: *Implied caplet volatilities for different values of* β_1 *(DD) and* γ_1 *(CEV) with the same ATM volatility* $\hat{\sigma}_1(0) = 10\%$.

tributed, for $\beta_i = \frac{1}{2}$ they almost follow the square-root process and for $\beta_i = 0$ they are normally distributed. As can be seen in Figure 4.5, setting $\gamma_i = \beta_i$ leads to very similar distributions and volatility skews for the DD and the CEV model. Since for $\beta_i = \gamma_i = 0$ and $\beta_i = \gamma_i = 1$ the two models are exactly equivalent, the small implied volatility differences are biggest for values between 0 and 1.[7]

This alternative notation with β_i has some advantages over the original notation with α_i. First, the normal distribution can be expressed exactly, not only approximated for $\alpha_i \to \infty$. Second, while in (4.15) β_i is usually chosen to be $\beta_i \in [0,1]$ this equation can also be used for larger domains of β_i. Negative values of β_i might be especially desirable. It has to be noted that for negative values of β_i a state $\hat{L}_i$ exists where:

$$\beta_i \hat{L}_i + (1-\beta_i) L_i(0) \;=\; 0.$$

This state has the unrealistic behavior of being a fix point, i.e. a forward rate with

[7] See [Reb02], p. 356-359.

the actual value $\hat{L}_i = \left(1 - \frac{1}{\beta_i}\right) L_i(0)$ cannot leave this state. However, as this state is not attainable it is sufficient to ensure β_i is a sufficiently small number.[8] Third, the volatility σ_{i,β_i} has the same magnitude independent of the chosen β_i. The only disadvantage is that the exact lognormal rolling out of the forward rate is no longer possible.

Comparing the CEV and the DD model, the CEV model lends itself more to an intuitive (and exact) interpretation regarding the normal, square-root and lognormal distribution it embraces. Furthermore, interest rates cannot get negative. The problems with the absorbing barrier at 0 and the better tractability of the DD model usually lead to the preference for evolving the forward rates over time with a displacement. Independent of the choice of the model as the biggest drawback remains the inability of both models to fit an existing volatility smile as these two basic models are only able to generate volatility smirks.

4.4 General Properties

The class of local volatility models is very flexible. The volatility $\sigma_i(t; L_i(t))$ can be parametrized in different ways, for example:[9]

$$\sigma_i(t; L_i(t)) \;=\; 1 - \frac{L_i(t)}{u_i} \tag{4.18}$$

with $u_i > 0$. In this model 0 is the lower and u_i is the upper boundary for the forward rate. Both boundaries as has been shown in [Ing97] are unattainable. Generally, to avoid negative interest rates one has to assure the condition

$$L_i(t)\sigma_i(t; L_i(t)) \;=\; 0 \qquad \text{for} \qquad L_i(t) \to 0 \tag{4.19}$$

is fulfilled.[10]

[8] This effect is an exact consequence of the domain $(-\alpha_i, \infty)$ in the first definition of the displaced diffusion model. See also [Pit03b], p. 5.

[9] For an overview see [Zuh02], p. 6-11.

[10] See [AA02], p. 163.

Other specifications for $\sigma_i(t;L_i(t))$ enable local volatility models even not only to generate volatility smirks but also volatility smiles. With an increasing number of parameters one is able to fit the market implied volatility smile better and better. Especially in lattice methods, e.g. Markov-Functional models[11], this way of smile modeling is widely used.

The main problem of local volatility models is that the generated smile will be non-stationary, i.e. the smile would not move when the interest rate moves. Therefore, such a model might be able to fit a certain volatility smile extremely well but might fail in providing a good estimate of future re-hedging costs. This issue will be discussed further in Part III.

4.5 Mixture of Lognormals

Another very different local volatility model was presented in [BM00a]. In this approach the evolution of interest rates does not follow a single lognormal distribution but a mixture of N lognormal densities with volatilities $\sigma_{i,j}(t)$ and positive weights $p_{i,j}$ under the condition $\sum_{j=1}^{N} p_{i,j} = 1$.

These assumptions lead in the terminal measure to the

Forward Rate Evolution:[12]

$$\frac{\mathrm{d}L_i(t)}{L_i(t)} = \sigma_{i,MoL}(t;L_i(t))\mathrm{d}z_i \tag{4.20}$$

with

$$\sigma_{i,MoL}(t;L_i(t)) = \sqrt{\frac{\sum_{j=1}^{N} p_{i,j}\frac{\sigma_{i,j}^2(t)}{\sigma_{i,j}}\exp\left\{-\frac{1}{2\sigma_{i,j}^2 T_i}\left(\ln\left[\frac{L_i(t)}{L_i(0)}\right]+\frac{1}{2}\sigma_{i,j}^2 T_i\right)^2\right\}}{\sum_{j=1}^{N} p_{i,j}\frac{1}{\sigma_{i,j}}\exp\left\{-\frac{1}{2\sigma_{i,j}^2 T_i}\left(\ln\left[\frac{L_i(t)}{L_i(0)}\right]+\frac{1}{2}\sigma_{i,j}^2 T_i\right)^2\right\}}} \tag{4.21}$$

[11] See [HKP00].
[12] See [BM01], p. 277-280.

where

$$\sigma_{i,j} \;=\; \sqrt{\frac{\int_0^{T_i}\sigma_{i,j}^2(u)\,\mathrm{d}u}{T_i}}.$$

For these dynamics one can write this easily computable

Caplet Pricing Formula:

$$\text{Caplet}\left(0,T_i,\delta,NP,K,\overrightarrow{\sigma}_i;\overrightarrow{p}_i\right) \;=\; NP\,\delta P(0,T_{i+1})\sum_{j=1}^{N} p_{i,j}\,\text{Bl}\left(K,L_i(0),\sigma_{i,j}\sqrt{T_i}\right). \tag{4.22}$$

The implied volatilities $\hat{\sigma}_i(M)$ for the moneyness M as defined in (3.1) are approximated via:

$$\hat{\sigma}_i(M) \;=\; \hat{\sigma}_i(0)\left\{1+\frac{M^2}{2}\sum_{j=1}^{N} p_{i,j}\left[\frac{\hat{\sigma}_i(0)}{\sigma_{i,j}}\mathrm{e}^{\frac{T_i}{8}\left(\hat{\sigma}_i^2(0)-\sigma_{i,j}^2\right)}-1\right]\right\}+O\left(M^4\right) \tag{4.23}$$

where the implied volatility for $M=0$ is given explicitly:

$$\hat{\sigma}_i(0) \;=\; \frac{2}{\sqrt{T_i}}\Phi^{-1}\left(\sum_{j=1}^{N} p_j\Phi\left(\frac{\sigma_{i,j}\sqrt{T_i}}{2}\right)\right). \tag{4.24}$$

The border cases are given by:[13]

$$\lim_{M\to\pm\infty}\hat{\sigma}_i(M)=\max\{\sigma_{i,1},\ldots,\sigma_{i,N}\}. \tag{4.25}$$

Calibration Quality w. r. t. a Fixed Maturity

When calibrating this model usually three different volatilities are sufficient. For $p_{i,j}=\frac{1}{3}$ and $\sigma_{i,2}=\hat{\sigma}_i(0)$ the other two volatilities can be quoted with a single

[13] See [Gat01], p. 3.

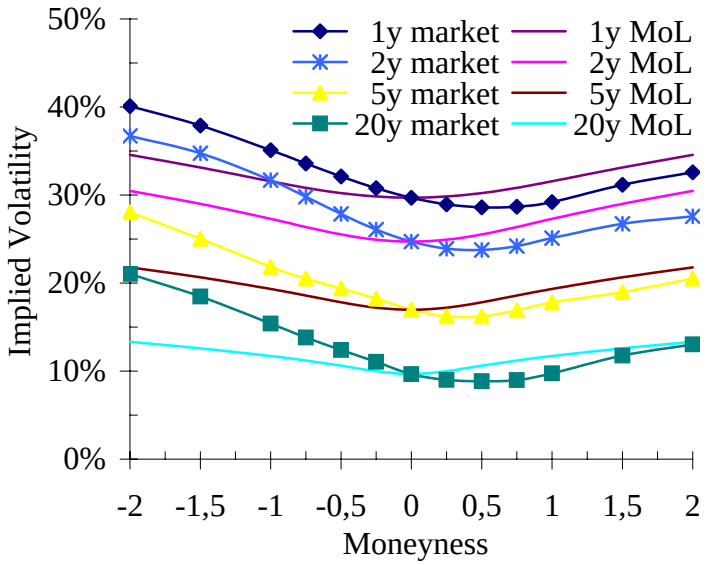

Figure 4.6: *The fit across moneynesses to the market implied caplet volatilities with the mixture of lognormals model for different expiries.* $\theta_1 = 57\%$, $\theta_2 = 45\%$, $\theta_5 = 36\%$ *and* $\theta_{20} = 19\%$.

parameter θ_i as the most important implied volatility is the ATM-volatility $\hat{\sigma}_i(0)$. To retain this volatility one can compute for a chosen $\sigma_{i,1} = \theta_i \sigma_{i,2}$ using (4.24):

$$\sigma_{i,3} = \frac{2}{\sqrt{T_i}} \Phi^{-1}\left(2\Phi\left(\frac{\sigma_{i,2}\sqrt{T_i}}{2}\right) - \Phi\left(\frac{\theta_i \sigma_{i,2}\sqrt{T_i}}{2}\right)\right). \tag{4.26}$$

The further generated Black implied volatilities can be calculated with equation (4.23). This procedure is especially noteworthy since it enables to separate the steps of first calibrating the ATM-volatilities with the plain-vanilla caplets and swaptions and then building on that calibrating the different smiles. When comparing the quality of the fit to a single volatility smile with other models, however, the calibration should not be carried out in this way as the result might clearly penalize this model as it would not have been calibrated to minimize the loss function computed as described in Section 3.4.

Calibrating this model with the one free parameter θ_i to market data leads to exactly symmetric smiles and hence is not able to fit market data having a volatility skew as can be seen in Figure 4.6 and even more clearly in Figure B.5.

This drawback of the basic mixture of lognormals model led to an extension that has been proposed in [BM00b]. Combining the "mixture of lognormals"-approach with another local volatility model, the displaced diffusion technique, provides a better fit to caplet volatilities as it enables the model to have the minimum implied volatility at a strike different from ATM and thereby generating the usual volatility skew in the market.[14]

This leads in the terminal measure to a shifted (compared to (4.20))

Forward Rate Evolution:

$$\frac{\mathrm{d}L_i(t)}{L_i(t)} = \sigma_{i,MoL,DD}(t;L_i(t))\mathrm{d}z_i \tag{4.27}$$

where

$$\sigma_{i,Mol,DD}(t;L_i(t)) = \frac{L_i(t)+\alpha_i}{L_i(t)}\sigma_{i,MoL}(t;L_i(t)+\alpha_i). \tag{4.28}$$

The resulting

Caplet Pricing Formula:

$$\begin{aligned}&\text{Caplet}\left(0,T_i,\delta,NP,K,\overrightarrow{\sigma_i};\overrightarrow{p}_i,\alpha_i\right)\\ &= NP\,\delta P(0,T+\delta)\sum_{j=1}^{N} p_{i,j}\,\text{Bl}\left(K+\alpha_i,L_i(0)+\alpha_i,\sigma_{i,j}\sqrt{T_i}\right).\end{aligned} \tag{4.29}$$

for the extension is therefore a blend of the basic "mixture of lognormals"-model and the displaced diffusion formula.

For a formula for the implied Black volatility $\hat{\sigma}_i(M)$, see [BM01], p. 281.

[14] See [BM01], p. 282.

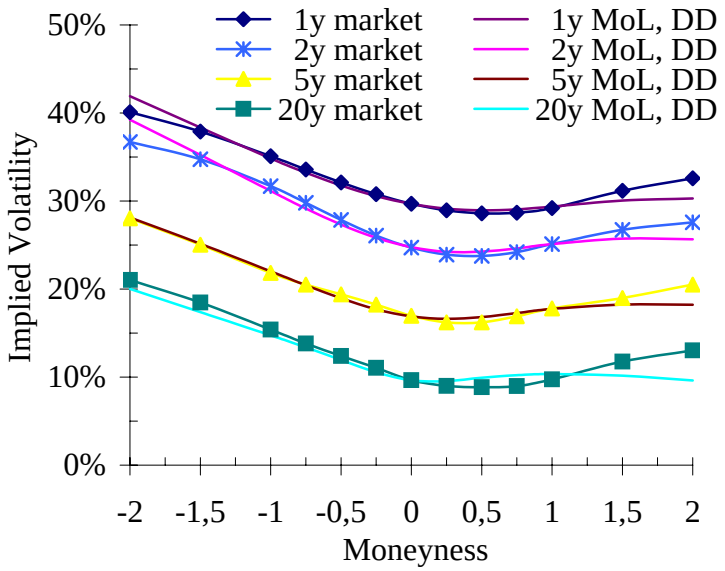

Figure 4.7: *The fit across moneynesses to the market implied caplet volatilities with the extended mixture of lognormals model for different expiries.* $\beta_1 = 35\%$, $\tilde{\sigma}_{1,1} = 18\%$, $\tilde{\sigma}_{1,2} = 41\%$, $\beta_2 = 27\%$, $\tilde{\sigma}_{2,1} = 12\%$, $\tilde{\sigma}_{2,2} = 37\%$, $\beta_5 = 31\%$, $\tilde{\sigma}_{5,1} = 7\%$, $\tilde{\sigma}_{5,2} = 26\%$, $\beta_{20} = 0.4\%$, $\tilde{\sigma}_{20,1} = 2\%$ *and* $\tilde{\sigma}_{20,2} = 17\%$.

Calibration Quality w. r. t. a Fixed Maturity

For calibrating this model only two lognormal densities were chosen. For clearer quotation all parameters are given level-adjusted via:

$$\begin{aligned} \beta_i &= \frac{L_i(0)}{L_i(0)+\alpha_i}, \\ \tilde{\sigma}_{i,j} &= \sigma_{i,j}\frac{L_i(0)+\alpha_i}{L_i(0)}. \end{aligned}$$

The fit both to € (Figure 4.7) and US-$ (Figure B.6) caplet volatility smiles is extremely better than with the previous models since this extended mixture of lognormals model can generate smiles with the minimum implied volatility at almost every reasonable moneyness.

4.6 Comparison of the Different Local Volatility Models

In this chapter different local volatility models have been introduced. The very basic displaced diffusion and constant elasticity of variance approaches have only one free parameter and hence are not very flexible regarding the generated volatility smiles. However, especially the DD model due to its extremely good tractability considering both mathematical and simulation properties is a candidate for enhancing other models.

A first example is the mixture of lognormals model that can in the basic version only generate symmetric volatility smiles. Combing it with displaced diffusion leads to a local volatility model that is able to fit market implied volatilities very well while having an easy Black-based caplet formula and a straightforward simulation mechanism.

All possible local volatility models share the drawback of a non-stationary volatility smile. That is when interest rates move the smile does not move. Therefore, the models are not able to produce self-similar smiles, i.e. future volatility smiles do not look similar to the current volatility smile independent of the future level of interest rates. This drawback while being inevitable when valuing derivatives in a one-dimensional lattice is avoidable in Monte Carlo simulations. Hence, other extensions of the LIBOR market model should offer more realistic market dynamics.

Chapter 5

Uncertain Volatility Models

While in the previous chapter local volatility (i.e. deterministic volatility) models have been discussed, in this and the following chapter non-deterministic volatility models shall be presented. The assumption of the local volatility models has been that the volatility at a certain time in future is a function of the level of the forward rate at that time. When assessing historical market data, however, this exact dependency cannot be observed. The volatility seems to fluctuate quite independently making future volatility non-deterministic when rolling out forward rates in the model. Generally, there are two possible ways to model this fluctuation. The easiest approach is to assume that volatility of today will jump shortly after today to one of several possible scenarios (= volatility levels). The advanced approach of volatility having its own stochastic process will be discussed in the next chapter.

Uncertain volatility models were presented in [Gat01] and [BMR03] suggesting in the terminal measure the following

Forward Rate Evolution:

$$\frac{\mathrm{d}L_i(t)}{L_i(t)} = \begin{cases} \sigma_i \, \mathrm{d}z_i & t \in [0, \varepsilon] \\ \sigma_i(t) \, \mathrm{d}z_i & t > \varepsilon \end{cases} \tag{5.1}$$

with $\sigma_i(t)$ being a discrete random variable, known for $t \geqq \varepsilon$, independent of the Wiener process dz, that is drawn at time ε. The volatility $\sigma_i(t)$ is drawn out of a

finite number of possible volatility scenarios:

$$(t \mapsto \sigma_i(t)) \;=\; \begin{cases} (t \mapsto \sigma_{i,1}(t)) & \text{with probability } p_{i,1} \\ (t \mapsto \sigma_{i,2}(t)) & \text{with probability } p_{i,2} \\ \quad\vdots & \qquad\vdots \\ (t \mapsto \sigma_{i,N}(t)) & \text{with probability } p_{i,N} \end{cases}$$

where $p_{i,j}$ is strictly positive with $\sum_{j=1}^{N} p_{i,j} = 1$. ⌟

The resulting process leads to a mixture of lognormal densities and therefore to the

Caplet Pricing Formula: ⌝

$$\text{Caplet}\left(0, T_i, \delta, NP, K, \vec{\sigma}_i; \vec{p}_i\right) \;=\; NP\,\delta P(0, T_{i+1}) \sum_{j=1}^{N} p_{i,j}\,\text{Bl}\left(K, L_i(0), \sigma_{i,j}\sqrt{T_i}\right). \tag{5.2}$$

with

$$\sigma_{i,j} \;=\; \sqrt{\frac{\int_0^{T_i} \sigma_{i,j}^2(u)\,\mathrm{d}u}{T_i}}$$

where $\sigma_{i,j}(t)$ is set to σ_i for $t < \varepsilon$. ⌟

Since this pricing formula is the same pricing formula as presented in Section 4.5 the same properties for implied volatilities as shown in equations (4.23) to (4.25) are valid.

Calibration Quality w. r. t. a Fixed Maturity

Due to the exact equality of pricing simple exotic derivatives as in the local volatility model the fit to caplets in both markets is the same as already shown in Figures 4.6 and B.5. To improve this fit one could again mix this model with the displaced diffusion approach as has been done in (4.29) to obtain a good fit to market data as shown in Figures 4.7 and B.6.

In spite of these equalities, however, there are a two big differences between those two models with the exact same pricing formula for caplets:[1]

- Exotic option prices can in the uncertain volatility model just be calculated as a mixture of prices for only time-dependent volatilities while in the local volatility model always numerics are needed to price more complex derivatives.
- The proposed dynamics for the forward rate is different. In the local volatility model it will be dependent upon the level of the forward rate while in the uncertain volatility model the future will be independent of this level. This difference will be discussed at length in Chapter 8.

[1] See [BMR03], p. 5.

Chapter 6

Stochastic Volatility Models

After the very basic uncertain volatility model in this chapter stochastic volatility models shall be presented. At the beginning models for equity options are introduced, after that two very basic models are discussed leading to an advanced model that also can incorporate the skew in stochastic volatility models.

6.1 General Characteristics and Problems

For modeling a continuous movement of the volatility again – as for the stock price or the forward rate – an Ito diffusion can be used. Several stochastic volatility models with different process for the volatility/variance have been proposed e.g. in [HW87], [Hes93] and [SZ98]. The problem there is to choose an appropriate process the volatility or variance should follow. This can hardly be determined as volatility is not directly observable in the market and has to be computed by time series analysis (= historical volatility) or market prices of options (= implied volatility). Unfortunately, these two ways of extracting volatilities from market data almost always leads to very different values for each stock, index or forward rate. While it has been found that different models with stochastic volatility and

correlation perform equally well for most options,[1] mathematical properties are also very important to ensure correct pricing of all options in the market.[2]

The importance of the stochastic volatility is most obvious when assessing the hedging activities and margins of the traders. In deterministic volatility models option prices are computed putting a probability of zero to volatilities different from the calibrated one. Therefore, traders have to shift the volatilities manually to calculate the risk of changing volatilities and to determine the correct hedge for that. Since this hedge is only correct in a static sense traders tend to avoid or to charge for options where this risk is not in their favor.[3]

Besides this Ito diffusion another possibility of modeling volatilities that change their level again and again in future are jumps of the volatility level.[4] Compared to an Ito diffusion as driving process for the volatility the main drawback is reduced tractability and less intuitive parameters. As these Ito diffusions – as will be shown in the following sections – are already producing an acceptable fit to smiles in the market this line of modeling shall not be pursued further in this thesis.

6.2 Andersen, Andreasen (2002)

There have been many approaches for pricing derivatives in a stochastic volatility context. The work in [Hes93] was a milestone as for the first time one did not have to use approximations to solve the partial differential equations with finite difference schemes or to use other inefficient methods but could compute an exact solution derived via Fourier transformation. Building on this original model and further work in [ABR01] a model for forward and swap rates with an exact solution for caplets and swaptions was presented in [AA02].[5]

[1] See [BS99], p. 22f.
[2] See also [AP04].
[3] See [Reb02], p. 370.
[4] See [Nai93], p. 1972.
[5] In this section only the stochastic volatility part of the model suggested in [AA02] is discussed. Combined models will be presented in Chapter 9.

In the respective swap rate measure one can give the

Swap Rate Evolution:

$$\mathrm{d}S_{r,s}(t) \;=\; S_{r,s}(t)\,\sigma_{r,s}\sqrt{V(t)}\mathrm{d}z_{r,s} \tag{6.1}$$

with

$$\mathrm{d}V(t) \;=\; \kappa(V(0)-V(t))\mathrm{d}t+\varepsilon\sqrt{V(t)}\mathrm{d}w \tag{6.2}$$

where

$$\begin{aligned}
\mathrm{d}z_{r,s} &= \sum_{k=1}^{m}\frac{\sigma_{r,s,k}}{\sigma_{r,s}}\mathrm{d}z_{(k)},\\
\sigma_{r,s}^2 &= \sum_{k=1}^{m}\sigma_{r,s,k}^2,\\
\sigma_{r,s,k} &= \text{the time-constant volatility of the logarithm of the swap rate } S_{r,s}(t) \text{ coming from factor } k,\\
\mathrm{d}w &= \text{the Brownian increment for the variance process and independent from } \mathrm{d}z,\\
\kappa &= \text{the so-called reversion speed with } \kappa\in[0;2),\\
\varepsilon &= \text{the so-called volatility of volatility.}
\end{aligned}$$

When simulating a forward rate over time with Monte Carlo techniques in the basic model, jumps from one reset date to the next are sufficient when using the appropriate corrections.[6] Special care has to be taken, however, when applying these discretization techniques for models with stochastic volatility as at the end of the discretization interval one not only has to account for changed forward rates but also for changed volatility levels (that had been piece-wise constant at the basic LIBOR market model). Since very often – like in this model – the stochastic volatility process is not lognormally or normally distributed, usually smaller steps for both the forward rates and the variance are chosen to ensure high accuracy of the simulation.

[6] See Chapter 2.5 and [Reb02], p. 123-131.

For the above model one can derive the exact

Swaption Pricing Formula:[7]

$$\begin{aligned}&\text{Swaption}(0,T_r,T_s,NP,K,\sigma_{r,s};\kappa,\varepsilon)\\ &= NP\delta\sum_{i=r}^{s-1}P(0,T_{i+1})\,f(S_{r,s}(0),T_r,K,\sigma_{r,s};\kappa,\varepsilon)\end{aligned} \tag{6.3}$$

where the following inverse Fourier integral has to be computed:[8]

$$\begin{aligned}f(S_{r,s}(0),T_r,K,\sigma_{r,s};\kappa,\varepsilon) &= S_{r,s}(0)-\frac{K}{2\pi}\int_{-\infty}^{\infty}\frac{e^{(\frac{1}{2}-i\omega)\ln[S_{r,s}(0)/K]}}{\omega^2+\frac{1}{4}}H(0,\omega)\,d\omega\\ &= S_{r,s}(0)-\frac{S_{r,s}(0)}{2\pi}\int_{-\infty}^{\infty}\frac{\cos\omega\sqrt{e}}{\omega^2+\frac{1}{4}}H(0,\omega)\,d\omega\end{aligned} \tag{6.4}$$

with $i=\sqrt{-1}$.

The function

$$H(0,\omega) = e^{A(0,\omega)+B(0,\omega)V(0)} \tag{6.5}$$

can be computed as A and B are the solutions to differential equations:

$$\frac{dA}{dt} = -\kappa V(0)B, \tag{6.6}$$

$$\frac{dB}{dt} = \frac{1}{2}\sigma_{r,s}^2\left(\omega^2+\frac{1}{4}\right)+\kappa B-\frac{1}{2}\varepsilon^2B^2. \tag{6.7}$$

Equation (6.7) corrects an error in the original article ([AA02], p. 165).

The final conditions are given as:

$$A(T_r,\omega) = 0, \qquad B(T_r,\omega)=0.$$

Closed form solutions exist for time-constant $\sigma_{r,s}$ that can be iteratively used for piece-wise constant $\sigma_{r,s}(t)$ as shown in Appendix A.3.

[7] See [AA02], p. 164f.
[8] See [Lew00], p. 54, 59, 330f.

The performance and stability of computing equation (6.4) can be increased by splitting the value of the integral into the Black price ($\varepsilon = 0$) and to the model induced difference:

$$\begin{aligned} & f(S_{r,s}(0), T_r, K, \sigma_{r,s}; \kappa, \varepsilon) \\ &= \mathrm{Bl}(K, S_{r,s}(0), v) - \frac{S_{r,s}(0)}{2\pi} \int_{-\infty}^{\infty} \frac{\cos\omega\sqrt{e}}{\omega^2 + \frac{1}{4}} \left(H(0,\omega) - e^{-\left(\omega^2+\frac{1}{4}\right)v^2/2} \right) d\omega \end{aligned} \quad (6.8)$$

with

$$v^2 = \int_0^{T_r} \sigma_{r,s}^2 V(0) du = \sigma_{r,s}^2 V(0) T_r.$$

A technique for efficiently performing this numerical integration is presented in Appendix A.2.

Calibration Quality w. r. t. a Fixed Maturity

When calibrating this model special care has to be taken considering the parameters κ and ε. These two parameters determine the model implied volatility smile. Since the effect of a change of one of these parameters has only a slight impact on the shape of the smile and can also be compensated by a change of the other parameter for every single caplet smile there exists many κ-ε-pairs that almost generate the same volatility smile. Therefore, and due to the reason that there is only one stochastic volatility process that has to be valid for all caplets and swaptions the κ-ε-pair is chosen which simultaneously fits all regarded options best.

In the original model there is even an additional free parameter, the so-called reversion level, instead of $V(0)$ that also influences the volatility smile. To avoid overfitting this parameter is set in all stochastic volatility models in this thesis to the actual level of the volatility process $V(0)$.

As can be seen in Figures 6.1 and B.7 the stochastic volatility model can only generate symmetric volatility smiles providing an insufficient fit to real market data.

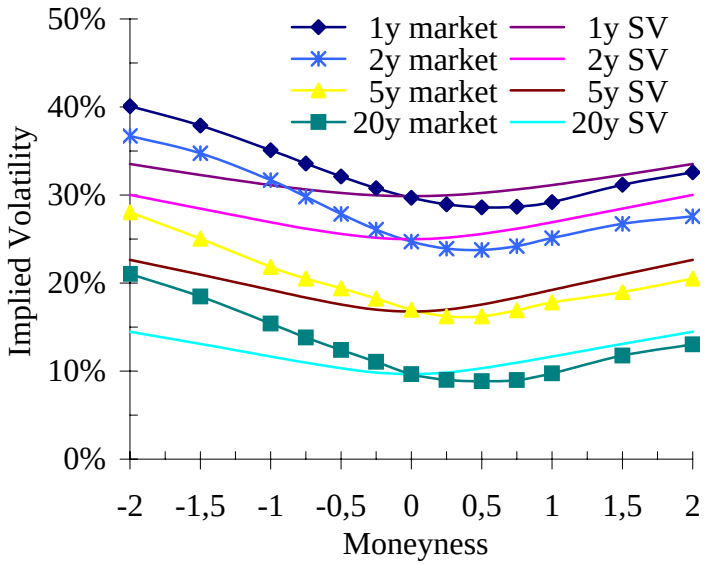

Figure 6.1: *The fit across moneynesses to the market implied caplet volatilities with Andersen/Andreasen's stochastic volatility model for different expiries.* $\sigma_{1,2} = 31\%$, $\sigma_{2,3} = 27\%$, $\sigma_{5,6} = 20\%$, $\sigma_{20,21} = 13\%$, $\kappa = 4\%$ *and* $\varepsilon = 100\%$.

In order to generate volatility skews with the stochastic volatility model one can introduce a correlation between the processes of the variance and of the forward rates (Section 6.4), combine it with jump processes and constant elasticity of variance (Section 9.1) or combine it with displaced diffusion (Section 9.2).

6.3 Joshi, Rebonato (2001)

Another very basic stochastic volatility model presented in [JR01] shall be discussed only briefly as no closed form solutions for caplets or swaptions exist. In this model the authors build on the term structure of volatility defined in (2.11) where these four parameters *a*, *b*, *c* and *d* instead of the general level of volatility as in the previous model are assumed to be stochastic following their own process with individual volatility, reversion speed and reversion level.

These characteristics leads to the following

Forward Rate Evolution: ⌝

$$\frac{\mathrm{d}L_i(t)}{L_i(t)} = \sigma_i(t)\mathrm{d}z_i \tag{6.9}$$

where

$$\begin{aligned}
\sigma_i(t) &= [a(t)+b(t)(T_i-t)]\,\mathrm{e}^{-c(t)(T_i-t)}+d(t),\\
\mathrm{d}a(t) &= \kappa_a(a_0-a(t))\mathrm{d}t+\sigma_a\,\mathrm{d}z_a,\\
\mathrm{d}b(t) &= \kappa_b(b_0-b(t))\mathrm{d}t+\sigma_b\,\mathrm{d}z_b,\\
\mathrm{d}\ln[c(t)] &= \kappa_c(\ln[c_0]-\ln[c(t)])\mathrm{d}t+\sigma_c\,\mathrm{d}z_c,\\
\mathrm{d}\ln[d(t)] &= \kappa_d(\ln[d_0]-\ln[d(t)])\mathrm{d}t+\sigma_d\,\mathrm{d}z_d.
\end{aligned}$$

The Brownian increments of these four additional processes are uncorrelated both among each other and with the Brownian motion driving the forward rate. ⌟

With the starting value $a(0)$, the reversion speed κ_a, the reversion level a_0 and the volatility σ_a (respective for b, c and d) there are altogether 16 free parameters that can be calibrated to fit the market prices best. As this number is certainly abundant the first step to reduce this number is usually to set the reversion levels equal to the starting values (e.g. $a_0 = a(0)$). For increasing stability of the calibrated parameters, usually only factor d is kept volatile what deteriorates the fit to market implied volatility skews only slightly but also reduces the model to a similar but less tractable version of the Andersen/Andreasen's model.[9] Independent of how many and which parameters are free to calibrate, due to the uncorrelated Brownian increments this model can only produce symmetric volatility smiles.

Due to the lack of closed form solutions for caplets and swaptions the calibration procedure has to be carried out numerically. While this is certainly less accurate and has higher computational costs it can be done quite efficiently by:

1. Simulating volatility paths (around 64 sample paths are sufficient),[10]

[9] See [JR01], p. 33.
[10] See [JR01], p. 18.

2. Integrating these paths numerically for each expiry,
3. Calculating the caplet prices as an average of the prices for each path,
4. Determining the sum of the absolute or squared differences between market and model prices,
5. Repeating steps 1-4 to calibrate the free parameters by minimizing the sum calculated in step 4.

6.4 Wu, Zhang (2002)

The main drawback of the two previously discussed models is their inability to fit a volatility skew. One possibility to model this skew is by assuming a correlation between the driving processes of interest rates and volatility. While there seem to be logical reasons for assuming this correlation between the underlying process and its volatility in the equity world[11] this fact is rather controversial in the interest rate world. For instance empirically it was shown in [CS01] that "the correlations between short-dated forward rates and their volatilities are indistinguishable from 0".[12] However, the ability to fit market data without having to mix a stochastic volatility model with one of the other basic models outweighs these concerns.

Since for correlated processes a change of measure has influence on both processes, it is preferable to start in the spot measure to ease a simultaneous simulation of all forward rates later on. This leads in the spot measure to the following dynamics for the forward rates and the variance:

$$\frac{\mathrm{d}L_i(t)}{L_i(t)} = \mu_i(t)V(t)\mathrm{d}t + \sigma_i(t)\sqrt{V(t)}\mathrm{d}z_i, \tag{6.10}$$

$$\mathrm{d}V(t) = \kappa(V(0) - V(t))\,\mathrm{d}t + \varepsilon\sqrt{V(t)}\mathrm{d}w \tag{6.11}$$

where the correlation between the two Brownian increments is denoted by $\rho_{i,V}(t)$.

[11] See [Mei03], p. 34.
[12] See [JLZ02], p. 8.

Changing to the forward measure results in the

Forward Rate Evolution:

$$\frac{\mathrm{d}L_i(t)}{L_i(t)} = \sigma_i(t)\sqrt{V(t)}\mathrm{d}z_i \tag{6.12}$$

where the variance evolves like

$$\mathrm{d}V(t) = [\kappa V(0) - (\kappa + \varepsilon\xi_i(t))V(t)]\,\mathrm{d}t + \varepsilon\sqrt{V(t)}\mathrm{d}w \tag{6.13}$$

with

$$\xi_i(t) = \sum_{k=1}^{i} \frac{\delta L_k(t)\rho_{k,V}(t)\sigma_k(t)}{1+\delta L_k(t)}.$$

To retain analytic tractability the forward rates in $\xi_i(t)$ are frozen at time 0:

$$\xi_i(t) \approx \sum_{k=1}^{i} \frac{\delta L_k(0)\rho_{k,V}(t)\sigma_k(t)}{1+\delta L_k(0)}. \tag{6.14}$$

Substituting

$$\widetilde{\xi}_i(t) = 1 + \frac{\varepsilon}{\kappa}\xi_i(t)$$

leads to:

$$\mathrm{d}V(t) = \kappa\left[V(0) - \widetilde{\xi}_i(t)V(t)\right] + \varepsilon\sqrt{V(t)}\mathrm{d}w. \tag{6.15}$$

For this model one can then write the

Caplet Pricing Formula:

$$\mathrm{Caplet}(0, T_i, \delta, NP, K, \sigma_i; \kappa, \varepsilon, \rho_{i,V}) = NP\,\delta P(0, T_{i+1})\,(L_i(0)\Pi_1 - K\Pi_2) \tag{6.16}$$

where

$$\Pi_1 = \frac{1}{2}+\frac{1}{\pi}\int_0^\infty \frac{\mathrm{Im}\left\{e^{-iu\ln[K/L_i(0)]}\Psi_{T_i}(1+iu)\right\}}{u}du, \tag{6.17}$$

$$\Pi_2 = \frac{1}{2}+\frac{1}{\pi}\int_0^\infty \frac{\mathrm{Im}\left\{e^{-iu\ln[K/L_i(0)]}\Psi_{T_i}(iu)\right\}}{u}du \tag{6.18}$$

with

$$\begin{aligned}\mathrm{Im}\{z\} &= \text{the imaginary part of the complex number } z,\\ \Psi_{T_i}(z) &= e^{A(T_i,z)+B(T_i,z)V(0)}.\end{aligned} \tag{6.19}$$

A and B follow the differential equations for τ being the time to expiry:

$$\begin{aligned}\frac{dA}{d\tau} &= \kappa V(0)B,\\ \frac{dB}{d\tau} &= \frac{1}{2}\varepsilon^2B^2+(\rho_{i,V}\,\varepsilon\,\sigma_i z-\kappa\widetilde{\xi}_i)B+\frac{1}{2}\sigma_i^2(z^2-z)\end{aligned}$$

with the initial conditions:

$$A(0,z) = 0, \qquad B(0,z) = 0.$$

Following Appendix A.3 one gets for piece-wise constant coefficients:

$$\begin{aligned}A(\tau,z) &= A(\tau_j,z)+\frac{\kappa V(0)}{\varepsilon^2}\left\{(a+d)(\tau-\tau_j)-2\ln\left[\frac{1-g_je^{d(\tau-\tau_j)}}{1-g_j}\right]\right\},\\ B(\tau,z) &= B(\tau_j,z)+\frac{\left(a+d-\varepsilon^2B(\tau_j,z)\right)\left(1-e^{d(\tau-\tau_j)}\right)}{\varepsilon^2\left(1-g_je^{d(\tau-\tau_j)}\right)}\end{aligned}$$

where

$$\begin{aligned}a &= \kappa\widetilde{\xi}_i-\rho_{i,V}\,\varepsilon\,\sigma_i z,\\ d &= \sqrt{a^2-\sigma_i^2\varepsilon^2(z^2-z)}\end{aligned}$$

and

$$g_j = \frac{a+d-\varepsilon^2 B(\tau_j,z)}{a-d-\varepsilon^2 B(\tau_j,z)}.$$

⌟

Furthermore, using (2.18) one can determine an approximative

Swaption Pricing Formula: ⌝

$$\text{Swaption}(0,T_r,T_s,NP,K,\sigma_{r,s};\kappa,\varepsilon,\rho_{r,s,V}) = NP\delta\sum_{i=r+1}^{s} P(0,T_i)\left(S_{r,s}(0)\Pi_1 - K\Pi_2\right) \tag{6.20}$$

where

$$\Pi_1 = \frac{1}{2}+\frac{1}{\pi}\int_0^\infty \frac{\text{Im}\left\{e^{-iu\ln[K/S_{r,s}(0)]}\Psi_{T_r}(1+iu)\right\}}{u}du, \tag{6.21}$$

$$\Pi_2 = \frac{1}{2}+\frac{1}{\pi}\int_0^\infty \frac{\text{Im}\left\{e^{-iu\ln[K/S_{r,s}(0)]}\Psi_{T_r}(iu)\right\}}{u}du. \tag{6.22}$$

The coefficients used for solving equation (6.19) are then substituted by:[13]

$$\begin{aligned}
\widetilde{\xi}_{r,s}(t) &= 1+\frac{\varepsilon}{\kappa}\sum_{i=r}^{s-1}\omega_i(0)\xi_i(t),\\
\sigma_{r,s}(t) &= \frac{\sum_{i=r}^{s-1}\overline{\omega}_i(0)L_i(0)\sigma_i(t)}{S_{r,s}(0)},\\
\rho_{r,s}(t) &= \frac{\sum_{i=r}^{s-1}\overline{\omega}_i(0)L_i(0)\sigma_i(t)\rho_i(t)}{S_{r,s}(0)\sigma_{r,s}(t)}
\end{aligned}$$

with $\omega_i(0)$ is given in equation (2.19) and $\overline{\omega}_i(0)$ in (2.22). ⌟

Additionally, it has to be noted that in a stochastic volatility model with correlation the market is not complete anymore since risk-neutral valuation is not possible.[14] For hedging an option a money market account and the underlying stock or forward rate are no longer sufficient but a second option is needed that already

[13] See [WZ02], p. 12-14.
[14] See [Reb99], p. 88.

implies the so-called market-price of risk.[15] For the special case where the correlation is perfect ($\rho = \pm 1$), this second option is not needed as this model then is reduced to local-volatility model that has been described in Chapter 4.

Calibration Quality w. r. t. a Fixed Maturity

Since in this model the closed form solution is valid for piece-wise constant parameters for the volatility $\sigma_i(t)$ and the correlation $\rho_{i,V}(t)$ a set of time-homogeneous parameters is straightforward to calibrate to. Therefore, the discussion of the calibration quality for a single volatility smile is deferred to the tests of the calibration quality w. r. t. the full term structure evolution.

Term Structure Evolution

When simulating the forward rates simultaneously the correlation between the variance and the forward rates has to be taken into consideration, too. As usually the number of Brownian factors m is smaller than the number of forward rates n in a simulation the parameters $\rho_{1,V}$, $\rho_{2,V}$, ..., $\rho_{n,V}$ can not be rebuilt exactly. Similar to the factor reduction for the basic model these correlation coefficients are reduced to a smaller number of factors. The process can then be simulated as described for the basic stochastic volatility model.

Calibration Quality w. r. t. the Full Term Structure Evolution

When calibrating this stochastic volatility model one has again to take special care of the parameters κ and ε. These parameters have to be identical for all different expiries. As the parameters σ_i and $\rho_{i,V}$ can be used in the caplet pricing formula as time-homogeneous parameters, the Figures 6.2 and B.8 were simultaneously calibrated. The results for the €-data are a very close fit to market data. For US-$ this fit is not sufficient since the skew seems to strong to be fitted by the correlation.

[15] This can be seen clearly when deriving the partial differential equation for Heston's model in Appendix A.4.

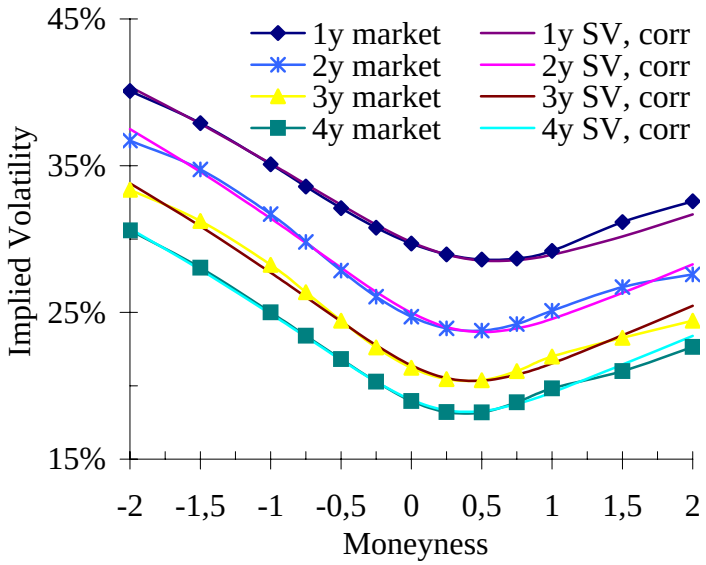

Figure 6.2: *The fit across moneynesses to the market implied caplet volatilities with Wu/Zhang's stochastic volatility model with correlation for different expiries.* $\sigma_1 = 33\%$, $\rho_{1,V} = -35\%$, $\sigma_2 = 28\%$, $\rho_{2,V} = -41\%$, $\sigma_3 = 22\%$, $\rho_{3,V} = -41\%$, $\sigma_4 = 18\%$, $\rho_{4,V} = -37\%$, $\kappa = 19\%$ *and* $\varepsilon = 160\%$.

6.5 Comparison of the Different Stochastic Volatility Models

Two main models have been introduced in this chapter. The basic model by Andersen/Andreasen without correlation is only able to produce a symmetric volatility smile. Besides mixing this approach with other basic models – as will be done in the third part of this thesis – one can also generate a volatility skew by correlating the volatility and the forward rate driving Brownian motions. Due to the market implied lower volatility for caplets out of the money this correlation is negative. The time-homogeneous fit to market data in this model is at least for the €-data very good.

The problems with Wu/Zhang's model, however, are a relatively time-consuming caplet pricing formula and also a very time-consuming and inefficient simulation of the forward rates as in this case the volatility paths cannot be simulated separately or be used for more than one forward rate path, but have to be computed

simultaneously with the forward rates. Two further minor disadvantages of this stochastic volatility model with correlation are the non 100%-exact caplet pricing formula and the fact that the calibrated $\rho_{i,V}(t)$ can not be simulated in a factor reduced model exactly.

Chapter 7

Models with Jump Processes

After testing in the previous chapters three different basic classes of models that modify volatility directly, models with jump processes as the last basic approach shall be presented in this chapter. With introducing jump processes to the evolution of the forward rates the assumption of a continuous evolution of forward rates over time is no longer retained.

First a general overview of these jump processes and reasons for their occurrence is given. Then the basics starting with Merton's formula are presented leading to more and more complex models. At the end of the chapter these different models are compared.

7.1 General Characteristics and Problems

The assumption in Black's formula of a continuous movement of the forward rates is not given in reality. The tick size and the time discretization of one second at exchanges are contradicting this assumption but this influence on prices is usually negligible. The real problems are, first, big movements of forward rates for this minimum step sizes due to new information during the opening hours and second, the closing times over night that lead to a jump every morning the exchange opens due to market movements that happened on other market places all over the world.

Big movements in the markets are mainly information induced. In the stock markets this information is usually a stock related announcement such as quarter earnings, a new analyst report or hostile bids. For fixed income securities mainly macroeconomic news have such a big effect on forward rates. One of the possible sources are the government rates announced on a regular basis by the European Central Bank (= ECB) for the € or by the Federal Reserve Bank for US-$. This regular announcement combined with the fact that the government rates have a big tick size with 25 basis points leads to frequent jumps in the forward rates.[1]

Furthermore, a study about the volatility smile in the stock option markets shows that the kurtosis of the distribution of stock returns is significantly higher for the overnight and weekend time where the exchange is closed than for the opening hours.[2] Since this fact can hardly be modeled by assuming a continuous movement of stocks during the closing times, it additionally amplifies the idea of jump events having an influence on interest rates when assuming that fixed income and stock markets are similar.

7.2 Merton's Fundament

The basic work for modeling jumps of the underlyings of financial derivatives has been done in [Mer76] where the assumption in the Black-Scholes model of a continuous development of stock prices is alleviated. The usual movements in stock prices are still described by a Brownian motion but for the unusual movements a Poisson process is introduced.[3]

A Poisson process is an integer-valued non-decreasing stochastic process with the parameter λ, the so-called arrival rate. This parameter denotes the expected number of events per unit time with $\frac{1}{\lambda}$ being the expected time till the next jump, the so-called interarrival time. This interarrival time (= for instance the time between the 2nd and the 3rd event) is exponentially distributed. Due to the independent

[1] See [Muc03], p. 7f and [Man02], p. 18f.
[2] Discussion by Robert Tompkins at the MathFinance Workshop 2004, Frankfurt.
[3] See [Fri03], p. 3f.

identically distributed (i.i.d.) jump times a Poisson process is memoryless, i.e. the expected time till the next jump at a certain point of time is independent of when the previous jump has occurred.

These Poisson distributed number of jumps per time interval can model the arrival of an important piece of information for the underlying stock. The intensity of these events, the so-called arrival rate, is denoted by λ, the random number of jump events up to time T is denoted by N_T. The probability of n jumps during a certain period of time can then be given by:

$$\mathrm{P}(N_T = n) = \frac{\mathrm{e}^{-\lambda T}(\lambda T)^n}{n!}. \tag{7.1}$$

The usual equation from Black-Scholes for the evolution of a stock in the risk-neutral measure:

$$\frac{\mathrm{d}A(t)}{A(t)} = r\,\mathrm{d}t + \sigma\,\mathrm{d}z \tag{7.2}$$

with

$$\begin{aligned} A(t) &= \text{the price of the underlying stock at time } t, \\ r &= \text{the risk free rate,} \\ \sigma &= \text{the volatility of the logarithm of the stock price} \end{aligned}$$

is then extended to:

$$\frac{\mathrm{d}A(t)}{A(t^-)} = (r - \lambda m)\mathrm{d}t + \sigma\,\mathrm{d}z + \mathrm{d}\left(\sum_{k=1}^{N}(J_k - 1)\right) \tag{7.3}$$

where

$$\begin{aligned} A(t^-) &= \text{the left side limit of the stock price at time } t, \\ N &= \text{a Poisson process with arrival rate } \lambda \end{aligned}$$

and

$$\begin{aligned} \{J_k\} &= \text{the sequence of independent identically distributed (i.i.d.) non-negative random variables,} \\ m &= E(J_i - 1), \text{ the expected proportional price change for one jump.} \end{aligned}$$

The formula of Black-Scholes for call options with maturity T:

$$\text{Call}(A,K,T,\sigma^2,r) = \text{BS}(A,K,T,\sigma^2,r) = S\Phi(d_1) - Ke^{-rT}\Phi(d_2) \qquad (7.4)$$

where

$$\begin{aligned} d_1 &= \frac{\ln[A/K] + \left(r + \frac{\sigma^2}{2}\right)T}{\sigma\sqrt{T}}, \\ d_2 &= d_1 - \sigma\sqrt{T}, \\ \sigma &= \text{the annualized volatility of the logarithm of the stock price} \end{aligned}$$

is accordingly extended with using equation (7.1) and the assumption that the jump size J is lognormally distributed $\left(J \sim LN(a,s^2)\right)$:[4]

$$\text{Call}(A,K,T,\sigma^2,r;\lambda,a,s) = \sum_{n=0}^{\infty} \frac{e^{-\lambda' T}(\lambda' T)^n}{n!} \text{BS}(A,K,T,v_n^2,r_n) \qquad (7.5)$$

where

$$\begin{aligned} \lambda' &= \lambda(1+m), \\ r_n &= r - \lambda m + \frac{n\ln(1+m)}{T}, \\ v_n^2 &= \sigma^2 + n\frac{s^2}{T}, \\ m &= e^{a+s^2/2} - 1. \end{aligned}$$

[4] See [Hul01], p. 630f., 646.

7.3 Glasserman, Kou (1999)

In [GK99] the authors build on Merton's formula for deriving a formula for caplets. Both intensity and density of the jump process are chosen as in the previous model. Since for deriving the formula of Black-Scholes the risk-neutral measure and for Black's formula the terminal measure is used, in the case of interest rates the jump process is added to the terminal measure leading to the

Forward Rate Evolution:[5] ⌝

$$\frac{\mathrm{d}L_i(t)}{L_i(t^-)} \;=\; -\lambda_i m_i \,\mathrm{d}t + \sigma_i(t)\mathrm{d}z_i + \mathrm{d}\left(\sum_{k=1}^{N_i}(J_k-1)\right) \tag{7.6}$$

where N_i is a Poisson process with the time-constant arrival rate λ_i. ⌟

For simulating this process with Monte Carlo techniques one has to discretize it for time steps of a finite size.[6] The jump process can be discretized by drawing a first random number to determine – using the CDF obtained with equation (7.1) – the number of jumps in this time interval (= N_δ) and according to the number of those jumps additional random numbers that are distributed as specified in the respective jump models (= in this case lognormally).

Due to the lognormal distribution of the diffusion and the fact that the forward rate is multiplied with the jump sizes, the step sizes for the simulation do not have to be increased. The level of the forward rate at time $t+\delta$ after the jumps is then a function of the stock price before accounting for the jumps (at time $(t+\delta)^-$):

$$L_i(t+\delta) \;=\; L_i((t+\delta)^-)\prod_{k=1}^{N_\delta} J_k. \tag{7.7}$$

[5] See [GK99], p. 13.
[6] For the discretization of the drift, see Section 2.5.

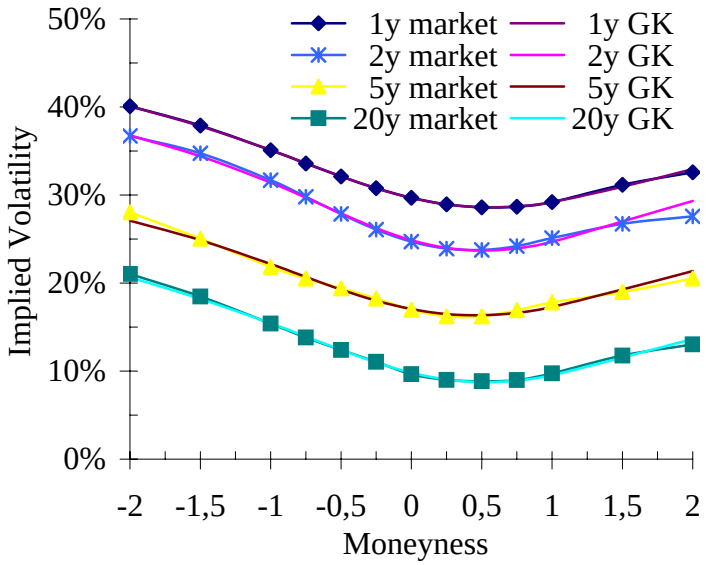

Figure 7.1: *The fit across moneynesses to the market implied caplet volatilities with Glasserman/Kou's jump model for different expiries.* $\sigma_1 = 17\%$, $\lambda_1 = 67\%$, $s_1 = 33\%$, $m_1 = -10\%$, $\sigma_2 = 13\%$, $\lambda_2 = 27\%$, $s_2 = 50\%$, $m_2 = -15\%$, $\sigma_5 = 9\%$, $\lambda_5 = 7\%$, $s_5 = 71\%$, $m_5 = -20\%$, $\sigma_{20} = 5\%$, $\lambda_{20} = 1\%$, $s_{20} = 223\%$ *and* $m_{20} = -62\%$.

Similar to Merton's formula in (7.4) one can then give a

Caplet Pricing Formula:

$$\begin{aligned} &\text{Caplet}(0, T_i, \delta, NP, K, \sigma_i; \lambda_i, m_i, s_i) \\ &= NP\delta P(0, T_{i+1}) e^{-\lambda_i T_i} \sum_{j=0}^{\infty} \frac{(\lambda_i T_i)^j}{j!} \text{Bl}(K, L_i^{(j)}(0), v_i^{(j)}) \end{aligned} \tag{7.8}$$

with

$$\begin{aligned} L_i^{(j)}(0) &= L_i(0) e^{-\lambda_i m_i T_i} (1 + m_i)^j, \\ v_i^{(j)} &= \sqrt{\sigma^2 T_i + j s_i^2}. \end{aligned}$$

Calibration Quality w. r. t. a Fixed Maturity

When testing the calibration quality of this model to market data one can see in markets with a pronounced volatility smile (€-data in Figure 7.1) instead of a volatility smirk (US-$-data in Figure B.9) a very good fit of the model implied volatilities to market implied volatilities. Examining the calibrated parameters for the caplet with one year expiry leads to very reasonable results: with a probability of 49% there will be one or more jumps with an expected jump size of -10%.

While the fit to market data stays good for longer maturities the obtained parameters change strongly: for a caplet with 20 years maturity with a probability of more than 80% no jump at all will occur, but if there will be a jump event it will lead to an average drop down of the interest rate by -62%. These parameters for the caplet that expires in 20 years are cumbersome by itself, but combing the resulting process with the process for a caplet with 1 year maturity would lead eventually to a very odd forward rate curve since those jumps of different parts of the curve are not connected at all.

Finding a forward rate process with additional parameters that can be interpreted to have an economic meaning is certainly an advantage of the jump process, but since these parameters are – as just shown – far away from realistic values, consequentially the suggested process does not match the real market dynamics. There are two possible improvements of this basic model. First, a different distribution of the jump sizes should be examined and second, a time-homogeneous evolution leading on all possible simulation paths to a smooth forward rate curve should be found. The first will be tested in the following section, the second in the section thereafter.

7.4 Kou (1999)

The lognormal distribution of the jump sizes proposed in [GK99] leads to a very simple pricing formula for caplets. However, since this is the same distribution as the underlying forward rate process it leads for longer maturities to a canceling

out of the effects of one or more jumps. Different distributions of the jump sizes exist with the same underlying

Forward Rate Evolution:

$$\frac{\mathrm{d}L_i(t)}{L_i(t^-)} = -\lambda_i m_i \,\mathrm{d}t + \sigma_i(t)\mathrm{d}z_i + \mathrm{d}\left(\sum_{k=1}^{N_i}(J_k - 1)\right). \tag{7.9}$$

In [Kou99] the author suggests a double exponential distribution for the logarithm of the jump size with the density:

$$f\left(\ln[J] = x\right) = \frac{1}{2\eta}\mathrm{e}^{-\frac{|x-\xi|}{\eta}} \tag{7.10}$$

where

$$\begin{aligned} \xi &= \text{the mean of the distribution,} \\ 2\eta^2 &= \text{the variance of the distribution with } 0 < \eta < 1. \end{aligned}$$

This can be stated differently by drawing an exponential random variable ν with mean η and variance η^2 and calculating the jump size J by:[7]

$$J = \begin{cases} \mathrm{e}^{\xi+\nu} & \text{with probability } \frac{1}{2}, \\ \mathrm{e}^{\xi-\nu} & \text{with probability } \frac{1}{2}. \end{cases} \tag{7.11}$$

Therefore, the distribution of $\ln[J]$ is symmetric in ξ and can produce values for $\ln[J]$ in the range $(-\infty, \infty)$. As in the basic model by Glasserman and Kou the logarithm ensures $J \in \mathbb{R}^+$ and hence prohibits interest rates from jumping to negative values.

The obtained density is similar to Student-*t* distributions and the main differences to the normal distribution used in [GK99] are the high peak and heavy tail features that should have a higher impact on the distribution of the forward rate. The

[7] See [Kou99], p. 10.

kurtosis is given by:

$$\text{Kurtosis} = \frac{E\left[(X-E(X))^4\right]}{Var(X)^2} - 3 \tag{7.12}$$

with the central normalized moment $M_4 = E\left[(X-E(X))^4\right]$ for the double exponential distribution ($= DE$) with $\xi = 0$:

$$M_4 = \int_{-\infty}^{\infty} \frac{x^4}{2\eta} e^{-\frac{|x|}{\eta}} = 24\eta^4. \tag{7.13}$$

The difference between this distribution and the normal distribution can then easily be seen by:

$$\begin{aligned} \text{Kurtosis}_{DE} &= \frac{M_4}{4\eta^4} - 3 = 3, \\ \text{Kurtosis}_N &= 0. \end{aligned}$$

The double exponential distribution can also be seen as a substitute for the more intuitive but less tractable Student-t distribution with 6 degrees of freedom with the density:

$$f(x) = \frac{\Gamma(3.5)}{\sqrt{6\pi}\Gamma(3)}\left(1+\frac{x^2}{6}\right)^{-3.5} = \frac{5\sqrt{6}}{32}\left(1+\frac{x^2}{6}\right)^{-3.5} \tag{7.14}$$

with

$$\Gamma(x) = \int_0^{\infty} t^{x-1}e^{-t}dt. \tag{7.15}$$

After scaling this density with $\sqrt{\frac{3}{2}}$:

$$f(x) = \frac{15}{32}\left(1+\frac{x^2}{4}\right)^{-3.5} \tag{7.16}$$

this distribution and the double exponential distribution have the same first five moments and can hardly be distinguished at sample market data.[8]

[8] See [Kou99], p. 10f.

The high peak and heavy tail features seem appealing due to two reasons. First, market observations show both under- and overreaction to market news, i.e. high peaks and heavy tails. Second, as the tails in the double exponential distribution are heavier than in the normal distribution, the effect of one jump on the volatility smile should be stronger and in the long run the canceling out of jumps should be slower than for the normal distribution.

The proposed dynamics lead to the

Caplet Pricing Formula:[9]

$$\begin{aligned}
\text{Caplet}(0,T_i,\delta,NP,K,\sigma_i;\lambda_i,\xi_i,\eta_i) \;=\; & NP\delta P(0,T_{i+1})\mathrm{e}^{-\lambda_i T_i} \\
\times\Bigg\{ & \sum_{n=1}^{\infty}\sum_{j=1}^{n}\frac{(\lambda_i T_i)^n}{n!\,2^{2n-j}}\binom{2n-j-1}{n-1}\times\Bigg[\mathrm{e}^{\frac{\sigma_i^2 T_i}{2\eta_i^2}}\frac{K}{\sqrt{2\pi}}\sum_{k=0}^{j-1}\left(\frac{\sigma_i\sqrt{T_i}}{\eta_i}\right)^k \\
& \times\left(\mathrm{e}^{-\frac{h_i}{\eta_i}}\left(\frac{1}{(1-\eta_i)^{j-k}}-1\right)\mathrm{Hh}_k(c_i^-)+\mathrm{e}^{\frac{h_i}{\eta_i}}\left(1-\frac{1}{(1+\eta_i)^{j-k}}\right)\mathrm{Hh}_k(c_i^+)\right) \\
& +L_i(0)\mathrm{e}^{-\lambda_i\zeta_i T_i+n\xi_i}\left(\frac{1}{(1-\eta_i)^j}+\frac{1}{(1+\eta_i)^j}\right)\Phi(a_i^+)-2K\Phi(a_i^-)\Bigg] \\
& +\Big[L_i(0)\mathrm{e}^{-\lambda_i\zeta_i T_i}\Phi(b_i^+)-K\Phi(b_i^-)\Big]\Bigg\} \qquad (7.17)
\end{aligned}$$

where

$$\begin{aligned}
a_i^{\pm} &= \frac{\ln\left[\frac{L_i(0)}{K}\right]\pm\frac{\sigma_i^2 T_i}{2}-\lambda_i\zeta_i T_i+n\xi_i}{\sigma_i\sqrt{T_i}}, \\
b_i^{\pm} &= \frac{\ln\left[\frac{L_i(0)}{K}\right]\pm\frac{\sigma_i^2 T_i}{2}-\lambda_i\zeta_i T_i}{\sigma_i\sqrt{T_i}}, \\
c_i^{\pm} &= \frac{\sigma_i\sqrt{T_i}}{\eta_i}\pm\frac{h_i}{\sigma_i\sqrt{T_i}}, \\
h_i &= \ln[K/L_i(0)]+\lambda_i\zeta_i T_i+\frac{\sigma_i^2 T_i}{2}-n\xi_i, \\
\zeta_i &= \frac{\mathrm{e}^{\xi_i}}{1-\eta_i^2}-1
\end{aligned}$$

[9] See [Kou99], p. 21, 23.

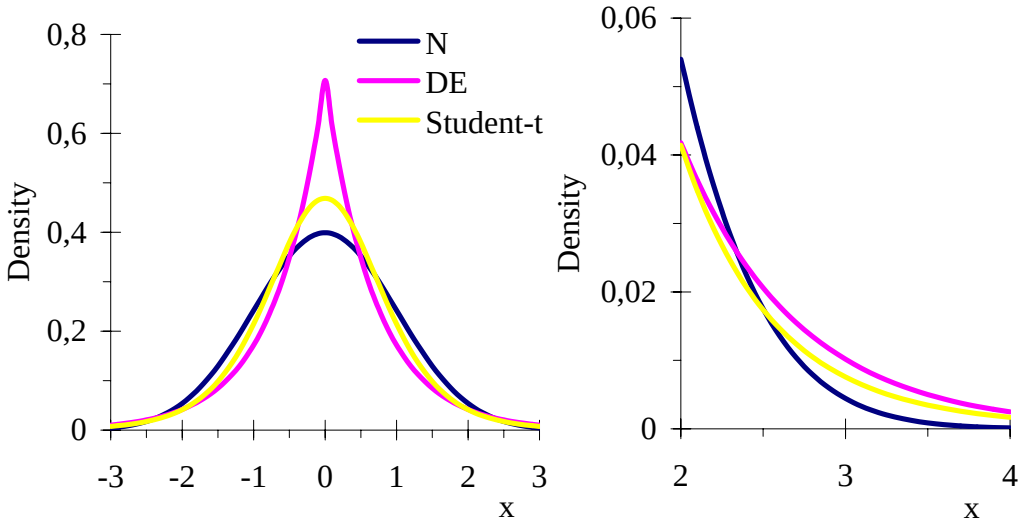

Figure 7.2: *Comparison between the normal distribution (N), the double exponential distribution (DE) and the Student-t distribution with six degrees of freedom (Student-t) for the variable x. All distributions have a mean of 0 and a variance of 1. N has a kurtosis of 0, DE and Student-t a kurtosis of 3.*

The *Hh* function is defined as follows:[10]

$$\begin{aligned} \mathrm{Hh}_{-1}(x) &= \mathrm{e}^{-x^2/2}, \\ \mathrm{Hh}_0(x) &= \sqrt{2\pi}\,\Phi(-x), \\ \mathrm{Hh}_n(x) &= \frac{\mathrm{Hh}_{n-2}(x) - x\,\mathrm{Hh}_{n-1}(x)}{n}. \end{aligned}$$

⌟

Calibration Quality w. r. t. a Fixed Maturity

The results obtained with this model (see Figures 7.3 and B.10) are very similar to the basic model proposed by [GK99]. With this model due to the strong leptokurtic feature of its jump size distribution all diffusion volatilities σ_i are higher and all jump arrival rates λ_i are smaller than in the previous model, but still the parameters are unrealistic and not apt for simulating all forward rates simultaneously.

[10] See [AS72], p. 299f, 691.

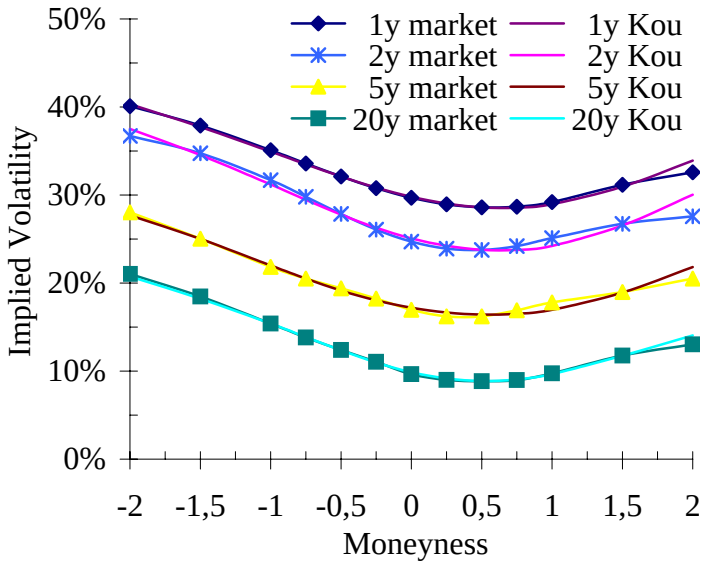

Figure 7.3: *The fit across moneynesses to the market implied caplet volatilities with Kou's jump model for different expiries.* $\sigma_1 = 18\%$, $\lambda_1 = 65\%$, $\eta_1 = 22\%$, $\xi_1 = -0.2$, $\sigma_2 = 16\%$, $\lambda_2 = 16\%$, $\eta_2 = 40\%$, $\xi_2 = -0.5$, $\sigma_5 = 11\%$, $\lambda_5 = 4\%$, $\eta_5 = 60\%$, $\xi_5 = -1.0$, $\sigma_{20} = 5\%$, $\lambda_{20} = 1\%$, $\eta_{20} = 95\%$ *and* $\xi_{20} = -3.5$.

Different distributions of jump sizes should be found but the difficulty might be to find an exact caplet pricing formula.

7.5 Glasserman, Merener (2001)

In the previous sections two different approaches with time-constant parameters for the jump process have been presented. Their shortcomings are both in fitting the smile of caplets with different maturities and in getting meaningful parameters to produce a comprehensive model that evolves all forward rates simultaneously over time.

A third model – clearly building on [GK99] – with time-dependent parameters has been proposed in [GM01a] and shall be presented and tested in this section.

The first step is again a closed form solution for caplets, the most important tool for calibrating the smile efficiently. As in this setting the parameters of the jump

processes are not time-constant but can even be chosen time-homogeneous, this model and the jump sizes can be calibrated by bootstrapping. The obtained parameters can then be used to model this evolution of forward rates over time for Monte Carlo simulations. Efficient ways for doing so are presented at the end of this section.

Starting in the respective terminal measure from a – compared to (7.6) – slightly modified

Forward Rate Evolution:

$$\frac{\mathrm{d}L_i(t)}{L_i(t^-)} = -\lambda_i(t)\,m_i(t)\mathrm{d}t + \sigma_i(t)\mathrm{d}z_i + \mathrm{d}\left(\sum_{k=1}^{N_i(t)}(J_k-1)\right) \tag{7.18}$$

with

$$N_i(t) = \text{a Poisson process with the time-dependent arrival rate } \lambda_i(t),$$

one gets a

Caplet Pricing Formula:[11]

$$\mathrm{Caplet}(0,T_i,\delta,NP,K,\overrightarrow{\sigma}_i;\overrightarrow{\lambda}_i,\overrightarrow{m}_i,\overrightarrow{s}_i) = NP\,\delta P(0,T_{i+1})\,(L_i(0)\Pi_1 - K\Pi_2) \tag{7.19}$$

with

$$\Pi_1 = \frac{1}{2} + \frac{1}{\pi}\int_0^\infty \frac{\mathrm{e}^{B_1(u)}\sin\left(B_2(u) - u\ln[K/L_i(0)]\right)}{u}\mathrm{d}u, \tag{7.20}$$

$$\Pi_2 = \frac{1}{2} + \frac{1}{\pi}\int_0^\infty \frac{\mathrm{e}^{B_3(u)}\sin\left(B_4(u) - u\ln[K/L_i(0)]\right)}{u}\mathrm{d}u, \tag{7.21}$$

where

$$B_1(u) = \delta\sum_{k=1}^{i}\lambda_k(0)\left[(1+m_k(0))\mathrm{e}^{-s_k^2(0)u^2/2}\cos(w_k(0)u) - 1\right] - \lambda_k(0)\,m_k(0) - \sigma_k^2(0)u^2/2$$

[11] See [GM01c], p. 6.

and

$$\begin{aligned}
B_2(u) &= \delta\sum_{k=1}^{i}\lambda_k(0)(1+m_k(0))\mathrm{e}^{-s_k^2(0)u^2/2}\sin(w_k(0)u)+\alpha_k(0)u+\sigma_k^2(0)u,\\
B_3(u) &= \delta\sum_{k=1}^{i}\lambda_k(0)\left[\mathrm{e}^{-s_k^2(0)u^2/2}\cos(a_k(0)u)-1\right]-\sigma_k^2(0)u^2/2,\\
B_4(u) &= \delta\sum_{k=1}^{i}\lambda_k(0)\mathrm{e}^{-s_k^2(0)u^2/2}\sin(a_k(0)u)+\alpha_k(0)u
\end{aligned}$$

with

$$\begin{aligned}
w_k(t) &= a_k(t)+s_k^2(t),\\
\alpha_k(t) &= -\lambda_k(t)\,m_k(t)-\sigma_k^2(t)/2,\\
a_k(t) &= \ln[m_k(t)+1]-\frac{s_k^2(t)}{2}
\end{aligned}$$

where all time-dependent $\sigma_k(t),\lambda_k(t),m_k(t)$ and $s_k(t)$ are chosen to be totally time-homogeneous analogous to equation (2.9) leading to:

$$\overrightarrow{\sigma}_i = \begin{pmatrix}\sigma_i(0)\\ \sigma_i(T_1)\\ \vdots\\ \sigma_i(T_{i-1})\end{pmatrix} = \begin{pmatrix}\sigma_i(0)\\ \sigma_{i-1}(0)\\ \vdots\\ \sigma_1(0)\end{pmatrix} \tag{7.22}$$

with respective vectors for $\overrightarrow{\lambda}_i$, $\overrightarrow{s}_i$ and $\overrightarrow{m}_i$. ⌟

With the closed form solution from (7.19) the parameters $\sigma_i(0),\lambda_i(0),m_i(0)$ and $s_i(0)$ can be obtained by bootstrapping, leading to a totally time-homogeneous behavior of the whole forward rate process where the forward rates $L_i(t)$ and $L_{i+k}(t)$

are notated in their respective (drift-free) forward measure:

$$\begin{aligned}\frac{\mathrm{d}L_i(t)}{L_i(t^-)} &= -\lambda_i(t)m_i(t)\mathrm{d}t + \sigma_i(t)\mathrm{d}z_i + \mathrm{d}\left(\sum_{k=1}^{N_i(t)}(J_k-1)\right)\\ &= -\lambda_{i+k}(t+k\delta)m_{i+k}(t+k\delta)\mathrm{d}t + \sigma_{i+k}(t+k\delta)\mathrm{d}z_{i+k} + \mathrm{d}\left(\sum_{k=1}^{N_{i+k}(t+k\delta)}(J_k-1)\right)\\ &= \frac{\mathrm{d}L_{i+k}(t+k\delta)}{L_{i+k}((t+k\delta)^-)}.\end{aligned}$$

Calibration Quality w. r. t. a Fixed Maturity

Calibrating the time-homogeneous jump model of Glasserman/Merener to market data is rather problematic since the obtained parameters are not similar, what means – as can be seen for example at the parameter s_2 with the extreme volatility of jump sizes – that these parameters for longer expiries have to take extreme values to ensure a good fit to market data as shown in Figure 7.4. In spite of these extreme values the obtained market fit is definitely worse than for time-constant parameters as shown in Figure 7.1.

An additional problem is that these parameters are calibrated in their respective forward measure. Therefore, an appropriate procedure has to be found, so that all parameters are valid in the same measure and ideally all these different Poisson processes can be implemented simultaneously and efficiently.[12]

Term Structure Evolution

The main problem with this simulation is that when changing the measure the Poisson process changes, too. The intensity of the jump process is different in every other measure and there exists no measure in which all processes are still Poisson simultaneously.[13]

[12] Compare to Section 2.4.
[13] See [GM01a], p. 9.

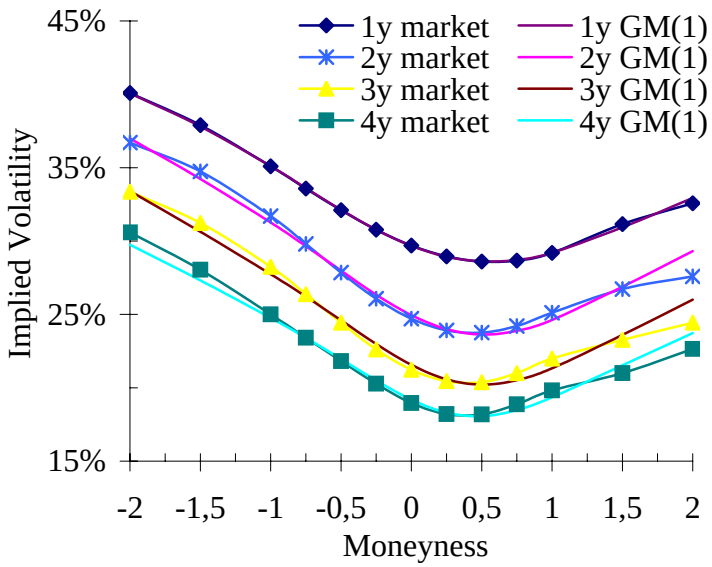

Figure 7.4: *The fit across moneynesses to the market implied caplet volatilities with Glasserman/Merener's jump model for different expiries.* $\sigma_1 = 17\%$, $\lambda_1(0) = 67\%$, $s_1(0) = 33\%$, $m_1(0) = -10\%$, $\sigma_2 = 11\%$, $\lambda_2(0) = 12\%$, $s_2(0) = 77\%$, $m_2(0) = -24\%$, $\sigma_3 = 9\%$, $\lambda_3(0) = 3\%$, $s_3(0) = 128\%$, $m_3(0) = -38\%$, $\sigma_4 = 7\%$, $\lambda_4(0) = 3\%$, $s_4(0) = 72\%$ *and* $m_4(0) = -1\%$.

As this change of measure leads to the fact that the jump process is no longer Poisson, the generated - more general - marked point process (MPP) has to be simulated when evolving the interest rates over time.

A marked point process exhibits two stochastic components: a stochastic point realization in time (= in this case influenced by the intensity of the jump process) and a stochastic size effect (= in this case the density of the jump size distribution). Further background on point processes can be found in [Bre81].

These MPPs are not that straightforward to implement, but they can be generated by having a Poisson process that is thinned. The main concept of this thinning algorithm is, first, to simulate a Poisson process with a sufficiently large arrival rate λ_0 and appropriate density for the jump sizes and then to determine probabilities for accepting these jumps of the Poisson process for the MPP.

In the special case of this model one starts with having n rates using n marked point processes (with the parameters $\sigma_i(0)$, $\lambda_i(0)$, $m_i(0)$ and $s_i(0)$ for the underly-

ing Poisson processes in the appropriate forward measure). Due to the thinning method it is sufficient to simulate one single Poisson process and then to thin all n marked point processes from this. This procedure leads to a very desirable property of the model: jumps of different forward rates occur at the same time and in the same direction.

In the market front end forward rates have a higher tendency to jump than rates with longer maturity. By appropriate choice of the parameters of the single jump processes, one can achieve that the set $I_i(t)$ of marked point processes, the forward rate $L_i(t)$ is sensitive to, equals:

$$I_i(t) \;=\; (i+1-\beta(t), i+2-\beta(t), \ldots, n) \tag{7.23}$$

with $\beta(t)$ is the index of the forward rate closest to its reset date.

With this construction, the rate that will mature next, $L_{\beta(t)}(t)$, is sensitive to all n MPPs, and if some rate $L_i(t)$ jumps then all rates maturing earlier than T_i also jump. Furthermore, if the term structure of volatilities is exactly time-homogeneous as e.g. in equation (2.11) "all rates follow, under their respective forward measures and for a fixed distance to their own maturities, the same stochastic differential equation."[14]

The appropriate choice of parameters mentioned to obtain the structure described in equation (7.23) is made if the parameters fulfill the restriction:

$$\begin{aligned} &\ln\left[\frac{s_{i+1}}{s_i}\right] - \frac{1}{2}z^2\left(\frac{1}{s_i^2} - \frac{1}{s_{i+1}^2}\right) + z\left(\frac{a_i}{s_i^2} - \frac{a_{i+1}}{s_{i+1}^2}\right) - \frac{1}{2}\left(\frac{a_i^2}{s_i^2} - \frac{a_{i+1}^2}{s_{i+1}^2}\right) \\ &\quad > \quad \ln\left[\frac{\lambda_{i+1}}{\lambda_i}\right] + \max\{0,z\} \;\text{ for } z \in \mathbb{R} \end{aligned} \tag{7.24}$$

where λ_i, a_i and s_i are short for $\lambda_i(0)$, $a_i(0)$ and $s_i(0)$

This restriction can be simplified to at least partially more intuitive restrictions:

1. $0 < w < 1$, i.e. the realistic assumption that forward rates jump more frequently the shorter the time to maturity is,

[14] See [GM01a], p. 10.

2. $0 < y < 1$, i.e. the realistic assumption that the closer the maturity date the more influence an information event has on the forward rate,
3. $y^2 s_i^2 \ln\left[\frac{y}{w}\right] - \frac{1}{2}a_i^2(y^2 - x^2) > 0$,
4. $\max\left\{a_i\frac{y^2-x}{y^2-1}; y^2 s_i^2 \ln\left[\frac{y}{w}\right] + \frac{1}{2}a_i^2\left(\frac{(y^2-x)^2}{y^2-1} - (y^2 - x^2)\right)\right\} > 0$,
5. $\max\left\{\frac{y^2 s_i^2 - a_i(y^2-x)}{y^2-1}; y^2 s_i^2\left(\ln\left[\frac{y}{w}\right] - \frac{a_i(y^2-x) - y^2 s_i^2}{y^2-1}\right) - \frac{1}{2}a_i^2(y^2 - x^2) + \frac{(a_i(y^2-x))^2 - y^4 s_i^4}{2y^2-2}\right\} > 0$

where

$$\begin{aligned} \lambda_{i+1} &= w\lambda_i, \\ a_{i+1} &= xa_i, \\ s_{i+1} &= ys_i. \end{aligned}$$

When one simulates the evolution of forward rates over time, the possible jump times of the underlying Poisson process can be determined even before simulating the evolution of the forward rates as they are not dependent upon the actual realization of the rates.[15]

Therefore, the arrival rate of the jumps for the underlying Poisson process is chosen to be:

$$\lambda_0 = \lambda_1 (2 + m_1). \tag{7.25}$$

and the density of the jump:

$$f(y) = \frac{f_1(y) + y f_1(y)}{2 + m_1}. \tag{7.26}$$

In the lognormal case of this model f_i has the density of $LN(a_n, s_n^2)$ leading to a mean of $1 + m_n$. The random value of y can then be computed as shown in Appendix A.5.

[15] See [GM01b], p. 7.

Then, the probability of a jump of the forward rate closest to maturity is given by:

$$p_{\beta(t)} = \frac{1+y\delta L_{\beta(t)}(t)}{1+\delta L_{\beta(t)}(t)}\frac{\lambda_1 f_1(y)}{\lambda_0 f(y)} = \frac{1+y\delta L_{\beta(t)}(t)}{\left(1+\delta L_{\beta(t)}(t)\right)(1+y)} \tag{7.27}$$

and for the forward rates $L_{\beta(t)+j+1}$, conditional on $L_{\beta(t)+j}$ jumping, by:

$$p_{\beta(t)+j+1} = \frac{1+y\delta L_{\beta(t)+j+1}}{1+\delta L_{\beta(t)+j+1}}\frac{\lambda_{j+2} f_{j+2}(y)}{\lambda_{j+1} f_{j+1}(y)}. \tag{7.28}$$

The result of the bootstrapping were the vectors $\overrightarrow{\sigma}_i$, $\overrightarrow{\lambda}_i$, $\overrightarrow{m}_i$ and $\overrightarrow{s}_i$. In this restricted model these values can also be used with an approximation where $T_r - t \gg T_s - T_r$ for a

Swaption Pricing Formula: ¬

$$\begin{aligned}&\text{Swaption}(0,T_r,T_s,NP,K,\overrightarrow{\sigma}_{r,s};\overrightarrow{\lambda}_{r,s},\overrightarrow{m}_{r,s},\overrightarrow{s}_{r,s})\\ &= NP\delta\sum_{i=r}^{s-1}P(0,T_{i+1})\left(S_{r,s}(0)\Pi_1 - K\Pi_2\right).\end{aligned} \tag{7.29}$$

For this approximation, using the previous results, the vectors $\overrightarrow{\sigma}_{r,s}$, $\overrightarrow{\lambda}_{r,s}$, $\overrightarrow{m}_{r,s}$ and $\overrightarrow{s}_{r,s}$ have to be computed.

Similar to equation (2.24) the volatility of the diffusion process can be determined by:[16]

$$\sigma^2_{r,s}(t) \approx \sum_{i=r}^{s-1}\sum_{j=r}^{s-1}\frac{\omega_i(0)\omega_j(0)L_i(0)L_j(0)\sigma_i(t)\sigma_j(t)\rho_{i,j}(t)}{S^2_{r,s}(0)}. \tag{7.30}$$

As the swap rate jumps with every forward rate resetting in T_i with $i = r,\ldots,s-1$ and in this restricted model the forward rate $L_i(t)$ can only jump when $L_{i-1}(t)$ is also jumping the arrival rate for jumps of the swap rate is given by:

$$\lambda_{r,s}(t) = \lambda_r(t). \tag{7.31}$$

[16] See [GM01c], p. 25-27.

The jump size and the volatility can be approximated by:

$$m_{r,s}(t) = \frac{\sum_{i=r}^{s-1} \lambda_i(t)\omega_i(0)L_i(0)m_i(t)}{\lambda_r(t)\sum_{j=r}^{s-1}\omega_j(0)L_j(0)}, \tag{7.32}$$

$$s_{r,s}^2(t) = \ln\left[\frac{\sum_{i=r}^{s-1}\sum_{j=r}^{s-1}\omega_{i,j}(0)\frac{\lambda_w(t)}{\lambda_r(t)}\left(e^{s_w^2(t)}(1+m_w(t))^2-2m_w(t)-1\right)}{(1+m_{r,s}(t))^2\sum_{i=r}^{s-1}\sum_{j=r}^{s-1}\omega_{i,j}(0)} + \frac{1+2m_{r,s}(t)}{(1+m_{r,s}(t))^2}\right] \tag{7.33}$$

where

$$\omega_{i,j}(0) = \omega_i(0)\omega_j(0)L_i(0)L_j(0),$$
$$w = \max\{i,j\}.$$

⌟

Calibration Quality w. r. t. the Full Term Structure Evolution

Glasserman/Merener's restricted jump model enables the time-homogeneous evolution with parameters that ensure a rather smooth development of the forward rate curve. Calibration of this model shows already for the caplet with expiry in two years an insufficient fit to the market implied volatility smile.

It can be seen at Figure 7.5 and the parameters s_1, s_2 and s_3 that are decreasing as slow as possible that the restriction $s_{i+1} < s_i$ is the main obstacle for a better fit to market data. Therefore, the thinning process ensures a meaningful joint evolution of forward rates but restricts degrees to freedom too much to enable a good fit to real market data.

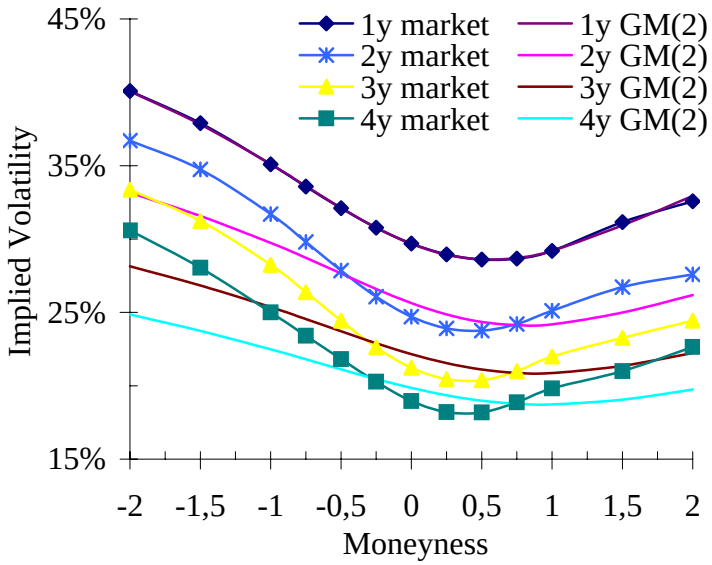

Figure 7.5: *The fit across moneynesses to the market implied caplet volatilities with Glasserman/Merener's restricted jump model for different expiries.* $\sigma_1 = 17\%$, $\lambda_1(0) = 67\%$, $s_1(0) = 33\%$, $m_1(0) = -10\%$, $\sigma_2 = 14\%$, $\lambda_2(0) = 27\%$, $s_2(0) = 31\%$, $m_2(0) = -19\%$, $\sigma_3 = 12\%$, $\lambda_3(0) = 6\%$, $s_3(0) = 30\%$, $m_3(0) = -19\%$, $\sigma_4 = 12\%$, $\lambda_4(0) = 4\%$, $s_4(0) = 20\%$ *and* $m_4(0) = -17\%$.

7.6 Comparison of the Different Models with Jump Processes

The basic model of Glasserman/Kou building on Merton's fundament with time-constant parameters for the density and the intensity of the jump process has been presented first in this chapter. This model is able to fit the volatility smile of forward rates close to maturity very good with reasonable parameters. For caplets with longer maturities the fit is still good but parameters are getting more and more cumbersome and unrealistic. This can only be slightly improved by a more leptokurtic distribution of the jump sizes in Kou's model.

Another problem of these two models are the time-constant parameters. They lead to very different jump processes for each forward rate when it is close to maturity. Besides that, the simultaneous simulation of the forward rates following such different jump processes would lead to a very uneven forward rate curve. A

model with time-dependent parameters for the jump process therefore has been introduced at length in the previous section. However, when using this model for calibrating one does not get a really good fit, but unrealistic parameters. When restricting these parameters to enable a simultaneous simulation of forward rates that leads to a realistic (i.e. smooth) forward rate curve, parameters are reasonable (by definition) but the fit already for caplets very close to expiry is insufficient. Therefore, jump models standing on their own fail to provide reasonable dynamics for the evolution of forward rates but might be interesting in combination with other previously discussed basic models.

Part III

Combined Models and Outlook

Chapter 8

Comparison of the Different Basic Models

In Part II of this thesis the four classes of basic extensions of the LIBOR market model have been introduced and several models been tested. All aspects mentioned in Section 3.3 have been discussed for each model separately with the exception of self-similar volatility smiles since one can examine this requirement best in a direct comparison of different models. After this little ”case study” a tabular overview of all models and their characteristic will be given leading eventually to a suggestion which models should be combined to approach the goal of a comprehensive smile model.

8.1 Self-Similar Volatility Smiles

The requirement of a smile model implying self-similar volatility smiles, i.e. forward volatility smiles that are similar to the actual volatility smile, is very often neglected when modeling the evolution of the forward rates since fitting caplet and swaption market data is a more obvious and compelling goal. Additionally, the future implied volatility smiles have influence on the prices of exotic options but these options are usually not liquid enough to extract these dynamics.

To clarify the effects of different model implied future volatility smiles a simplified pricing example is given. Since in all basic classes there are models that can generate symmetric volatility smiles the exemplary "market data" is:

$$\begin{aligned} L_2(0) &= 2\%, \\ \hat{\sigma}(0) &= 20\%, \\ \hat{\sigma}(\pm 2) &= 25\% \end{aligned}$$

with $\hat{\sigma}(M)$ being the annualized Black implied volatility for a caplet with moneyness M. This set of data has been chosen to enable all models to match the given volatilities exactly.

The following four models – one for each class of basic models – are compared:

1. **Mixture of Lognormals (Section 4.5),**
2. **Uncertain Volatility (Chapter 5),**
3. **Stochastic Volatility without Correlation (Section 6.2),**
4. **Lognormally Distributed Jumps (Section 7.3).**

The calibrated model parameters are given as:

- **For the local volatility and the uncertain volatility model (since both share exactly the same pricing formula):**
  $\theta = 41.5\%$ (i.e. $\sigma_1 = 8.3\%$, $\sigma_2 = 20\%$ and $\sigma_3 = 31.8\%$).
- **For the stochastic volatility model:**
  $\kappa = 10\%$ (chosen manually), $\varepsilon = 122\%$ and $\sigma = 22\%$.
- **For the jump model:**
  $\lambda = 20\%$ (chosen manually), $s = 38\%$, $a = -\frac{s^2}{2} = -7.1\%$ and $\sigma = 14\%$.

These parameters lead to the volatility smiles shown in Figure 8.1.

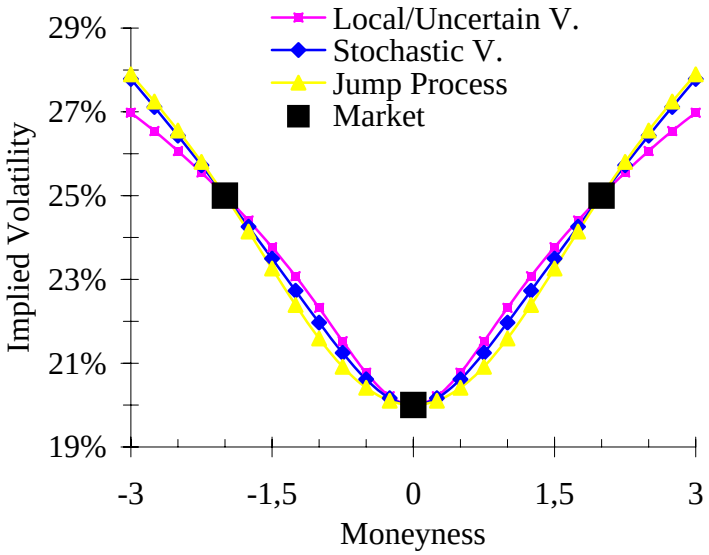

Figure 8.1: *Market data and implied volatility smiles for four different basic models for a caplet expiring in two years.*

Determining the model implied future volatility smile not only means to fix parameters but also in some cases to account for different underlying dynamics. More explicit, the ways to compute the future model implied volatility smile in each model are given as follows:

- **For the local volatility model:**
  The future volatility is still determined by (4.20). Therefore, one has to perform a simulation for time $t = 1$ to $t = 2$ for this given dynamics with $L_2(0) = 2\%$.

- **For the uncertain volatility model:**
  Since the time for the draw of the random variable is already over at time $t = 1$, the chosen scenario and the connected volatility $\sigma_{2,j}$ is already fixed with the probability $p_{2,j}$. In this case, the three scenarios occur with a probability of $\frac{1}{3}$ each.

- **For the stochastic volatility model:**
  To determine $V(1)$ one has to roll out the variance level. From the dis-

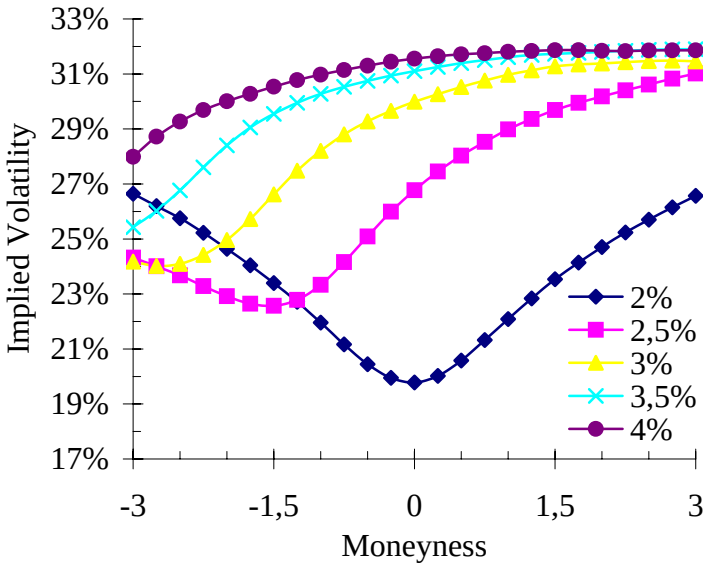

Figure 8.2: *Future volatility smiles implied by the local volatility model for different levels of the forward rate* $L_2(1)$.

tribution of $V(1)$ different possible future implied volatility smiles can be computed with (6.5) and (6.8).

- **For the model with a jump process:**
  Since the jump process is memoryless the future implied volatilities $\hat{\sigma}(M)$ are deterministic and the caplets can be priced for the expiry in 1 year with (7.8) with the same parameters as computed for expiry in 2 years previously.

To compare these future implied volatilities the volatility smiles are given in Figures 8.2 to 8.5. For comparability reasons the moneyness is computed with $\sigma = 20\%$ independent of the model implied volatility $\hat{\sigma}(0)$.

The only model where the future volatility smile depends upon the level of the forward rate is the local volatility model. Different smiles from different levels of the forward rate $L_2(1)$ are given in Figure 8.2. There it can be seen that the volatility smile is so-called "sticky strike", i.e. the minimum local volatility $\sigma(t; L_i(t))$ stays at the same strike independent of the level of the forward rate in future.

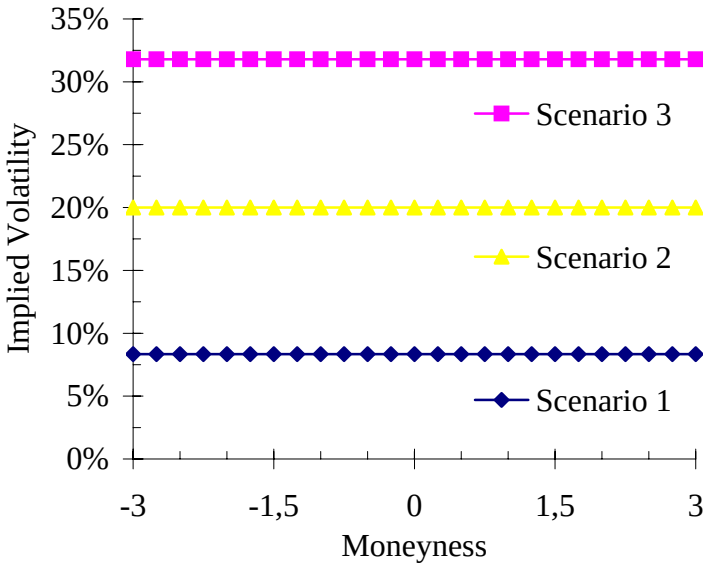

Figure 8.3: *Set of future volatility smiles implied by the uncertain volatility model.*

The other model with exactly the same pricing formula, the uncertain volatility model, leads to flat volatility smiles. One of the possible volatility scenarios is chosen directly after time 0. In this case each of the scenarios shown in Figure 8.3 occurs with a probability of 33.3%.

The stochastic volatility model leads to a far range of possible future volatility scenarios. In Figure 8.4 possible future volatility smiles are given. Since the process (6.2) is a martingale, the mean is $V(1) = 1$. The other volatility smiles are the 25%, the 50% (= median) and the 75% quantile of $V(1)$.

Finally, Figure 8.5 depicts the future smile implied by the jump model. This smile is independent of both the level of the forward rate and the number of jumps having occurred in the past.

In summary, the future smile implied by the local and the uncertain volatility model are not self-similar at all. Opposed to that the stochastic volatility model and the jump processes lead to volatility smiles that can be observed in the markets.

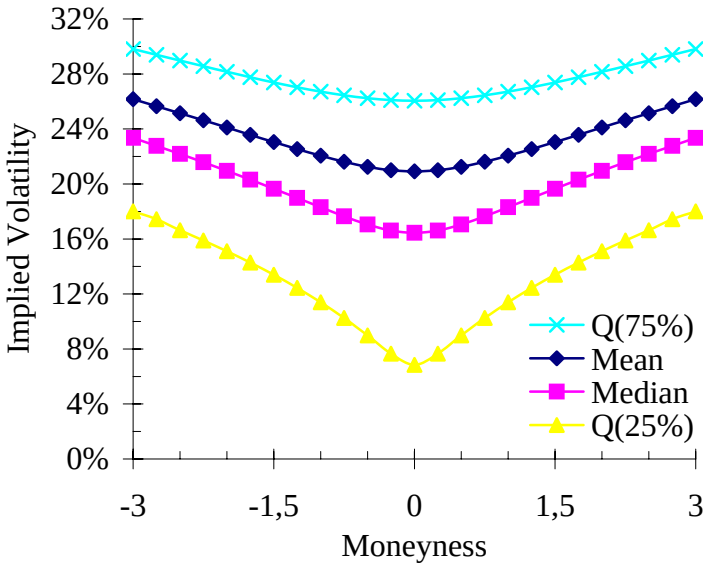

Figure 8.4: *Representatives of the future implied volatility smile by the stochastic volatility model.*

These findings certainly have a strong influence on the prices of exotic derivatives and further research should be done in this area. For example calculations how much exotic option prices depend upon the chosen model for the evolution of the interest rate and/or the volatility, see [BJN00], p. 851-855.

8.2 Conclusions from the Different Basic Models

After having discussed all possible aspects of these basic models from Section 4.1 to Section 8.1 in length a tabular overview of their characteristics is given in Table 8.1. While most of the fields in this table are obvious some classifications might also be chosen different, i.e. choosing ”true” instead of ”partially true” and vice versa. Furthermore, due to space restrictions not all fields for every single model have been reasoned throughout this thesis but in most cases should be apparent.

The ”uncombined” model seeming best to fit market data and implying reasonable dynamics is Wu/Zhang’s stochastic volatility model with correlation. However,

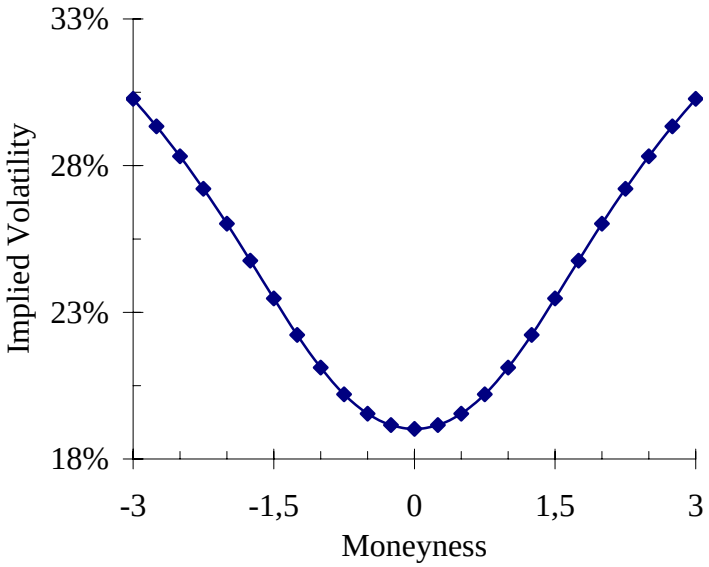

Figure 8.5: *Future volatility smile implied by the jump model.*

the tractability and also the fit for example to the US-$ data shown in Figure B.8 are not totally convincing.

The combination of some models might provide further possibilities. Since both stochastic volatility and jumps are observed in the market, this might be a very promising approach and will be presented in Chapter 9.1 additionally including CEV.

While this model including jumps, stochastic volatility and CEV seems like the ideal model for fitting the market implied volatility smiles a better tractable comprehensive smile model might be the combination of stochastic volatility and displaced diffusion. This DD approach can also be seen as a better tractable way of generating correlation between the forward rates and the volatility than Wu/Zhang's model. This model will be presented in Chapter 9.2.

Step (See Chapter 3.5)		1			2				3	4	5	6
Criteria / Model Name	Chapter	Number of Free Parameters	Exact Roll Out	No Substeps Needed	Only Positive Interest Rates	Exact Pricing Formula	Symmetric Volatility Smiles	Volatility Smirks	Volatility Skews	Fit to Market Data (Single Smile)	Time-Homogeneous	Fit to Market Data (Term Structure)	Self-Similar Smiles
Displaced Diffusion (DD)	4.1	1	X	X	-	X	-	X	-	-	-	-	(X)
Constant Elasticity of Variance (CEV)	4.2	1	X	-	(X)	X	-	X	-	-	-	-	(X)
Limited CEV	4.2	1	X	-	X	(X)	-	X	-	-	-	-	(X)
Mixture of Lognormals (MoL)	4.5	1+	X	-	X	X	X	-	-	-	(X)	-	-
Extended MoL	4.5	2+	X	-	-	X	X	X	X	X	(X)	(X)	-
Uncertain Volatility	5	1+	X	X	X	X	X	-	-	-	(X)	-	-
Stochastic Volatility (SV)	6.2	2	X	-	X	X	X	-	-	-	(X)	-	X
Joshi/Rebonato	6.3	2+	X	-	X	-	X	-	-	-	(X)	-	X
SV with Correlation	6.4	3	(X)	-	X	(X)	X	-	X	X	X	(X)	X
Lognormally Distributed Jumps (GK)	7.3	3	X	X	X	X	X	-	X	(X)	-	-	X
Leptokurtic Distributed Jumps (Kou)	7.4	3	X	X	X	X	X	-	X	(X)	-	-	X
Time-Homogeneous GK (GM)	7.5	3	X	X	X	X	X	-	X	(X)	(X)	(X)	X
Restricted GM	7.5	3	X	X	X	X	X	-	X	(X)	X	-	X

Table 8.1: *Comparison of the basic models and their characteristics. X = true, - = false, (X) = partially true.*

Chapter 9

Combined Models

At the end of the previous chapter two combined models have been suggested for being tested how they fit market data. Both imply reasonable joint forward rate dynamics that are important for exotic option pricing. For a good fit both models have to include stochastic volatility as this is the only way to generate a volatility smile for long-term options with realistic dynamics.

In the first model this stochastic volatility will be combined with jump processes and constant elasticity of variance. Since jumps are observed in the market and the CEV approach prohibits interest rates from becoming negative this might be a big step towards the ideal model for the forward rate dynamics.

The second model, the combination of stochastic volatility with the displaced diffusion approach, will be more tractable, e.g. efficient ways for calibrating the whole swaption matrix can be presented for the latter model.

Both models will be tested the same way as the basic models according to the scheme presented at the end of Section 3.5.

9.1 Stochastic Volatility with Jump Processes and CEV

Jarrow, Li and Zhao present in their paper this combined model with the following

Forward Rate Evolution:[1] ⌝

$$\frac{\mathrm{d}L_i(t)}{L_i(t^-)} = -\lambda_i m_i \,\mathrm{d}t + \left[L_i(t^-)\right]^{\gamma_i - 1} \sigma_i(t)\sqrt{V(t)}\,\mathrm{d}z_i + \mathrm{d}\left(\sum_{k=1}^{N_i}(J_k - 1)\right) \tag{9.1}$$

where $L_i(t^-)$ is the left side limit of the forward rate at time t and the other parameters are as given in the basic models discussed in Sections 4.2 and 7.3. The evolution of the variance is given by:

$$\mathrm{d}V(t) = \kappa(V(0) - V(t))\mathrm{d}t + \varepsilon\sqrt{V(t)}\mathrm{d}w \tag{9.2}$$

with the parameters as described in Section 6.2. ⌟

These dynamics lead to the

Caplet Pricing Formula: ⌝

$$\begin{aligned}&\mathrm{Caplet}(0, T_i, NP, K, \sigma_i; \gamma_i, \kappa, \varepsilon, \lambda_i, m_i, s_i)\\ &= NP\,\delta P(0, T_{i+1}) \sum_{j=0}^{\infty} \mathrm{e}^{-\lambda_i T_i} \frac{(\lambda_i T_i)^j}{j!} G\left(0, L_i^{(j)}, V(0), j\right)\end{aligned} \tag{9.3}$$

where[2]

$$L_i^{(j)} = L_i(0)\mathrm{e}^{-\lambda_i m_i T_i}(1 + m_i)^j, \tag{9.4}$$

$$G\left(0, L_i^{(j)}, V(0), j\right) = L_i^{(j)}\Phi(d_1) - K\Phi(d_2) \tag{9.5}$$

[1] See [JLZ02], p. 9f.
[2] See [JLZ02], p. 19.

with

$$\begin{aligned} d_1 &= \frac{\ln[L_i^{(j)}/K] + \frac{1}{2}\Omega^{(j)}\left(0, L_i^{(j)}, c\right)^2}{\Omega^{(j)}\left(0, L_i^{(j)}, c\right)}, \\ d_2 &= d_1 - \Omega^{(j)}\left(0, L_i^{(j)}, c\right), \\ \Omega^{(j)}\left(0, L_i^{(j)}, c\right) &= \sqrt{\Omega\left(0, L_i^{(j)}, c\right) + js_i^2}. \end{aligned}$$

For calculating Ω an expansion can be computed:

$$\begin{aligned} \Omega\left(0, L_i^{(j)}, c\right) &= \Omega_0\left(L_i^{(j)}\right)(cT_i)^{\frac{1}{2}} + \Omega_1\left(L_i^{(j)}\right)(cT_i)^{\frac{3}{2}} + O\left((T_i)^{\frac{5}{2}}\right), \quad (9.6) \\ \Omega_0\left(L_i^{(j)}\right) &= \frac{\ln\left[L_i^{(j)}/K\right]}{\int_K^{L_i^{(j)}} u^{-\gamma_i}\,\mathrm{d}u}, \\ \Omega_1\left(L_i^{(j)}\right) &= -\frac{\Omega_0\left(L_i^{(j)}\right)}{\left(\int_K^{L_i^{(j)}} u^{-\gamma_i}\,\mathrm{d}u\right)^2} \ln\left[\Omega_0\left(L_i^{(j)}\right)\sqrt{\left(L_i^{(j)}K\right)^{1-\gamma_i}}\right]. \end{aligned}$$

The variance c can be approximated by:

$$c = \bar{c} + \alpha_0\varepsilon^2 + \alpha_1\varepsilon^2 \ln\left[L_i^{(j)}/K\right]^2 + O\left(\varepsilon^4\right) \quad (9.7)$$

where[3]

$$\begin{aligned} \bar{c} &= \frac{V(0)}{T_i}\int_0^{T_i}\sigma_i^2(u)\mathrm{d}u, \\ \alpha_0 &= \frac{l_{1,2}}{(T_i)^2}\left(\Omega_{21} - \frac{1}{4}\Omega\left(0, L_i^{(j)}, \bar{c}\right)^2\Omega_{10}\right), \\ \alpha_1 &= \frac{l_{1,2}}{(T_i)^2}\Omega\left(0, L_i^{(j)}, \bar{c}\right)^{-2}\Omega_{10}. \end{aligned}$$

[3] See [ABR01], p. 31f.

with

$$\begin{aligned}
\Omega_{mn} &= \frac{\partial^m \Omega\left(0, L_i^{(j)}, \bar{c}\right)/\partial \bar{c}^m}{\partial^n \Omega\left(0, L_i^{(j)}, \bar{c}\right)/\partial \bar{c}^n}, \\
\Omega_{10} &= \frac{\Omega_0\left(L_i^{(j)}\right) + 3\bar{c}\,T_i\,\Omega_1\left(L_i^{(j)}\right)}{2\bar{c}\,\Omega_0\left(L_i^{(j)}\right) + 2\bar{c}^2 T_i\,\Omega_1\left(L_i^{(j)}\right)}, \\
\Omega_{21} &= \frac{-\Omega_0\left(L_i^{(j)}\right) + 3\bar{c}\,T_i\,\Omega_1\left(L_i^{(j)}\right)}{2\bar{c}\,\Omega_0\left(L_i^{(j)}\right) + 6\bar{c}^2 T_i\,\Omega_1\left(L_i^{(j)}\right)}
\end{aligned}$$

and[4]

$$\begin{aligned}
l_{1,2} &= \frac{1}{2}V(0)\int_0^{T_i} p^2(u)\mathrm{d}u, \\
p(t) &= \int_t^{T_i} \sigma_i^2(u)\mathrm{e}^{-\kappa(u-t)}\mathrm{d}u.
\end{aligned}$$

⌟

The problem of this closed form solution are the two approximations in (9.6) and (9.7). The first expansion for computing Ω makes the formula inaccurate for big T_i. The second expansion for computing c leads to convergence problems for $\varepsilon > 1$, i.e. for values that are usually obtained when calibrating to market data.[5]

One can improve the second expansion by increasing the order of the approximation with substituting in (9.7):

$$O\left(\varepsilon^4\right) = \varepsilon^4\left(\beta_0 + \beta_1 \ln\left[L_i^{(j)}/K\right]^2 + \beta_2 \ln\left[L_i^{(j)}/K\right]^4\right) + O\left(\varepsilon^6\right). \tag{9.8}$$

The values for β_0, β_1 and β_2 are given in Appendix A.6.

For options deep in or out of the money where $\ln\left[L_i^{(j)}/K\right]^4$ tends to grow to ∞ the

[4] See [ABR01], p. 12.
[5] See [ABR01], p. 35f.

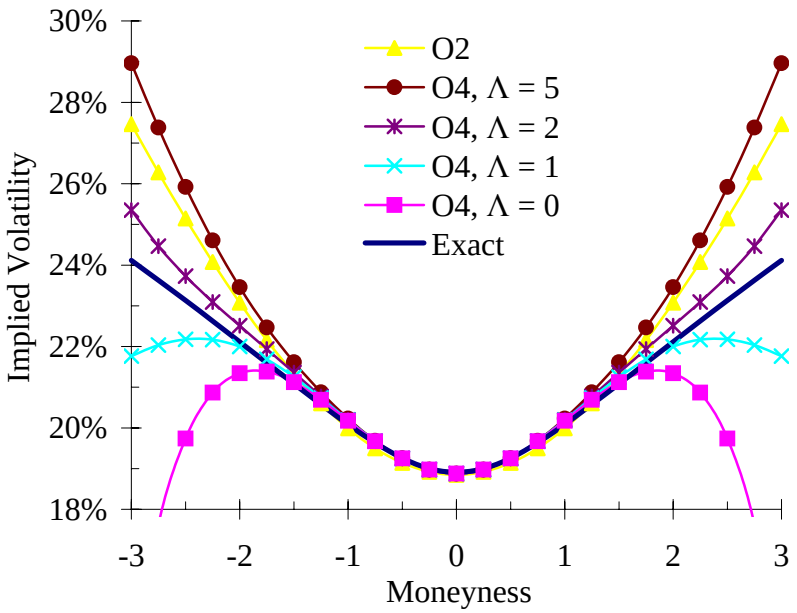

Figure 9.1: *Comparison between the exact solution from* (6.3) *and the basic expansion from* (9.7) *(= O2) and the higher order expansion from* (9.8) *(= O4) for different values of* Λ*. To be able to get a better comparison of these expansions the CEV and the jump processes are switched off.* $\sigma_1 = 20\%$, $\varepsilon = 120\%$ *and* $\kappa = 10\%$.

results are deteriorated. To avoid this β_2 is substituted by

$$\widehat{\beta}_2 = \beta_2 e^{-\Lambda\varepsilon^2 \ln\left[L_i^{(j)}/K\right]^2} \tag{9.9}$$

where Λ is some arbitrary small number (usually chosen between 1 and 10).

The implied volatility smiles for different expansions are shown in Figure 9.1. The problem is that different maturities and different sets of moneynesses would imply different Λ that best approximate the exact solution. This exact solution from Section 6.2 can not be used for pricing since the expansions are needed to incorporate jump processes and CEV for the closed form solution. Since usually a very low reversion speed κ fits market data best, these expansions could most probably not even be improved easily to a reasonable level since for small κ the approximate pricing formulæ are most inaccurate.[6]

[6] See [ABR01], p. 17.

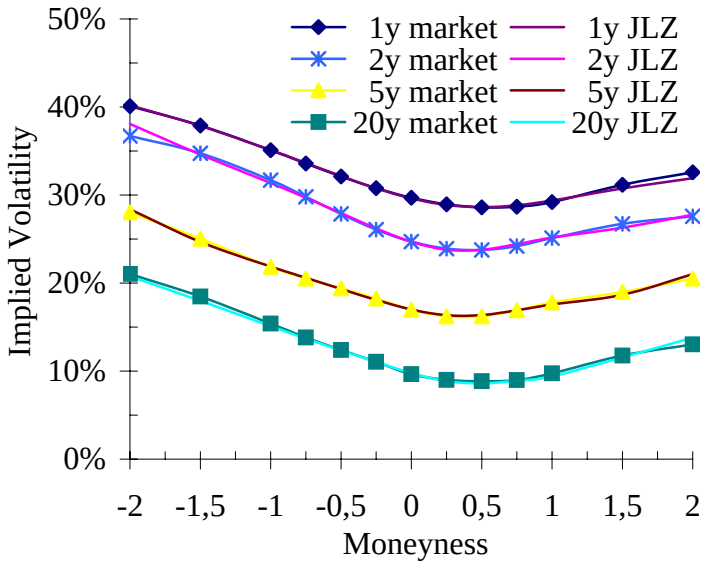

Figure 9.2: *The fit across moneynesses to the market implied caplet volatilities with Jarrow/Li/Zhao's combined model for different expiries.* $\varepsilon = 110\%$, $\kappa = 15\%$, $\sigma_1 = 19\%$, $\lambda_1 = 57\%$, $m_1 = -12\%$, $s_1 = 32\%$, $\gamma_1 = 98\%$, $\sigma_2 = 1.0\%$, $\lambda_2 = 32\%$, $m_2 = -11\%$, $s_2 = 42\%$, $\gamma_2 = 18\%$, $\sigma_5 = 2.9\%$, $\lambda_5 = 10\%$, $m_1 = -17\%$, $s_1 = 41\%$, $\gamma_5 = 51\%$, $\sigma_{20} = 0.3\%$, $\lambda_{20} = 0.9\%$, $m_{20} = -53\%$, $s_{20} = 171\%$, $\gamma_{20} = 0.3\%$

An exact closed form solution without convergence problems could be very useful in testing – similar to the work in [BCC97] – which of the basic models included is most important in providing a good fit to the market implied volatility smile.

Calibration Quality w. r. t. a Fixed Maturity

This comparison was performed in [JLZ02]. The parameters obtained in their paper rather show how easily a model with such a myriad of free parameters can be overfitted. Especially at meaningful parameters like the reversion level of the stochastic volatility process that logically should be at least at the same magnitude as the actual volatility this overfitting is obvious. For instance, calibrating a reversion level of 8.4 for caplets with 7 years maturity and 0.014 for caplets with 5 years maturity as was done in [JLZ02] can be regarded as an extremely problematic example.

For this reason when calibrating to market data as shown in Figure 9.2 the parameters for the stochastic volatility were set equal for all maturities. The reversion level has been set – as always throughout this thesis – to the actual level of volatility. Extremely little loss of accuracy is obtained when doing so, but both analytic tractability and parameter stability are improved. The results show how easily most volatility smiles can be fitted with this model. Parameters for the jump processes and the CEV, however, are not consistent for different expiries.

The main problem of this model remains the analytic tractability and the lack of methods to evolve the term structure of interest rates simultaneously.

9.2 Stochastic Volatility with DD

After the non-exact caplet pricing formula in the previous model a combination of stochastic volatility with displaced diffusion only needs slight modifications of the closed form solution from (6.3).

This model was presented in [AA02] with the following

Swap Rate Evolution: ⌝

$$\mathrm{d}S_{r,s}(t) \;=\; [\beta_{r,s}S_{r,s}(t)+(1-\beta_{r,s})S_{r,s}(0)]\,\sigma_{r,s}\sqrt{V(t)}\,\mathrm{d}z_{r,s} \tag{9.10}$$

and the evolution of the variance

$$\mathrm{d}V(t) \;=\; \kappa(V(0)-V(t))\mathrm{d}t+\varepsilon\sqrt{V(t)}\,\mathrm{d}w \tag{9.11}$$

where the parameters are as given in Section 6.2. ⌟

These dynamics lead to the

Swaption Pricing Formula: ⌝

$$\begin{aligned}&\mathrm{Swaption}(0,T_r,T_s,NP,K,\sigma_{r,s};\beta_{r,s},\kappa,\varepsilon)\\ &\quad=\; NP\,\delta\sum_{i=r}^{s-1}P(0,T_{i+1})\,\frac{f(S_{r,s}(0),T_r,K,\sigma_{r,s};\beta_{r,s},\kappa,\varepsilon)}{\beta_{r,s}}\end{aligned} \tag{9.12}$$

where

$$
\begin{aligned}
&f(S_{r,s}(0), T_r, K, \sigma_{r,s}; \beta_{r,s}, \kappa, \varepsilon) \\
&= \mathrm{Bl}(K', S_{r,s}(0), v) - \frac{S_{r,s}(0)}{2\pi} \int_{-\infty}^{\infty} \frac{\cos\omega\sqrt{e}}{\omega^2 + \frac{1}{4}} \left(H(0,\omega) - e^{-\left(\omega^2+\frac{1}{4}\right)v^2/2} \right) d\omega \quad (9.13)
\end{aligned}
$$

with

$$
\begin{aligned}
K' &= \beta_{r,s} K + (1-\beta_{r,s}) S_{r,s}(0), \\
v^2 &= \beta_{r,s}^2 \sigma_{r,s}^2 V(0) T_r.
\end{aligned}
$$

To compute $H(0,\omega)$ with (6.5) one has to substitute equation (6.7) with

$$
\frac{dB}{dt} = \frac{1}{2}\beta_{r,s}^2 \sigma_{r,s}^2 \left(\omega^2 + \frac{1}{4} \right) + \kappa B - \frac{1}{2}\varepsilon^2 B^2 \qquad (9.14)
$$

and the following calculations are as described in Section 6.2. ⌟

Calibration Quality w. r. t. a Fixed Maturity

When calibrating this model to market data again for the process of the variance the same parameters for all different expiries are used. For €-data this generates an acceptable fit (Figure 9.3), for US-$-data (Figure B.11) the same problem as for other models occurs: the skew is too strong to be fit by the model. Since the results are similar to the results of a stochastic volatility with correlation model (Section 6.4) the displaced diffusion can be regarded as a (mathematically) "cheap" way of modeling the correlation between volatility and the level of forward rates.

With the parameters κ and ε calibrated to the caplet volatility surface one can also fit swaptions with different tenors sufficiently in both markets (Figures 9.4 and B.12).

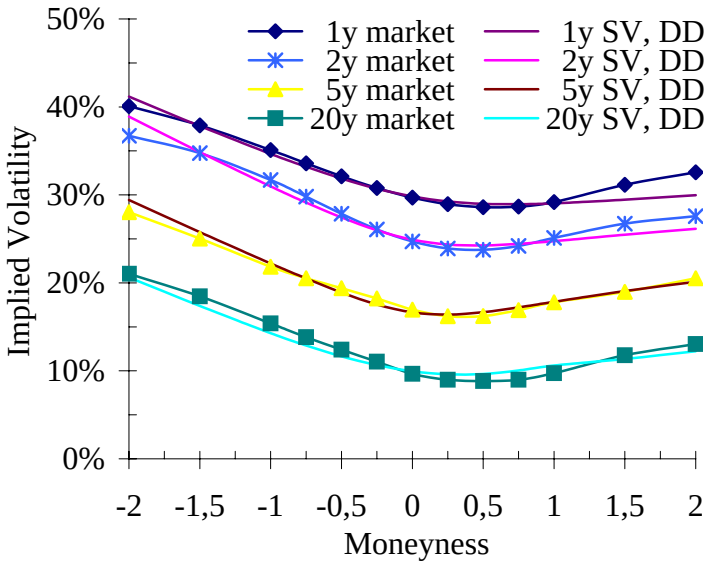

Figure 9.3: *The fit across moneynesses to the market implied caplet volatilities with the stochastic volatility and displaced diffusion model for different expiries.* $\sigma_{1,2} = 32\%$, $\beta_{1,2} = 35\%$, $\sigma_{2,3} = 28\%$, $\beta_{2,3} = 26\%$, $\sigma_{5,6} = 20\%$, $\beta_{5,6} = 27\%$, $\sigma_{20,21} = 14\%$, $\beta_{20,21} = 3\%$, $\varepsilon = 121\%$ *and* $\kappa = 4\%$.

Term Structure Evolution

Volatility smiles could be fitted sufficiently well with this underlying model. The missing part, however, is the connection between the time-constant parameters $\beta_{r,s}$ and $\sigma_{r,s}$ and a process for the forward rates so that these can be simulated. This has to be done since no general β and σ can be found that enables a sufficient fit to all market data.[7] A way of generating these dependencies efficiently was presented in [Pit03b].

Starting from the dynamics of the forward rate with time-dependent parameters under the terminal measure:

$$\mathrm{d}L_i(t) = [\beta_i(t)L_i(t) + (1-\beta_i(t))L_i(0)]\,\sigma_i(t)\sqrt{V(t)}\mathrm{d}z_i \qquad (9.15)$$

[7] See [Pit03b], p. 7f.

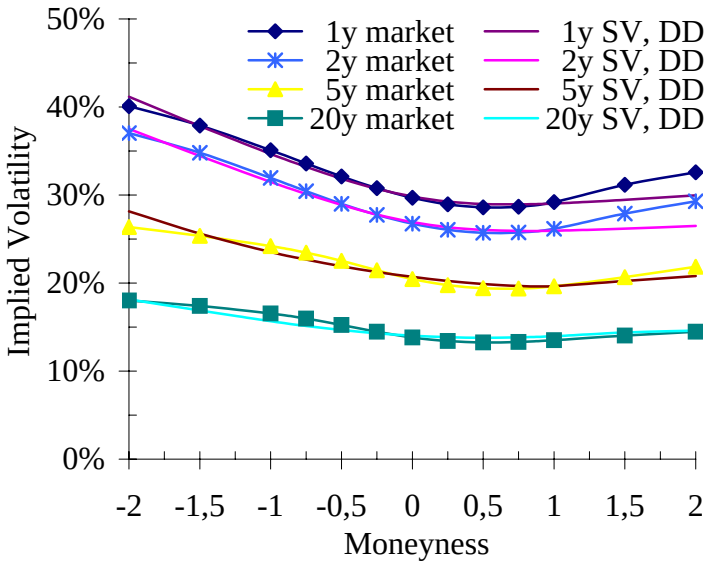

Figure 9.4: *The fit across moneynesses to the market implied swaption volatilities with the stochastic volatility and displaced diffusion model for expiry in one year and different tenors.* $\sigma_{1,2} = 32\%$, $\beta_{1,2} = 35\%$, $\sigma_{1,3} = 28\%$, $\beta_{1,3} = 21\%$, $\sigma_{1,6} = 22\%$, $\beta_{1,6} = 4\%$, $\sigma_{1,21} = 15\%$, $\beta_{1,21} = 8\%$, $\varepsilon = 121\%$ *and* $\kappa = 4\%$.

with the usual

$$\sigma_i(t)\mathrm{d}z_i \;=\; \sum_{k=1}^{m} \sigma_{ik}(t)\mathrm{d}z_{(k)}$$

one can approximate the dynamics of a swap rate in the drift free measure by

$$\mathrm{d}S_{r,s}(t) \;=\; \left[\beta_{r,s}(t)S_{r,s}(t) + (1-\beta_{r,s}(t)S_{r,s}(0)\right]\sqrt{V(t)}\sum_{k=1}^{m}\sigma_{r,s,k}(t)\mathrm{d}z_{(k)} \qquad (9.16)$$

where

$$\sigma_{r,s,k}(t) \;=\; \sum_{i=r}^{s-1} q_{r,s,i}\,\sigma_{ik}(t), \qquad (9.17)$$

$$\beta_{r,s}(t) \;=\; \sum_{i=r}^{s-1} p_{r,s,i}\,\beta_i(t) \qquad (9.18)$$

with

$$\begin{aligned} q_{r,s,i} &= \frac{L_i(0)}{S_{r,s}(0)} \frac{\partial S_{r,s}(0)}{\partial L_i(0)}, \\ \frac{\partial S_{r,s}(0)}{\partial L_i(0)} &= \overline{\omega}_i(0) \text{ from equation (2.22)}, \\ p_{r,s,i} &= ^{8} \frac{\sum_{k=1}^{m} \sigma_{ik}(t)\sigma_{r,s,k}(t)}{(s-r)\sum_{k=1}^{m} \sigma_{r,s,k}^2(t)} \end{aligned}$$

where m is the number of factors.

With this result, the approximate volatility and skew for every swaption can be calculated from the volatilities and skews of the forward rates. These values, however, are time-dependent as opposed to the time-constant values from calibrating market data with formula (9.12).

The time-constant skew can be calculated via:[9]

$$\beta_{r,s} = \int_0^{T_r} \beta_{r,s}(t) w_{r,s}(t) \mathrm{d}t \tag{9.19}$$

with

$$\begin{aligned} w_{r,s}(t) &= \frac{v_{r,s}^2(t)\sigma_{r,s}^2(t)}{\int_0^{T_r} v_{r,s}^2(t)\sigma_{r,s}^2(t)\mathrm{d}t}, \\ v_{r,s}^2(t) &= V(0)^2 \int_0^t \sigma_{r,s}^2(u)\mathrm{d}u + V(0)\varepsilon^2 \mathrm{e}^{-\kappa t} \int_0^t \sigma_{r,s}^2(u) \frac{\mathrm{e}^{\kappa u} - \mathrm{e}^{-\kappa u}}{2\kappa} \mathrm{d}u. \end{aligned}$$

The time-constant volatility can be calculated as the solution to:

$$\varphi_0\left(-\frac{g''(\zeta)}{g'(\zeta)}\sigma_{r,s}^2\right) = \varphi\left(-\frac{g''(\zeta)}{g'(\zeta)}\right) \tag{9.20}$$

[8] This equation corrects an error in the original article ([Pit03b], p. 8, 24).
[9] See [Pit03b], p. 11-14.

where

$$\begin{aligned} \zeta &= V(0)\int_0^{T_r}\sigma_{r,s}^2(t)\mathrm{d}t, \\ g(x) &= \frac{S_{r,s}(0)}{\beta_{r,s}}\left(2\Phi\left(\frac{\beta_{r,s}\sqrt{x}}{2}\right)-1\right). \end{aligned} \tag{9.21}$$

Then one can compute:

$$\begin{aligned} \frac{g''(x)}{g'(x)} &= \left(\ln\left[g'(x)\right]\right)' \\ &= \left(\ln\left[\frac{S_{r,s}(0)}{2\sqrt{x}}\phi\left(\frac{\beta_{r,s}\sqrt{x}}{2}\right)\right]\right)' \\ &= \left(\ln\left[\frac{S_{r,s}(0)}{2\sqrt{2x\pi}}\mathrm{e}^{-\beta_{r,s}^2 x/8}\right]\right)' \\ &= \left(\ln\left[\frac{S_{r,s}(0)}{2\sqrt{2\pi}}\right]-\frac{1}{2}\ln[x]-\frac{\beta_{r,s}^2 x}{8}\right)' \\ &= -\frac{1}{2x}-\frac{\beta_{r,s}^2}{8}. \end{aligned} \tag{9.22}$$

The function

$$\varphi(x) = \mathrm{e}^{A(0,x)-V(0)B(0,x)} \tag{9.23}$$

with $A(t,x)$ and $B(t,x)$ satisfying the differential equations

$$\begin{aligned} \frac{\mathrm{d}A}{\mathrm{d}t} &= -\kappa V(0)B, \\ \frac{\mathrm{d}B}{\mathrm{d}t} &= -\frac{1}{2}\varepsilon^2 B^2-\kappa B+x\sigma(t) \end{aligned}$$

and the final conditions

$$A(T_r,x) = 0, \qquad B(T_r,x) = 0$$

can be solved explicitly when using equations (A.21) and (A.22) in Appendix A.3 iteratively.[10]

[10] See [Pit03b], p. 31f.

The function $\varphi_0(x)$ can be solved as:

$$\begin{aligned}
\varphi_0(x) &= e^{A(0,x)-V(0)B(0,x)}, \\
B(0,x) &= \frac{2x\left(1-e^{-\gamma T_r}\right)}{(\kappa+\gamma)\left(1-e^{-\gamma T_r}\right)+2\gamma e^{-\gamma T_r}}, \\
A(0,x) &= {}^{11} \frac{2\kappa V(0)}{\varepsilon^2}\ln\left[\frac{2\gamma}{(\kappa+\gamma)\left(1-e^{-\gamma T_r}\right)+2\gamma e^{-\gamma T_r}}\right]-2\kappa V(0)\frac{x}{\kappa+\gamma}T_r, \\
\gamma &= \sqrt{\kappa^2+2\varepsilon^2 x}.
\end{aligned}$$

Calibration Quality w. r. t. the Full Term Structure Evolution

Using the just derived dependencies between the forward rate parameters $\sigma_i(t)$ and $\beta_i(t)$ and the time-constant swap rate parameters $\sigma_{r,s}$ and $\beta_{r,s}$ one does not have to calibrate the forward rate parameters directly to market implied volatilities but can divide this calibration into two steps. These dependencies are also summarized graphically in Figure 9.5.

First, the parameters of the stochastic volatility process ε and κ and for each expiry-tenor pair the parameters $\sigma_{r,s}$ and $\beta_{r,s}$ are calibrated to fit market implied volatilities best.

This step can be divided into two substeps:

1. **Calibration of ε and κ:**
   As there is exactly one variance process generating the volatility smile for all different expiries and tenors the parameters have to be the same for pricing all swaptions and caplets. To determine these two parameters the implied volatility smile is calibrated for different expiries and tenors simultaneously and the ε and κ leading to the minimum combined error are chosen.

2. **Calibration of $\beta_{r,s}$ and $\sigma_{r,s}$:**
   Using the two parameters for the stochastic volatility process the matrixes $\beta_{r,s}$ and $\sigma_{r,s}$ can be calibrated.

[11] This equation corrects an error in the original article ([Pit03b], p. 32).

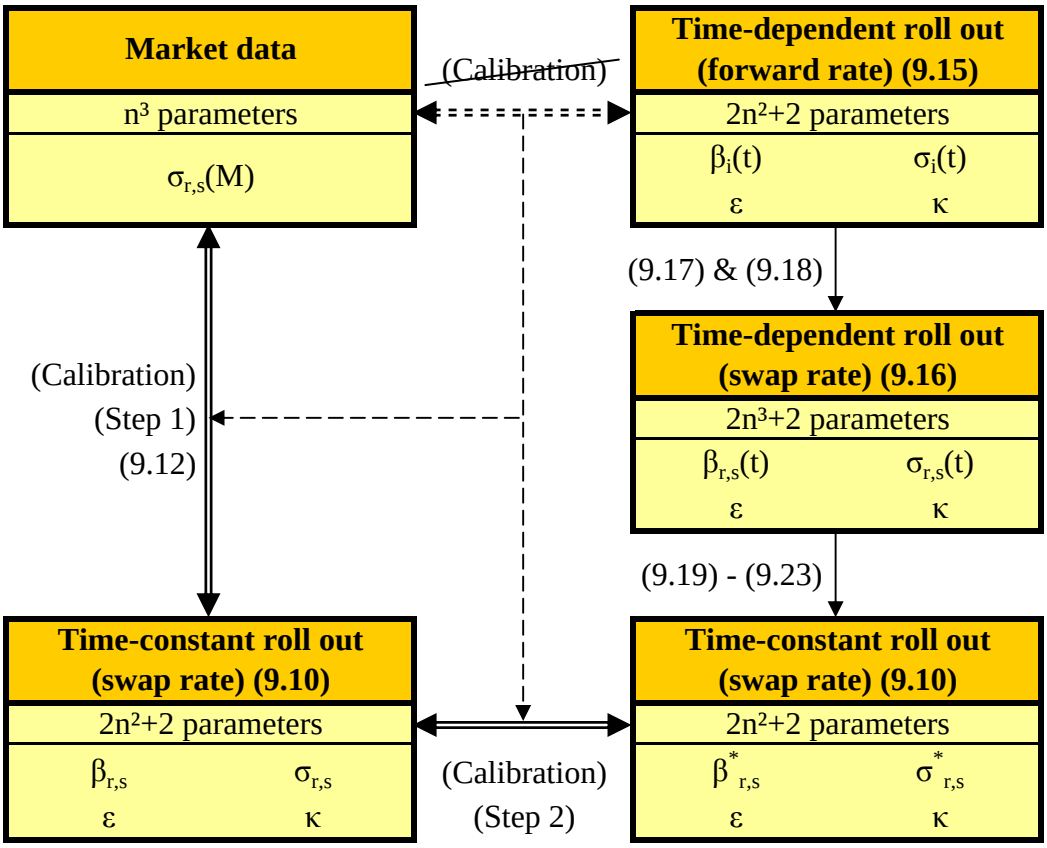

Figure 9.5: *The dependencies between the parameters of the forward rate and variance processes and swaption implied volatilities for the stochastic volatility and displaced diffusion model.*

Second, the forward rate parameters $\sigma_i(t)$ and $\beta_i(t)$ are calibrated to fit the just obtained swap rate skews and volatilities as good as possible.[12]

The second step can be further divided into 3 to 4 substeps:

1. **Calibration of $\sigma_i(t)$:**
   The matrix of parameters $\sigma_{r,s}$ is used to bootstrap the time-dependent forward rate volatilities $\sigma_i(t)$.

[12] The aim of exact time-homogeneous parameters can usually not be reached while maintaining an acceptable fit to market implied volatilities. Since this problem is always persistent when calibrating to market data even in the pure LIBOR market model, it should not be regarded as a problem caused by this specific model.

2. **Improving time-homogeneity of $\sigma_i(t)$:**
   These $\sigma_i(t)$ are calibrated with penalty functions for being more time-homogeneous while only slightly deteriorating the previously exact fit to the matrix $\sigma_{r,s}$.

3. **Calibration of $\beta_i(t)$:**
   The matrix of parameters $\beta_{r,s}$ is used to bootstrap the time-dependent forward rate skews $\beta_i(t)$. The obtained parameters are afterwards simultaneously calibrated to the matrix of $\beta_{r,s}$ improving the calibration.

4. **Improving time-homogeneity of $\beta_i(t)$:**
   These $\beta_i(t)$ could be optionally calibrated with penalty functions for being more time-homogeneous. However, an approximate time-homogeneity would lead to a heavy deterioration of the previously exact fit to the matrix $\beta_{r,s}$ and hence is usually not carried out.

Substeps 3 to 4 can be executed after substeps 1 and 2 since these two optimization problems are almost orthogonal.[13]

For better understanding this calibration procedure an example with real market data will be given. The parameters obtained are given in Tables C.1 to C.5 in Appendix C. Figures 9.6 and 9.7 show the obtained results on page 120. The calibration will be carried out for € market data for the swaption matrix with $s \leqq 11$, i.e. for a triangle matrix with expiries up to ten years and tenors up to ten years.

The calibration to market data leads in the first step to:[14]

$$\varepsilon = 134\%, \qquad \kappa = 12\%$$

and different $\beta_{r,s}$ and $\sigma_{r,s}$ for each expiry-tenor pair. The results are given in Table C.1.

[13] See [Pit03b], p. 15f.

[14] This result is different from the result obtained when calibrating data for Figure 9.3 since a different set of options has been chosen to calibrate to and a wide range of different ε-κ-pairs leads to very similar effects on the volatility smiles.

In the second step, simple bootstrapping of time-dependent but not time-homogeneous parameters $\sigma_i(t)$ as substep 1 leads to the values given in Table C.2. Further calibrating these $\sigma_i(t)$ with a function that additionally penalizes for non time-homogeneous values leads in substep 2 to the values given in Table C.3.

In substep 3 finally, the skew parameters $\beta_i(t)$ are bootstrapped and afterwards optimized leading to the values in Table C.4. The values 100% and -50% have been set as boundaries for any $\beta_i(t)$ since values outside this interval are considered unrealistic and especially for highly negative $\beta_i(t)$ also mathematically cumbersome. Both values are marked red in this table to show the problem of this bootstrapping and how far away from time-homogeneous parameters the bootstrapped parameters are. It has to be noted that imposing these boundaries leads – like in the unavoidable case of the volatility ($\sigma_i(t) \geq 0$) – to the fact that the bootstrapping cannot always exactly rebuild the matrix $\beta_{r,s}$.

The differences between the $\sigma_{r,s}$ and $\beta_{r,s}$ from step 1 and $\sigma^*_{r,s}$ and $\beta^*_{r,s}$ from step 2 are given in Table C.5.

For the two swaptions with the highest difference in the skew ($S_{5,6}$) and in the volatility grid ($S_{1,11}$) the calibrations are compared in Figures 9.6 and 9.7. There one can see clearly that 5.1% difference in $\beta_{r,s}$ leads to much smaller calibration differences than a 0.7% difference in $\sigma_{r,s}$. In both cases considering that these are the worst examples for the complete swaption matrix the fit seems sufficient.

Therefore, this model is able to fit the whole volatility surface of the swaption matrix, has approximately time-homogeneous volatilities and can be calibrated efficiently. The remaining problem are the skew parameters of the forward rates $\beta_i(t)$ since these parameters are not remotely time-homogeneous and both borders for possible values (-50% and 100%) are frequently touched in Table C.4. However, due to the strong effect of the stochastic volatility, future volatility smiles are more self-similar than for other models that provide a good fit to the volatility surface.

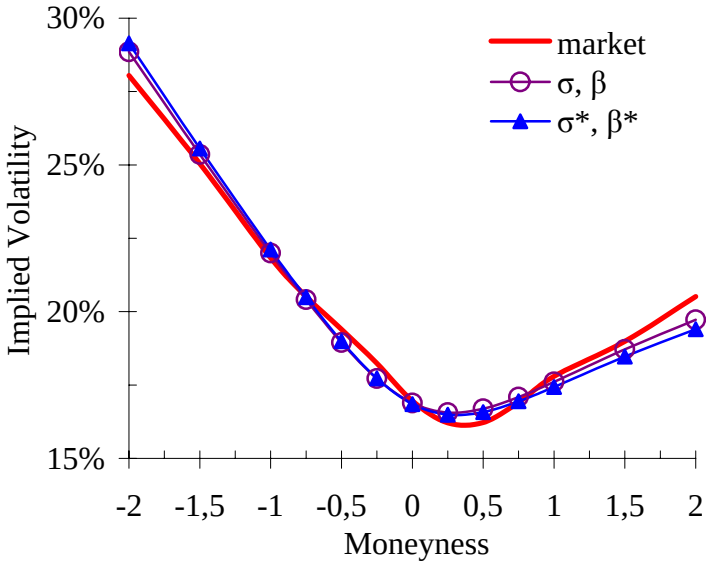

Figure 9.6: *Comparison between market and model implied volatilities in the SV & DD model for a caplet with expiry in 5 years.* σ *and* β *are the best parameters obtained in step 1,* σ^* *and* β^* *are the parameters obtained in steps 2 where the volatility was calibrated to be more time-homogeneous and the skew was bootstrapped.*

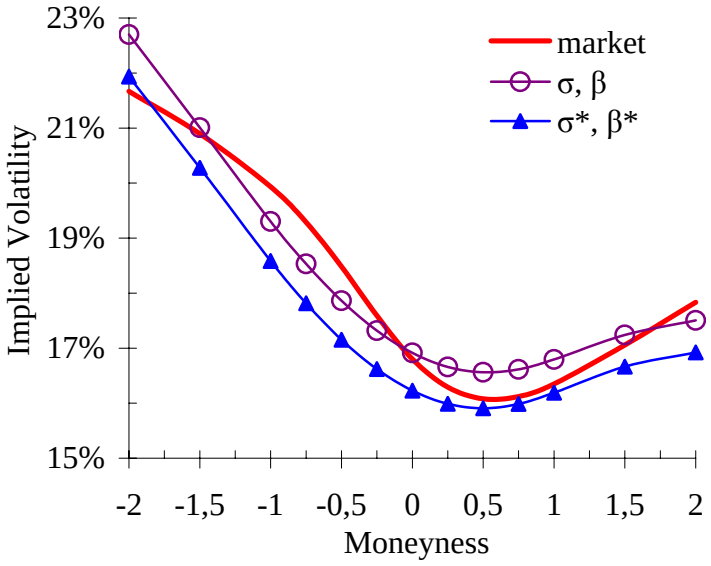

Figure 9.7: *Comparison between market and model implied volatilities in the SV & DD model for a swaption with expiry in one year and a tenor of 10 years.*

Chapter 10

Summary

The LIBOR market model is one of the most important interest rate models recently. The most demanding problem for using it successfully as a benchmark model is the volatility smile.

The LIBOR market model is usually simulated with Monte Carlo techniques, the most flexible implementation. Therefore, the forward process lends itself to a myriad of different extensions. The four most important extensions, in this thesis called ”basic models”, have been presented in Part II. While there are many ways of fitting a market given volatility smile the class of stochastic volatility models seems most important as these are the only models that can generate volatility smiles for long-term options implying reasonable future forward rate dynamics.

These dynamics – as has been discussed in Chapter 8 – are cumbersome for local and uncertain volatility models. Due to their analytic tractability and easy implementation these models are, however, the most popular for pricing derivatives including a volatility smile.

In Chapter 9 two combined models have been introduced. The first one, the combination of stochastic volatility with both jump processes and constant elasticity of variance, causes problems with the pricing formula and the time-homogeneous behavior of the forward rates. The second model does not share these drawbacks.

Since it combines stochastic volatility with displaced diffusion it has the shortcoming of possible negative interest rates.

As this second model – due to the extensions presented in [Pit03b] – can connect swaption implied volatilities to the forward rate parameters, it offers the possibility of exact time-homogeneous joint forward rate dynamics. When calibrating to market data, however, this exact time-homogeneity could only be reached for the cost of insufficient calibration results.

Future interesting developments for smile modeling in the LIBOR market model might be especially closed form solutions, e.g. for stochastic volatility combined with jump processes, for jump models with a more leptokurtic distribution for the jump size, and for more realistic distributions of the stochastic volatility process, since the lack of exact solutions makes many interesting ways of evolving the forward rates over time untractable or inefficient.

Appendix

Appendix A

Mathematical Methods

A.1 Determining the Implied Distribution from Market Prices

To determine the implied distribution $f_{L_i(T_i)}$ of the forward rate $L_i(T_i)$ at its reset date one starts with the option price $C(K)$ as a function of the strike K expressed as the expected payoff of the option in the terminal measure ($P(T_{i+1}, T_{i+1}) = 1$):[1]

$$C(K) \;=\; P(t, T_{i+1}) \int_{-\infty}^{\infty} \max\{s-K, 0\}\, f_{L_i(T_i)}(s)\mathrm{d}s. \tag{A.1}$$

The first derivative is then:

$$\begin{aligned} \frac{\partial C(K)}{\partial K} &= P(t, T_{i+1}) \int_{-\infty}^{\infty} -\mathbf{1}_{s \geqq K}\, f_{L_i(T_i)}(s)\mathrm{d}s & \text{(A.2)} \\ &= P(t, T_{i+1}) \int_{K}^{\infty} -f_{L_i(T_i)}(s)\mathrm{d}s. & \text{(A.3)} \end{aligned}$$

The second derivative equals:

$$\frac{\partial^2 C(K)}{\partial K^2} \;=\; P(t, T_{i+1})\, f_{L_i(T_i)}(K). \tag{A.4}$$

[1] See [BL78], p. 627 and [Fri04], p. 56f.

As this derivative can be approximated with differences of market prices:[2]

$$\frac{\partial^2 C(K)}{\partial K^2} \approx \frac{C(K+\Delta K)+C(K-\Delta K)-2C(K)}{\Delta K^2} \tag{A.5}$$

one can calculate the implied distribution as:

$$f_{L_i(T_i)}(K) = \frac{1}{P(t,T_{i+1})}\frac{C(K+\Delta K)+C(K-\Delta K)-2C(K)}{\Delta K^2}. \tag{A.6}$$

For better comparison of different distributions and calculating the skew and kurtosis, the moneyness $M = \frac{\ln\left[\frac{K}{L_i(t)}\right]}{\sigma_i\sqrt{T_i}}$ of the forward rate can be used. Since

$$\begin{aligned}\int_K^\infty f_{L_i(T_i)}(s)\mathrm{d}s &= \mathrm{Prob}\left(L_i(T_i) < K\right) \\ &= \mathrm{Prob}\left(M(T_i) < M\right) = \int_M^\infty f_{M(T_i)}(y)\mathrm{d}y\end{aligned}$$

with

$$M(T_i) = \frac{\ln\left[\frac{L_i(T_i)}{L_i(t)}\right]}{\sigma_i\sqrt{T_i}} \tag{A.7}$$

one can re-phrase (A.4) as

$$\frac{\partial^2 C(K)}{\partial K^2} = P(t,T_{i+1})\frac{f_{M(T_i)}(M)}{K\sigma_i\sqrt{T_i}}. \tag{A.8}$$

The implied distribution of the logarithm of the forward rate can then be calculated via:

$$f_{M(T_i)}(M) = \frac{K\sigma_i\sqrt{T_i}}{P(t,T_{i+1})}\frac{C\left(K+\Delta K\right)+C\left(K-\Delta K\right)-2C\left(K\right)}{\Delta K^2}. \tag{A.9}$$

Since these procedures are independent of the actual model the implied distributions of market and model prices can be easily compared.

[2] See [Sey00], p. 82.

A.2 Numerical Integration with Adaptive Step Size

When numerically integrating a fixed step size is usually not efficient as there are sections like singularities where small step sizes are important and other sections (especially when integrating a converging function to ∞) where extremely big step sizes are sufficient. The main idea of adaptive step sizes then is to integrate

$$I = \int_a^b f(x)\mathrm{d}x \tag{A.10}$$

with two different algorithms to obtain two approximations $I_1(a,b)$ and $I_2(a,b)$.[3] If the difference between these values is smaller then a chosen tolerance level (minimum tolerance is the machine precision), the better (i.e. the one with the higher expected accuracy) approximation is chosen as the value of the integral. Otherwise, one divides the integral in two parts

$$I = \int_a^m f(x)\mathrm{d}x + \int_m^b f(x)\mathrm{d}x \tag{A.11}$$

with $m = \frac{1}{2}(a+b)$ and then performs their integration independently.

For computing the approximative integrals in [GG98] the authors suggest the Simpson quadrature with

$$I_0(a,b) = (b-a)\frac{f(a)+4f(m)+f(b)}{6}, \tag{A.12}$$

$$\begin{aligned} I_1(a,b) &= I_0(a,m)+I_0(m,b) \\ &= (b-a)\frac{f(a)+4f\left(\frac{a+m}{2}\right)+2f(m)+4f\left(\frac{m+b}{2}\right)+f(b)}{12}. \end{aligned} \tag{A.13}$$

For improving the residual errors one step of Romberg extrapolation is used:[4]

$$I_2(a,b) = \frac{16I_1(a,b)-I_0(a,b)}{15}. \tag{A.14}$$

[3] See [GG98], p. 3-5.
[4] See [Ern02], p. 376.

For a termination criterion one can choose:

$$I_s \;\widehat{=}\; I_s + (I_2(a,b) - I_1(a,b)) \tag{A.15}$$

where I_s is a first (computational) guess (e.g. with Monte Carlo) for the value of the integral $[a,b]$ and $\widehat{=}$ denotes computational equivalence, i.e. with machine precision. When dividing the integral iteratively into more and more parts the same I_s is used even for all these subintervals as increasing the absolute accuracy for partial integrals with less weight is unnecessary and inefficient.

For every interval $[a,b]$ the integral is computed with 5 function calls in the first step. With handing over the obtained results to the computation of the partial integrals ($f(a), f\left(\frac{a+m}{2}\right)$ and $f(m)$ respective $f(m), f\left(\frac{m+b}{2}\right)$ and $f(b)$) only two additional function calls per each partial integral have to be computed leading to an efficient algorithm.

For well behaving and converging functions such as (6.8), (6.17), (6.18), (7.20), and (7.21) the main problem of numerical integration, the correctness of the obtained results, is usually not given.

A.3 Deriving a Closed-Form Solution to Riccati Equations with Piece-Wise Constant Coefficients

Given the general problem where coefficients are constant

$$\frac{\mathrm{d}A}{\mathrm{d}\tau} = a_0 B, \tag{A.16}$$

$$\frac{\mathrm{d}B}{\mathrm{d}\tau} = b_2 B^2 + b_1 B + b_0 \tag{A.17}$$

with the initial conditions

$$A(0) = A_0 \qquad \text{and} \qquad B(0) = B_0$$

one starts with solving for B as it is independent of A. The equation[5]

$$b_2 Y^2 + b_1 Y + b_0 \;=\; 0 \tag{A.18}$$

has two solutions

$$Y_\pm \;=\; \frac{-b_1 \pm d}{2b_2} \qquad \text{with} \qquad d \;=\; \sqrt{b_1^2 - 4b_0 b_2}. \tag{A.19}$$

Choosing Y_+ we consider the difference between Y_+ and B

$$Y_1 \;=\; B - Y_+.$$

Obviously, Y_1 satisfies

$$\begin{aligned}
\frac{\mathrm{d}Y_1}{\mathrm{d}\tau} &= \frac{\mathrm{d}(Y_1 + Y_+)}{\mathrm{d}\tau} \\
&= b_2(Y_1 + Y_+)^2 + b_1(Y_1 + Y_+) + b_0 \\
&\overset{\text{(A.19)}}{=} b_2 Y_1^2 + \overbrace{(2b_2 Y_+ + b_1)}\, Y_1 \\
&= b_2 Y_1^2 + dY_1
\end{aligned}$$

with the initial condition

$$Y_1(0) \;=\; B_0 - Y_+.$$

This Bernoulli equation can be solved explicitly

$$Y_1 \;=\; \frac{d}{b_2}\frac{g\mathrm{e}^{d\tau}}{\left(1 - g\mathrm{e}^{d\tau}\right)} \qquad \text{where} \qquad g \;=\; \frac{-b_1 + d - 2B_0 b_2}{-b_1 - d - 2B_0 b2} \tag{A.20}$$

[5] See [WZ02], p. 29f.

leading to the solution for B

$$\begin{aligned} B(\tau) &= Y_+ + Y_1 \\ &= \frac{-b_1+d}{2b_2} + \frac{d}{b_2}\frac{g\mathrm{e}^{d\tau}}{\left(1-g\mathrm{e}^{d\tau}\right)} \\ &= B_0 + \frac{(-b_1+d-2b_2B_0)\left(1-\mathrm{e}^{d\tau}\right)}{2b_2\left(1-g\mathrm{e}^{d\tau}\right)} \end{aligned} \tag{A.21}$$

and through integrating this result also to the solution of A

$$\begin{aligned} A(\tau) &= A_0 + a_0\int_0^\tau B(s)\mathrm{d}s \\ &= A_0 + a_0B_0\tau + \frac{a_0(-b_1+d-2b_2B_0)}{2b_2}\int_0^\tau \frac{1-\mathrm{e}^{d\tau}}{1-g\mathrm{e}^{d\tau}}\mathrm{d}\tau \\ &= A_0 + a_0B_0\tau + \frac{a_0(-b_1+d-2b_2B_0)}{2b_2}\left[\tau - \int_0^\tau \frac{(1-g)\mathrm{e}^{d\tau}}{1-g\mathrm{e}^{d\tau}}\mathrm{d}\tau\right] \\ &= A_0 + \frac{a_0(-b_1+d)\tau}{2b_2} - \frac{a_0(-b_1+d-2b_2B_0)}{2b_2d}\int_1^{\mathrm{e}^{d\tau}} \frac{1-g}{1-gu}\mathrm{d}u \\ &= A_0 + \frac{a_0(-b_1+d)\tau}{2b_2} - \frac{a_0(-b_1+d-2b_2B_0)}{2b_2d}\frac{g-1}{g}\ln\left[\frac{1-g\mathrm{e}^{d\tau}}{1-g}\right] \\ &= A_0 + \frac{a_0}{2b_2}\left((-b_1+d)\tau - 2\ln\left[\frac{1-g\mathrm{e}^{d\tau}}{1-g}\right]\right). \end{aligned} \tag{A.22}$$

A.4 Deriving the Partial Differential Equation for Heston's Stochastic Volatility Model

Similar to the Black-Scholes framework the partial differential equation in Heston's stochastic volatility model can be derived by a replication strategy.[6] The price of the derivative C is replicated by a portfolio X of the underlying stock A, the money market account (with the risk-free interest rate r) and another derivative

[6] See [Wys00], p. 4f.

W. The initial value X_0 of the portfolio evolves according to:

$$\mathrm{d}X = a\mathrm{d}A + b\mathrm{d}W + r(X - aA - bW)\mathrm{d}t \tag{A.23}$$

with a is the number of stocks and b is the number of the derivatives W in the portfolio.[7] From the exact equality for all times t:

$$X(t) = C(A,V,t) \tag{A.24}$$

follows the equality of the differentials:[8]

$$\begin{aligned}\mathrm{d}A &= \underbrace{\left\{\frac{\partial A}{\partial t} + \kappa(\theta - V)\frac{\partial C}{\partial V} + \mu A\frac{\partial C}{\partial A} + \frac{1}{2}\varepsilon^2 V\frac{\partial^2 C}{\partial V^2} + \frac{1}{2}VA^2\frac{\partial^2 C}{\partial A^2} + \rho\varepsilon VA\frac{\partial^2 C}{\partial A \partial V}\right\}}_{\tilde{C}}\mathrm{d}t \\ &\quad + \varepsilon\sqrt{V}\frac{\partial C}{\partial V}\mathrm{d}w + \sqrt{V}A\frac{\partial C}{\partial A}\mathrm{d}z \qquad (A.25)\\ \mathrm{d}X &= aA(\mu - r)\mathrm{d}t + a\sqrt{V}A\mathrm{d}z + rX\mathrm{d}t + b\mathrm{d}W - rbW\mathrm{d}t \qquad (A.26)\end{aligned}$$

with

$$\rho = \text{the correlation between the two Wiener processes } \mathrm{d}z \text{ and } \mathrm{d}w.$$

Since (A.25) is also valid for the second derivative W, one can insert this in equation (A.26) and write:

$$\begin{aligned}\varepsilon\sqrt{V}\frac{\partial C}{\partial V}\mathrm{d}w + \sqrt{V}A\frac{\partial C}{\partial A}\mathrm{d}z + \tilde{C}\mathrm{d}t &= aA(\mu - r)\mathrm{d}t + a\sqrt{V}A\mathrm{d}z + rX\mathrm{d}t \\ &\quad - rbW\mathrm{d}t + b\tilde{W}\mathrm{d}t + b\varepsilon\sqrt{V}\frac{\partial W}{\partial V}\mathrm{d}w + b\sqrt{V}A\frac{\partial W}{\partial A}\mathrm{d}z. \qquad (A.27)\end{aligned}$$

When setting the coefficients of the Wiener processes $\mathrm{d}z$ and $\mathrm{d}w$ equal on both

[7] The parameters a and b are time-dependent as they are the weight factors of a self-financing replication strategy but stay unchanged in the equation for the evolution of the portfolio. See [KK99], p. 62f, 67f, 70f.

[8] This can be derived with a two-dimensional version of Ito's Lemma, see [FPS00], p. 44.

sides of equation (A.27) one can write:

$$\begin{aligned} a\sqrt{V}A + b\sqrt{V}A\frac{\partial W}{\partial A} &= \sqrt{V}A\frac{\partial C}{\partial A}, \\ b\varepsilon\sqrt{V}\frac{\partial W}{\partial V} &= \varepsilon\sqrt{V}\frac{\partial C}{\partial V}. \end{aligned} \tag{A.28}$$

This leads to:

$$b = \frac{\frac{\partial C}{\partial V}}{\frac{\partial W}{\partial V}}, \tag{A.29}$$

$$a = \frac{\partial C}{\partial A} - \frac{\frac{\partial C}{\partial V}}{\frac{\partial W}{\partial V}}\frac{\partial W}{\partial A}. \tag{A.30}$$

From inserting (A.29) and (A.30) in (A.28) follows:

$$\begin{aligned} &\frac{1}{\frac{\partial W}{\partial V}}\left\{\frac{\partial W}{\partial t} + \kappa(\theta - V)\frac{\partial W}{\partial V} + rA\frac{\partial W}{\partial A} + \frac{1}{2}\varepsilon^2 V\frac{\partial^2 W}{\partial V^2}\right. \\ &\qquad \left. + \frac{1}{2}VA^2\frac{\partial^2 W}{\partial A^2} + \rho\varepsilon VA\frac{\partial^2 W}{\partial V\partial A} - rW\right\} \\ = \;& \frac{1}{\frac{\partial C}{\partial V}}\left\{\frac{\partial W}{\partial t} + \kappa(\theta - V)\frac{\partial C}{\partial V} + rA\frac{\partial C}{\partial A} + \frac{1}{2}\varepsilon^2 V\frac{\partial^2 C}{\partial V^2}\right. \\ &\qquad \left. + \frac{1}{2}VA^2\frac{\partial^2 C}{\partial A^2} + \rho\varepsilon VA\frac{\partial^2 C}{\partial V\partial A} - rC\right\} \end{aligned} \tag{A.31}$$

Since the left side of this equation only depends upon W, the right side only upon C and the derivative W can be chosen to be an arbitrary derivative with the same underlying stock, both sides of the equation must be equal to a function $\lambda(A,V,t)$, the so-called market price of risk/volatility. This function is chosen to be time-constant and independent of the actual stock price level and assumed to be proportional to the variance level:[9]

$$\lambda(A,V,t) = \lambda V. \tag{A.32}$$

[9] For stock price options the market price of risk is always positive.

Equations (A.31) and (A.32) lead to the following partial differential equation for Heston's model:

$$\begin{aligned} &\frac{1}{2}VA^2\frac{\partial^2 C}{\partial A^2}+\rho\varepsilon VA\frac{\partial^2 C}{\partial A\partial V}+\frac{1}{2}\varepsilon^2 V\frac{\partial^2 C}{\partial V^2}+rA\frac{\partial C}{\partial A} \\ &+ \quad [\kappa(\theta-V)-\lambda V]\frac{\partial C}{\partial V}-rC+\frac{\partial C}{\partial t} \;=\; 0. \end{aligned} \tag{A.33}$$

This partial differential equations can then be used to evolve an exact solution via Fourier transformation.[10] Similar equations lead to the exact caplet pricing formulæ in Chapter 6.

A.5 Drawing the Random Jump Size for Glasserman, Merener (2001)

To determine the random jump size in this model one has to produce a table with the cumulated distribution function (CDF), drawing an equally distributed random number and looking up the jump size in the table.

The density is given by:

$$f(y) \;=\; \frac{f_1(y)+y f_1(y)}{2+m_1} \tag{A.34}$$

with

$$\begin{aligned} f_1(y) &\sim LN(a_1, s_1^2), \\ m_1 &= \mathrm{e}^{a_1+s_1^2/2}-1. \end{aligned}$$

Then the density of $f_1(y)$:

$$f_1(y) \;=\; \frac{1}{\sqrt{2\pi}s_1 y}\mathrm{e}^{-\frac{1}{2}(\ln[y]-a_1)^2/s_1^2} \tag{A.35}$$

[10] See [Hes93], p. 330f.

leads to:

$$f(y) = \frac{1+y}{2+m_1} f_1(y) = \frac{1+y}{(2+m_1)\sqrt{2\pi}s_1 y} e^{-\frac{1}{2}(\ln[y]-a_1)^2/s_1^2}. \tag{A.36}$$

The CDF can then be computed via:

$$\begin{aligned}
F(y) &= \frac{1}{(2+m_1)\sqrt{2\pi}s_1} \underbrace{\int_0^y \frac{1+v}{v} e^{-\frac{1}{2}(\ln[v]-a_1)^2/s_1^2} dv}_{\text{substituting } x=\ln[v]} \\
&= \frac{1}{(2+m_1)\sqrt{2\pi}s_1} \int_{-\infty}^{\ln[y]} (1+e^x) e^{-\frac{1}{2}(x-a_1)^2/s_1^2} dx \\
&= \frac{1}{2+m_1} \left[\int_{-\infty}^{\ln[y]} \frac{1}{\sqrt{2\pi}s_1} e^{-\frac{1}{2}(x-a_1)^2/s_1^2} dx + \int_{-\infty}^{\ln[y]} \frac{e^x}{\sqrt{2\pi}s_1} e^{-\frac{1}{2}(x-a_1)^2/s_1^2} dx \right] \\
&\overset{11}{=} \frac{1}{2+m_1} \left[\Phi\left(\frac{\ln[y]-a_1}{s_1} \right) + e^{a_1+s_1^2/2} \Phi\left(\frac{\ln[y]-a_1-s_1^2}{s_1} \right) \right] \\
&= \frac{1}{2+m_1} \left[\Phi\left(\frac{\ln[y]-a_1}{s_1} \right) + (1+m_1) \Phi\left(\frac{\ln[y]-a_1-s_1^2}{s_1} \right) \right].
\end{aligned} \tag{A.37}$$

A.6 Parameters for Jarrow, Li, Zhao (2002)

The additional parameters β_0, β_1 and β_2 in the model of Jarrow, Li and Zhao introduced in Section 9.1 are given as follows:[12]

$$\begin{aligned}
\beta_0 &= -\frac{l_{2,3}}{(T_i)^3} \left(\Omega_{31} - \Omega_{21}^2 - \frac{1}{4}\Omega^2 \left(\Omega_{20} + \Omega_{10}^2 \right) + \left(\Omega_{21} - \frac{1}{4}\Omega^2 \Omega_{10} \right)^2 \right) \\
&\quad + \frac{1}{2} \frac{l_{1,2}^2}{(T_i)^4} \left[\Omega_{41} - 3\Omega_{31}\Omega_{21} + 2\Omega_{21}^3 - \frac{1}{4}\Omega^2\Omega_{30} - \frac{3}{4}\Omega^2\Omega_{10}\Omega_{20} \right. \\
&\quad \left. + 3 \left(\Omega_{21} - \frac{1}{4}\Omega^2\Omega_{10} \right) \left(\Omega_{31} - \Omega_{21}^2 - \frac{1}{4}\Omega^2 \left(\Omega_{20} + \Omega_{10}^2 \right) \right) \right]
\end{aligned} \tag{A.38}$$

[11] See [Fri04], p. 152.
[12] See [ABR01], p. 32.

and

$$\begin{aligned}\beta_1 &= \Omega^{-2}\Bigg\{-\frac{l_{2,3}}{(T_i)^3}\left(\Omega_{20}-3\Omega_{10}^2+2\Omega_{10}\left(\Omega_{21}-\frac{1}{4}\Omega^2\Omega_{10}\right)\right)\\ &\quad+\frac{1}{2}\frac{l_{1,2}^2}{(T_i)^4}\Bigg[\Omega_{30}-9\Omega_{10}\Omega_{20}+3\Omega_{10}\left(\Omega_{31}-\Omega_{21}^2-\frac{1}{4}\Omega^2\left(\Omega_{20}+\Omega_{10}^2\right)\right)\\ &\quad+12\Omega_{10}^3+3\left(\Omega_{21}-\frac{1}{4}\Omega^2\Omega_{10}\right)\left(\Omega_{20}-3\Omega_{10}^2\right)\Bigg]\Bigg\}, \qquad \text{(A.39)}\\ \beta_2 &= \Omega^{-4}\left(-\frac{l_{2,3}}{(T_i)^3}\Omega_{10}^2+\frac{3}{2}\frac{l_{1,2}^2}{(T_i)^4}\Omega_{10}\left(\Omega_{20}-3\Omega_{10}^2\right)\right) \qquad \text{(A.40)}\end{aligned}$$

where[13]

$$\begin{aligned}\Omega &= \Omega\left(0,L_i^{(j)},\bar{c}\right), \qquad \text{(A.41)}\\ l_{2,3} &= -\frac{1}{2}V(0)\int_0^{T_i}\mathrm{e}^{\kappa u}p(u)\int_u^{T_i}\mathrm{e}^{-\kappa v}p^2(v)\mathrm{d}v\,\mathrm{d}u. \qquad \text{(A.42)}\end{aligned}$$

Due to the nested nature of the triple integral $l_{2,3}$ ($p(t)$ is an integral itself) it can be numerically integrated in a single loop.

[13] See [ABR01], p. 12f.

Appendix B

Additional Figures

All figures given in this appendix are for US-$ caplets and swaptions.

To Section 3.2 Sample Data

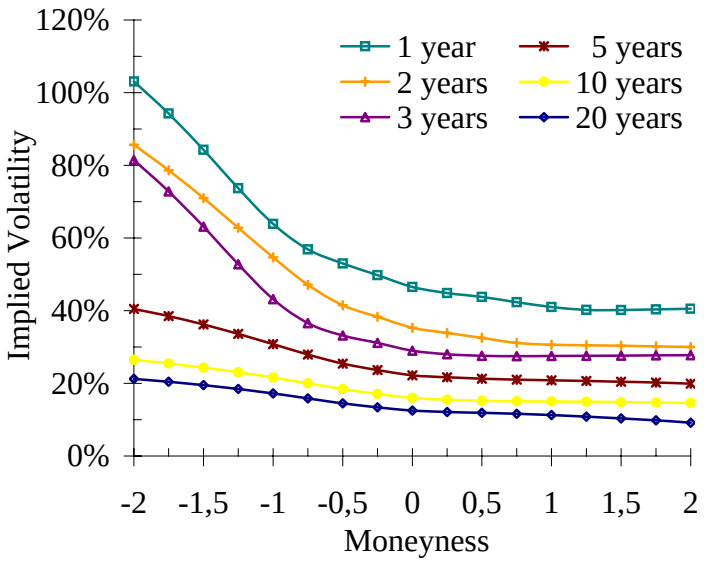

Figure B.1: *Caplet volatility smiles for different expiries.*

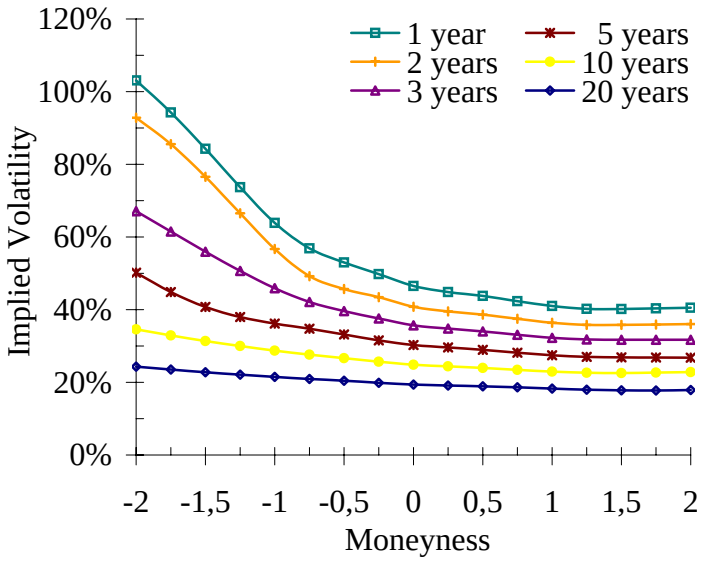

Figure B.2: *Swaption volatility smiles for 1 year expiry and different tenors.*

To Section 4.1 Displaced Diffusion

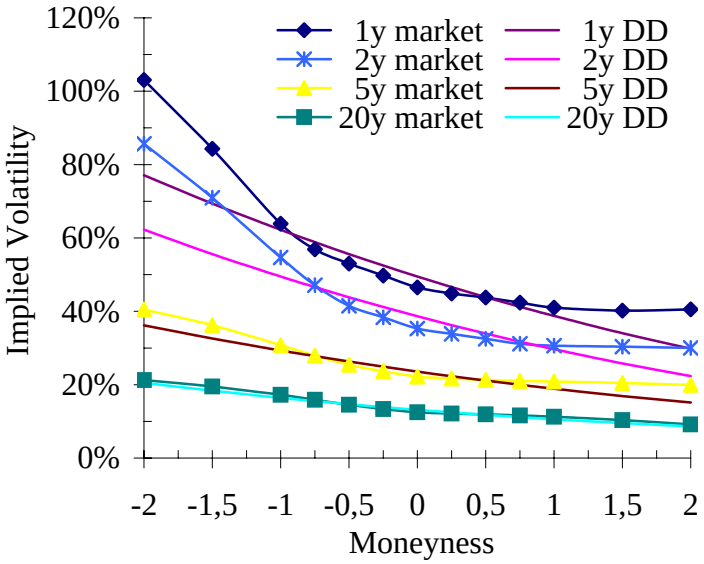

Figure B.3: *The fit across moneynesses to the market implied caplet volatilities with the displaced diffusion model for different expiries.* $\alpha_1 = 3300\%$, $\alpha_2 = 7700\%$, $\alpha_5 = 41.2\%$ *and* $\alpha_{20} = 21.1\%$.

To Section 4.2 Constant Elasticity of Variance

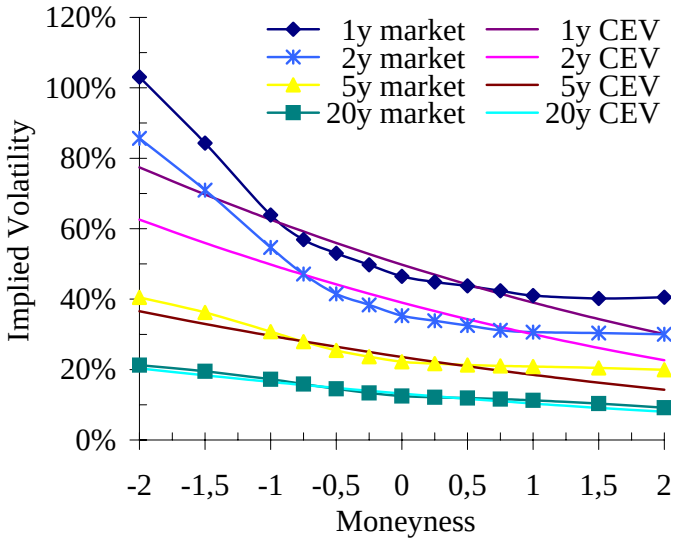

Figure B.4: *The fit across moneynesses to the market implied caplet volatilities with the constant elasticity of variance model for different expiries.* $\gamma_1 = 0.004$, $\gamma_2 = 0.008$, $\gamma_5 = 0.07$ *and* $\gamma_{20} = 0.18$.

To Section 4.5 Mixture of Lognormals

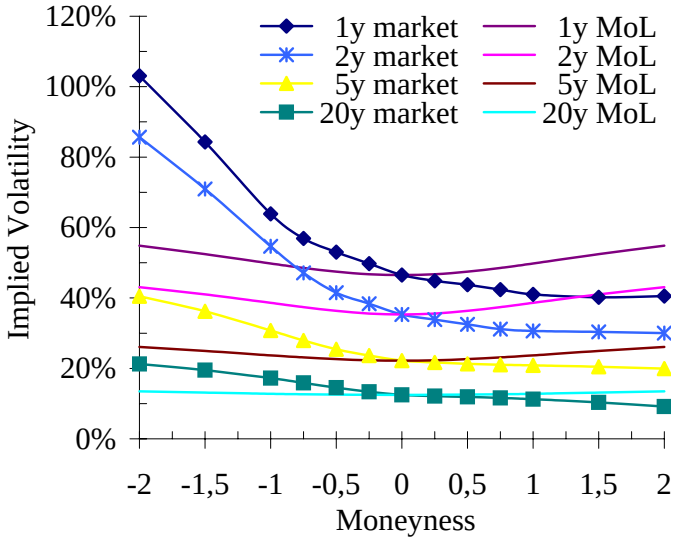

Figure B.5: *The fit across moneynesses to the market implied caplet volatilities with the mixture of lognormals model for different expiries.* $\theta_1 = 55\%$, $\theta_2 = 48\%$, $\theta_5 = 56\%$ *and* $\theta_{20} = 74\%$.

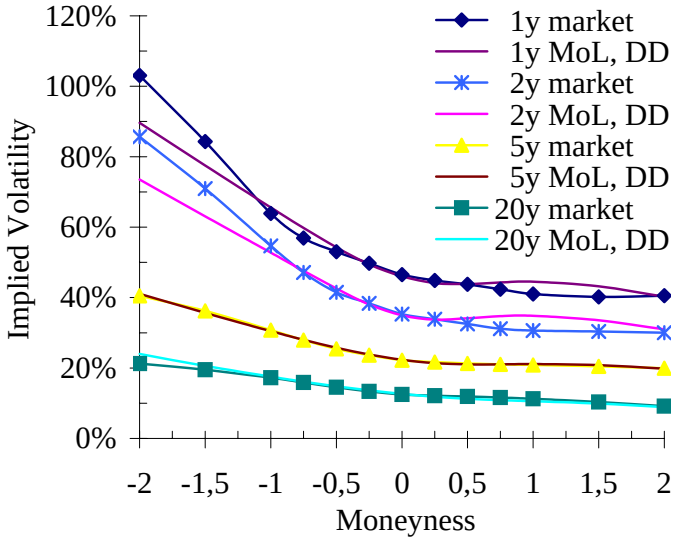

Figure B.6: *The fit across moneynesses to the market implied caplet volatilities with the extended mixture of lognormals model for different expiries.* $\beta_1 = 0\%$, $\tilde{\sigma}_{1,1} = 19\%$, $\tilde{\sigma}_{1,2} = 72\%$, $\beta_2 = 0\%$, $\tilde{\sigma}_{2,1} = 11\%$, $\tilde{\sigma}_{2,2} = 58\%$, $\beta_5 = 14\%$, $\tilde{\sigma}_{5,1} = 11\%$, $\tilde{\sigma}_{5,2} = 33\%$, $\beta_{20} = 0.2\%$, $\tilde{\sigma}_{20,1} = 8\%$ *and* $\tilde{\sigma}_{20,2} = 17\%$.

To Section 6.2 Andersen, Andreasen (2002)

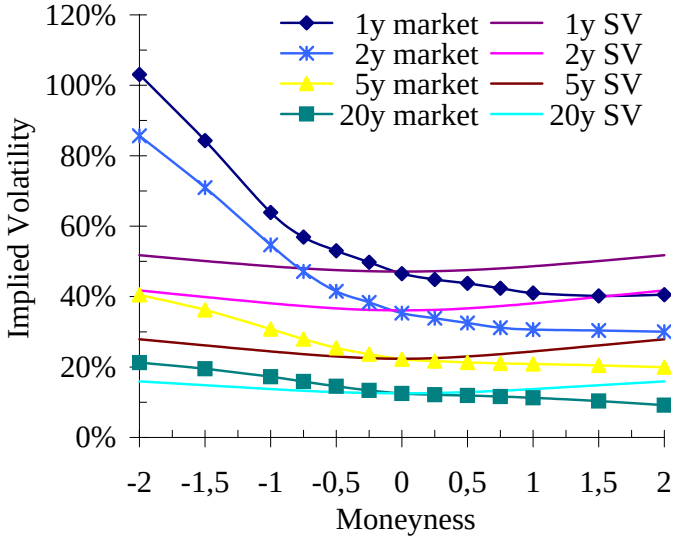

Figure B.7: *The fit across moneynesses to the market implied caplet volatilities with Andersen/Andreasen's stochastic volatility model for different expiries.* $\sigma_{1,2} = 49\%$, $\sigma_{2,3} = 38\%$, $\sigma_{5,6} = 25\%$, $\sigma_{20,21} = 14\%$, $\kappa = 12\%$ *and* $\varepsilon = 91\%$.

To Section 6.4 Wu, Zhang (2002)

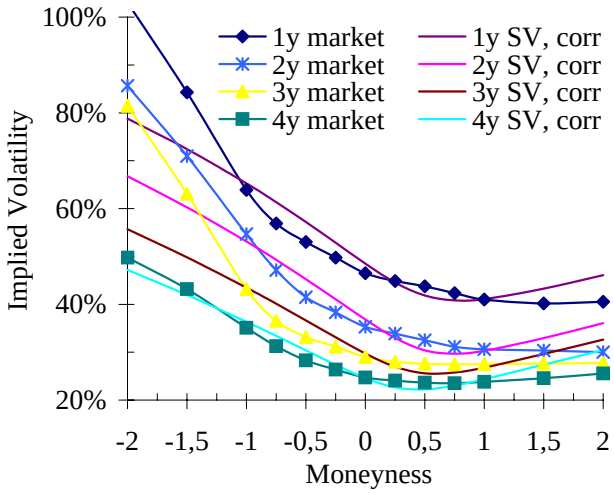

Figure B.8: *The fit across moneynesses to the market implied caplet volatilities with Wu/Zhang's stochastic volatility model with correlation for different expiries.* $\sigma_1 = 66\%$, $\rho_{1,V} = -65\%$, $\sigma_2 = 62\%$, $\rho_{2,V} = -73\%$, $\sigma_3 = 53\%$, $\rho_{3,V} = -65\%$, $\sigma_4 = 43\%$, $\rho_{4,V} = -55\%$, $\kappa = 4\%$ *and* $\varepsilon = 221\%$.

To Section 7.3 Glasserman, Kou (1999)

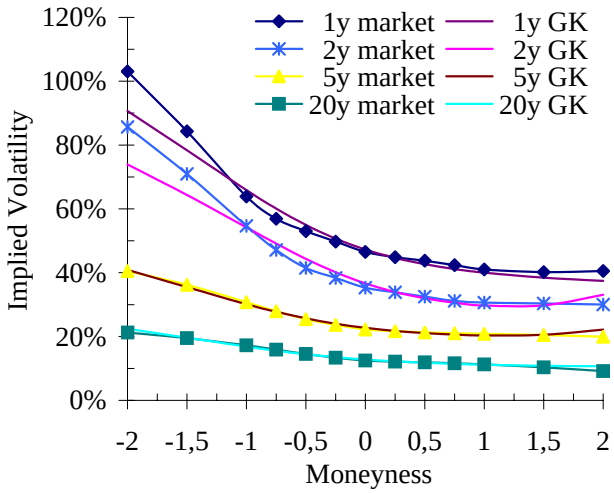

Figure B.9: *The fit across moneynesses to the market implied caplet volatilities with Glasserman/Kou's jump model for different expiries.* $\sigma_1 = 34\%$, $\lambda_1 = 11\%$, $s_1 = 357\%$, $m_1 = -99.99\%$, $\sigma_2 = 23\%$, $\lambda_2 = 8\%$, $s_2 = 546\%$, $m_2 = -97\%$, $\sigma_5 = 17\%$, $\lambda_5 = 2\%$, $s_5 = 254\%$, $m_5 = -89\%$, $\sigma_{20} = 10\%$, $\lambda_{20} = 1\%$, $s_{20} = 151\%$ *and* $m_{20} = -92\%$.

To Section 7.4 Kou (1999)

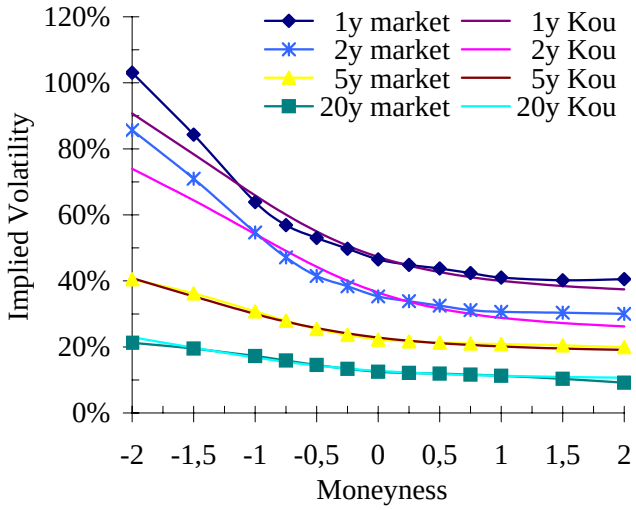

Figure B.10: *The fit across moneynesses to the market implied caplet volatilities with Kou's jump model for different expiries.* $\sigma_1 = 34\%$, $\lambda_1 = 11\%$, $\eta_1 = 500\%$, $\xi_1 = -15$, $\sigma_2 = 23\%$, $\lambda_2 = 8\%$, $\eta_2 = 500\%$, $\xi_2 = -18.6$, $\sigma_5 = 17\%$, $\lambda_5 = 2\%$, $\eta_5 = 254\%$, $\xi_5 = -5.4$, $\sigma_{20} = 10\%$, $\lambda_{20} = 1\%$, $\eta_{20} = 151\%$ *and* $\xi_{20} = -3.7$.

To Section 9.2 Stochastic Volatility with DD

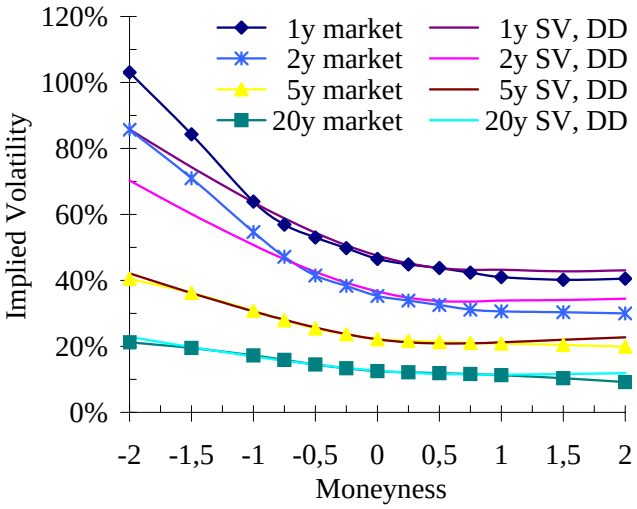

Figure B.11: *The fit across moneynesses to the market implied caplet volatilities with the stochastic volatility and displaced diffusion model for different expiries.* $\sigma_{1,2} = 53\%$, $\beta_{1,2} = 3\%$, $\sigma_{2,3} = 42\%$, $\beta_{2,3} = 3\%$, $\sigma_{5,6} = 26\%$, $\beta_{5,6} = 10\%$, $\sigma_{20,21} = 14\%$, $\beta_{20,21} = 20\%$, $\varepsilon = 200\%$ *and* $\kappa = 35\%$.

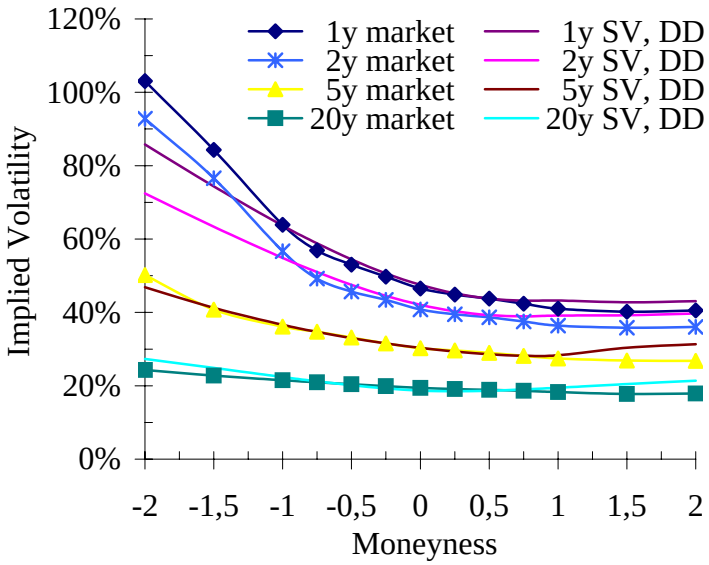

Figure B.12: *The fit across moneynesses to the market implied swaption volatilities with the stochastic volatility and displaced diffusion model for expiry in one year and different tenors.* $\sigma_{1,2} = 53\%$, $\beta_{1,2} = 3\%$, $\sigma_{1,3} = 47\%$, $\beta_{1,3} = 3\%$, $\sigma_{1,6} = 33\%$, $\beta_{1,6} = 2\%$, $\sigma_{1,21} = 21\%$, $\beta_{1,21} = 15\%$, $\varepsilon = 200\%$ *and* $\kappa = 35\%$.

Appendix C

Calibration Tables for SV and DD

$\sigma_{r,s}$		Tenors (T_s-T_r)									
		1y	2y	3y	4y	5y	6y	7y	8y	9y	10y
Expiries (T_r)	1y	31,7%	28,6%	25,6%	23,4%	21,8%	20,9%	20,0%	19,3%	18,7%	18,0%
	2y	27,8%	24,4%	22,5%	20,9%	19,4%	18,7%	17,9%	17,4%	16,8%	-
	3y	24,7%	22,4%	20,6%	19,1%	17,8%	17,3%	16,7%	16,2%	-	-
	4y	22,4%	20,6%	18,9%	17,7%	16,7%	16,2%	15,7%	-	-	-
	5y	20,2%	18,9%	17,4%	16,4%	15,7%	15,3%	-	-	-	-
	6y	18,7%	17,8%	16,5%	15,8%	15,2%	-	-	-	-	-
	7y	17,2%	16,5%	15,6%	15,1%	-	-	-	-	-	-
	8y	16,6%	15,9%	15,1%	-	-	-	-	-	-	-
	9y	15,9%	15,3%	-	-	-	-	-	-	-	-
	10y	15,2%	-	-	-	-	-	-	-	-	-

$\beta_{r,s}$		Tenors (T_s-T_r)									
		1y	2y	3y	4y	5y	6y	7y	8y	9y	10y
Expiries (T_r)	1y	34,7%	20,7%	6,2%	6,2%	3,7%	4,0%	6,8%	6,8%	7,0%	7,1%
	2y	25,6%	10,5%	5,5%	5,8%	2,8%	5,6%	3,0%	3,2%	3,4%	-
	3y	28,1%	11,4%	6,6%	2,9%	2,7%	2,8%	2,9%	2,9%	-	-
	4y	25,2%	17,0%	8,7%	3,2%	3,1%	2,9%	2,7%	-	-	-
	5y	27,5%	14,1%	12,6%	2,7%	2,9%	2,7%	-	-	-	-
	6y	18,0%	12,7%	5,3%	3,1%	3,0%	-	-	-	-	-
	7y	5,3%	3,4%	3,0%	3,3%	-	-	-	-	-	-
	8y	3,4%	3,3%	3,1%	-	-	-	-	-	-	-
	9y	3,2%	3,1%	-	-	-	-	-	-	-	-
	10y	3,0%	-	-	-	-	-	-	-	-	-

Table C.1: *Calibrated parameters $\sigma_{r,s}$ and $\beta_{r,s}$ after step 1.*

$\sigma_i(t)$		Forward rate resetting in (T_i-t)									
		1y	2y	3y	4y	5y	6y	7y	8y	9y	10y
Time t	0y	31,7%	26,5%	22,1%	19,9%	19,3%	21,0%	19,2%	20,5%	19,3%	17,4%
	1y	29,0%	21,6%	21,2%	17,4%	11,3%	19,9%	11,8%	18,5%	17,8%	-
	2y	29,5%	21,3%	17,7%	18,2%	5,4%	22,3%	13,8%	17,6%	-	-
	3y	26,6%	22,1%	15,5%	18,4%	5,0%	17,7%	13,4%	-	-	-
	4y	23,6%	23,2%	13,0%	15,0%	7,7%	17,8%	-	-	-	-
	5y	20,2%	26,0%	14,6%	14,1%	6,1%	-	-	-	-	-
	6y	9,6%	28,5%	11,2%	15,8%	-	-	-	-	-	-
	7y	3,0%	29,5%	7,0%	-	-	-	-	-	-	-
	8y	3,0%	26,4%	-	-	-	-	-	-	-	-
	9y	3,0%	-	-	-	-	-	-	-	-	-

Table C.2: *Bootstrapped parameters $\sigma_i(t)$ after step 2, substep 1.*

$\sigma_i(t)$		Forward rate resetting in (T_i-t)									
		1y	2y	3y	4y	5y	6y	7y	8y	9y	10y
Time t	0y	31,2%	26,9%	22,9%	20,7%	19,0%	18,1%	17,6%	17,2%	16,5%	15,6%
	1y	27,6%	23,9%	20,6%	18,1%	16,5%	15,7%	15,4%	15,3%	15,3%	-
	2y	25,6%	22,5%	19,1%	16,7%	15,1%	14,4%	14,0%	14,1%	-	-
	3y	23,8%	21,0%	18,2%	15,9%	14,6%	13,9%	13,2%	-	-	-
	4y	22,8%	20,6%	18,0%	16,1%	14,9%	14,1%	-	-	-	-
	5y	21,7%	19,7%	17,5%	15,8%	14,6%	-	-	-	-	-
	6y	20,6%	19,0%	17,1%	15,5%	-	-	-	-	-	-
	7y	20,0%	18,6%	16,8%	-	-	-	-	-	-	-
	8y	19,4%	18,3%	-	-	-	-	-	-	-	-
	9y	18,9%	-	-	-	-	-	-	-	-	-

$\sigma^*_{r,s}$		Tenors (T_s-T_r)									
		1y	2y	3y	4y	5y	6y	7y	8y	9y	10y
Expiries (T_r)	1y	31,2%	28,6%	25,9%	23,8%	22,1%	20,8%	19,7%	18,8%	18,0%	17,3%
	2y	27,2%	24,9%	22,9%	21,2%	19,9%	18,8%	17,9%	17,2%	16,5%	-
	3y	24,1%	22,4%	20,8%	19,3%	18,2%	17,3%	16,5%	15,9%	-	-
	4y	21,9%	20,4%	19,0%	17,8%	16,9%	16,1%	15,5%	-	-	-
	5y	20,1%	18,9%	17,7%	16,8%	16,0%	15,3%	-	-	-	-
	6y	18,7%	17,7%	16,8%	16,0%	15,3%	-	-	-	-	-
	7y	17,6%	16,8%	16,0%	15,3%	-	-	-	-	-	-
	8y	16,9%	16,2%	15,5%	-	-	-	-	-	-	-
	9y	16,3%	15,7%	-	-	-	-	-	-	-	-
	10y	15,7%	-	-	-	-	-	-	-	-	-

Table C.3: *Optimized parameters $\sigma_i(t)$ and the resulting $\sigma^*_{r,s}$ after step 2, substep 2.*

$\beta_i(t)$		Forward rate resetting in (T_i-t)									
		1y	2y	3y	4y	5y	6y	7y	8y	9y	10y
Time t	0y	34,7%	4,5%	-30,8%	10,9%	-24,2%	24,1%	28,5%	19,7%	-3,5%	8,9%
	1y	51,1%	22,1%	-25,0%	34,6%	-40,6%	2,4%	-50%	22,2%	-7,2%	-
	2y	100%	20,4%	-26,0%	-39,2%	-50%	15,7%	25,5%	19,0%	-	-
	3y	100%	100%	32,1%	-50%	-50%	-50%	-50%	-	-	-
	4y	100%	100%	100%	-50%	-50%	37,1%	-	-	-	-
	5y	100%	100%	100%	100%	100%	-	-	-	-	-
	6y	100%	-50%	-50%	-50%	-	-	-	-	-	-
	7y	-23,5%	7,5%	23,6%	-	-	-	-	-	-	-
	8y	7,8%	2,6%	-	-	-	-	-	-	-	-
	9y	0,9%	-	-	-	-	-	-	-	-	-

$\beta^*_{r,s}$		Tenors (T_s-T_r)									
		1y	2y	3y	4y	5y	6y	7y	8y	9y	10y
Expiries (T_r)	1y	34,7%	20,8%	6,4%	6,7%	1,9%	4,2%	6,6%	7,8%	7,1%	7,2%
	2y	25,4%	11,3%	6,0%	4,2%	2,9%	4,6%	3,5%	3,7%	3,6%	-
	3y	26,1%	14,8%	7,4%	2,9%	2,5%	1,9%	2,6%	2,9%	-	-
	4y	21,1%	17,3%	10,6%	6,9%	4,3%	3,7%	3,1%	-	-	-
	5y	22,4%	16,1%	12,6%	6,9%	4,9%	4,2%	-	-	-	-
	6y	13,1%	12,3%	5,5%	3,3%	2,6%	-	-	-	-	-
	7y	4,8%	1,1%	1,5%	2,5%	-	-	-	-	-	-
	8y	3,4%	3,3%	3,1%	-	-	-	-	-	-	-
	9y	3,2%	3,1%	-	-	-	-	-	-	-	-
	10y	3,0%	-	-	-	-	-	-	-	-	-

Table C.4: *Optimized parameters $\beta_i(t)$ and the resulting $\beta^*_{r,s}$ after step 2, sub-step 3.*

$\sigma_{r,s} - \sigma^*_{r,s}$		Tenors (T_s-T_r)									
		1y	2y	3y	4y	5y	6y	7y	8y	9y	10y
Expiries (T_r)	1y	0,5%	0,0%	-0,3%	-0,4%	-0,3%	0,1%	0,3%	0,5%	0,7%	0,7%
	2y	0,5%	-0,5%	-0,4%	-0,3%	-0,4%	-0,1%	0,0%	0,2%	0,3%	-
	3y	0,5%	0,0%	-0,2%	-0,2%	-0,4%	0,0%	0,1%	0,3%	-	-
	4y	0,4%	0,2%	-0,1%	-0,2%	-0,2%	0,1%	0,2%	-	-	-
	5y	0,1%	0,1%	-0,3%	-0,4%	-0,3%	0,0%	-	-	-	-
	6y	-0,1%	0,1%	-0,3%	-0,2%	-0,1%	-	-	-	-	-
	7y	-0,4%	-0,4%	-0,5%	-0,3%	-	-	-	-	-	-
	8y	-0,3%	-0,3%	-0,4%	-	-	-	-	-	-	-
	9y	-0,4%	-0,3%	-	-	-	-	-	-	-	-
	10y	-0,6%	-	-	-	-	-	-	-	-	-

$\beta_{r,s} - \beta^*_{r,s}$		Tenors (T_s-T_r)									
		1y	2y	3y	4y	5y	6y	7y	8y	9y	10y
Expiries (T_r)	1y	0,0%	-0,1%	-0,2%	-0,5%	1,8%	-0,2%	0,2%	-0,9%	-0,1%	-0,1%
	2y	0,2%	-0,8%	-0,5%	1,6%	-0,1%	1,0%	-0,5%	-0,6%	-0,3%	-
	3y	2,0%	-3,4%	-0,8%	0,0%	0,2%	0,9%	0,3%	0,1%	-	-
	4y	4,1%	-0,3%	-1,9%	-3,7%	-1,2%	-0,8%	-0,4%	-	-	-
	5y	5,1%	-2,0%	0,0%	-4,3%	-2,0%	-1,5%	-	-	-	-
	6y	4,9%	0,3%	-0,2%	-0,2%	0,4%	-	-	-	-	-
	7y	0,5%	2,4%	1,5%	0,8%	-	-	-	-	-	-
	8y	0,0%	0,0%	0,0%	-	-	-	-	-	-	-
	9y	0,0%	0,0%	-	-	-	-	-	-	-	-
	10y	0,0%	-	-	-	-	-	-	-	-	-

Table C.5: *The differences between the parameters obtained in step 1 ($\sigma_{r,s}$ and $\beta_{r,s}$) and the parameters determined by the forward rate parameters obtained in step 2.*

Bibliography

[AA97] **Andersen, Leif; Andreasen, Jesper (1997):** *Volatility Skews and Extensions of the Libor Market Model;* Working Paper

[AA02] **Andersen, Leif; Andreasen, Jesper (2002):** *Volatile volatilities;* RISK, Volume 15, No. 12, p. 163-168

[ABR01] **Andersen, Leif; Brotherton-Ratcliffe, Rupert (2001):** *Extended Libor Market Models with Stochastic Volatility;* Working Paper

[AP04] **Andersen, Leif; Piterbarg, Vladimir (2004):** *Moment Explosions in Stochastic Volatility Models;* Working Paper

[AS72] **Abramowitz, Milton; Stegun, Irene (1972):** *Handbook of Mathematical Functions;* U. S. National Bureau of Standards, 10th Printing

[BCC97] **Bakshi, Gurdip; Cao, Charles; Chen, Zhiwu (1997):** *Empirical Performance of Alternative Option Pricing Models;* Journal of Finance, Volume 52, p. 2003-2049

[BGM97] **Brace, Alan; Gatarek, Dariusz; Musiela, Marek (1997):** *The Market Model of Interest Rate Dynamics;* Mathematical Finance, Volume 7, No. 2, p. 127-147

[BJN00] **Britten-Jones, Mark; Neuberger, Anthony (2000):** *Option Prices, Implied Price Processes, and Stochastic Volatility;* The Journal of Finance, Volume 55, No. 2, p. 839-866

[BL78] **Breeden, Douglas; Litzenberger, Robert (1978):** *Prices of State-Contingent Claims Implicit in Option Prices;* The Journal of Business, Volume 51, No. 4, p. 621-651

[Bla76] **Black, Fischer (1976):** *The pricing of commodity contracts;* Journal of Financial Economics, Issue 3, p. 167-179

[BM00a] **Brigo, Damiano; Mercurio, Fabio (2000):** *Fitting Volatility Smiles with Analytically Tractable Asset Price Models;* Internal Report, Banca IMI, Milan

[BM00b] **Brigo, Damiano; Mercurio, Fabio (2000):** *A Mixed-up Smile;* RISK, Volume 13, No. 9, p. 123-126

[BM01] **Brigo, Damiano; Mercurio, Fabio (2001):** *Interest Rate Models – Theory and Practice;* Springer Verlag, Heidelberg

[BM04] **Brigo, Damiano; Morini, Massimo (2004):** *An empirically efficient analytical cascade calibration of the LIBOR Market Model based only on directly quoted swaptions data;* Working Paper

[BMR03] **Brigo, Damiano; Mercurio, Fabio; Rapisarda, Francesco (2003):** *Smile at the Uncertainty;* Working Paper

[BNMR01] **Barndorff-Nielsen, Ole; Mikosch, Thomas; Resnick, Sidney (2001):** *Levy Processes;* Birkhauser Boston

[Bre81] **Bremaud, Pierre (1981):** *Point Processes and Queues: Martingale Dynamics;* Springer Verlag, New York

[BS96] **Borodin, Andrei N.; Salminen, Paavo (1996):** *Handbook of Brownian Motion – Facts and Formulae;* Birkhäuser, Basel

[BS99] **Belledin, Michael; Schlag, Christian (1999):** *An Empirical Comparison of Alternative Stochastic Volatility Models;* Working Paper, Johann Wolfgang Goethe-Universität, Frankfurt am Main

[CJ02] **Christoffersen, Peter; Jacobs, Kris (2004):** *The Importance of the Loss Function in Option Valuation;* Working Paper

[CR76] **Cox, John C.; Ross, Stephen A. (1976):** *The Valuation of Options for Alternative Stochastic Processes;* Journal of Financial Economics, Volume 3, p. 145-166

[CS01] **Chen, Ren-Raw; Scott, Louis (2001):** *Stochastic Volatility and Jumps in Interest Rates: An Empirical Analysis;* Working paper, Rutgers University

[Din89] **Dinges, Hermann (1989):** *Special Cases of Second Order Wiener Germ Approximations;* Probability Theory and Related Fields, Volume 83, p. 5-57

[DK94] **Derman, Emanuel; Kani, Iraj (1994):** *Riding on a smile;* RISK, Volume 7, No. 2, p. 32-39

[Dup94] **Dupire, Bruno (1994):** *Pricing with a smile;* RISK, Volume 7, No. 1, p. 18-20

[Ern02] **Ernst, Oliver (2002):** *Numerische Mathematik I;* Technische Universität Bergakademie Freiberg

[FPS00] **Fouque, Jean-Pierre; Papanicolaou, George; Sircar, K. Ronnie (2000):** *Derivatives in Financial Markets with Stochastic Volatility;* Cambridge University Press

[Fri03] **Friederichs, Marcel (2003):** *Optionsbewertung bei Sprüngen;* Working Paper, University of Karlsruhe

[Fri04] **Fries, Christian (2004):** *Bewertung von Zinsderivaten: Theorie, Modellierung, Implementierung;* University of Mainz, Lecture Notes

[Gat01] **Gatarek, Dariusz (2001):** *LIBOR market model with stochastic volatility;* Working Paper

[Gat03] **Gatheral, Jim (2003):** *Stochastic Volatility and Local Volatility;* Courant Institute of Mathematical Sciences, Course Notes

[GG98] **Gander, Walter; Gautschi, Walter (1998):** *Adaptive Quadrature - Revisited;* Working paper, ETH Zürich

[GK99] **Glasserman, Paul; Kou, S. G. (1999):** *The Term Structure of Simple Forward Rates with Jump Risk;* Working Paper

[GM01a] **Glasserman, Paul; Merener, Nicolas (2001):** *Numerical Solution of Jump-Diffusion LIBOR Market Models;* Working Paper

[GM01b] **Glasserman, Paul; Merener, Nicolas (2001):** *Convergence of a Discretization Scheme for Jump-Diffusion Processes with State-Dependent Intensities;* Working Paper

[GM01c] **Glasserman, Paul; Merener, Nicolas (2001):** *Cap and Swaption Approximations in LIBOR Market Models with Jumps;* Working Paper

[Hen03] **Hentschel, Ludger (2003):** *Errors in Implied Volatility Estimation;* Working Paper, Forthcoming in Journal of Financial and Quantitative Analysis, University of Rochester

[Hes93] **Heston, Steven (1993):** *A Closed-Form Solution for Options with Stochastic Volatility with Applications to Bond and Currency Options;* The Review of Financial Studies, Volume 6, No. 2, p. 327-343

[HKP00] **Hunt, Phil; Kennedy, Joanne; Pelsser, Antoon (2000):** *Markov-Functional Interest Rate Models;* Finance and Stochastics, Volume 4, No. 4, p. 391-408

[Hul01] **Hull, John (2001):** *Optionen, Futures und andere Derivate;* Fourth Edition, Oldenbourg Verlag, München

[HW87] **Hull, John; White, Alan (1987):** *The Pricing of Options on Assets with Stochastic Volatilities;* The Journal of Finance, Volume 42, No. 2, p. 281-300

[Ing97] **Ingersoll, Jonathan A. (1997):** *Valuing Foreign Exchange Rate Derivatives with a Bounded Exchange Process;* Review of Derivatives Research, Volume 1, p. 159-181

[Jac02] **Jäckel, Peter (2002):** *Monte Carlo Methods in Finance;* Wiley, Chichester

[Jam97] **Jamshidian, Farshid (1997):** *LIBOR and swap market models and measures;* Finance and Stochastics, Volume 1, No. 4, p. 293-330

[JLZ02] **Jarrow, Robert; Li, Haitao; Zhao, Feng (2002):** *Interest Rate Caps "Smile" Too! But can the LIBOR Market Models Capture It?* Working Paper

[JR01] **Joshi, Mark; Rebonato, Ricardo (2001):** *A stochastic-volatility, displaced-diffusion extension of the LIBOR market model;* Working Paper, Royal Bank of Scotland Quantitative Research Centre

[KK99] **Korn, Ralf; Korn, Elke (1999):** *Optionsbewertung und Portfolio-Optimierung – Moderne Methoden der Finanzmathematik;* Vieweg Verlag, Braunschweig

[Kou99] **Kou, S. G. (1999):** *A Jump Diffusion Model for Option Pricing with Three Properties: Leptokurtic Feature, Volatility Smile, and Analytical Tractability;* Working Paper

[Lew00] **Lewis, Alan (2000):** *Option Valuation Under Stochastic Volatility With Mathematica Code;* Finance Press, Newport Beach

[Man02] **Mandler, Martin (2002):** *Comparing risk-neutral probability density functions implied by option prices - market uncertainty and ECB-council meetings;* EFA 2002 Berlin Meetings Presented Paper

[Mar99] **Marris, D. G. H. (1999):** *Financial option pricing and skewed volatility;* Statistical Laboratory, University of Cambridge

[Mei03] **Meister, Markus (2003):** *Optionsbewertung bei stochastischer Volatilität;* Working Paper, University of Karlsruhe

[Mei04] **Meister, Markus (2004):** *Wird das Marktmodell zum Benchmarkmodell für die Bewertung von Zinsderivaten?* Working Paper, University of Karlsruhe

[Mey03] **Meyer, Michael (2003):** *Monte Carlo Simulation With Java and C++;* http://martingale.berlios.de/Martingale.html

[Mer76] **Merton, Robert (1976):** *Option pricing when underlying stock returns are discontinuous;* Journal of Financial Economics, Volume 3, No. 1/2, p. 125-144

[MSS97] **Miltersen, Kristian; Sandmann, Klaus; Sondermann, Dieter (1997):** *Closed Form Solutions for Term Structure Derivatives with Log-Normal Interest Rates;* The Journal of Finance, Volume 52, Issue 1, p. 409-430

[Muc03] **Muck, Matthias (2003):** *Do Surprising Central Bank Moves Influence Interest Rate Derivatives Prices? Empirical Evidence From the European Caps and Swaptions Market;* Working Paper, WHU - Otto Beisheim Graduate School of Management

[Nai93] **Naik, Vasanttilak (1993):** *Option Valuation and Hedging Strategies with Jumps in the Volatility of Asset Returns;* The Journal of Finance, Volume 48, No. 5, p. 1969-1984

[Pit03a] **Piterbarg, Vladimir (2003):** *A Practitioner's Guide to Pricing and Hedging Callable Libor Exotics in Forward Libor Models;* Working Paper

[Pit03b] **Piterbarg, Vladimir (2003):** *A Stochastic Volatility Forward LIBOR Model with a Term Structure of Volatility Smiles;* Working Paper

[PR00] **Penev, Spiridon; Raykov, Tenko (2000):** *A Wiener Germ Approximation of the Non-Central Chi-Square Distribution and of its Quantiles;* Computational Statistics, Volume 15, No. 2, p. 19-28

[Reb99] **Rebonato, Ricardo (1999):** *Volatility and Correlation – In the Pricing of Equity, FX and Interest-Rate Options;* Wiley, Chichester

[Reb00] **Rebonato, Ricardo (2000):** *Interest-Rate Option Models – Understanding, analysing and using models for exotic interest-rate options;* Second Edition, Wiley, Chichester

[Reb02] **Rebonato, Ricardo (2002):** *Modern Pricing of Interest-Rate Derivatives – The LIBOR Market Model and Beyond;* Princeton University Press, Princeton

[Rub83] **Rubinstein, Mark (1983):** *Displaced diffusion option pricing;* The Journal of Finance, Volume 38, No. 1, p. 213-217

[SC00] **Schoenmakers, John; Coffey, Brian (2000):** *Stable implied calibration of a multi-factor LIBOR model via a semi-parametric correlation structure;* Working Paper No. 611, Weierstrass-Institut für Angewandte Analysis und Stochastik, Berlin

[Sey00] **Seydel, Rüdiger (2000):** *Einführung in die numerische Berechnung von Finanz-Derivaten – Computational Finance;* Springer Verlag, Heidelberg

[SZ98] **Schöbel, Rainer; Zhu, Jianwei (1998):** *Stochastic volatility with an Ornstein-Uhlenbeck process: An extension;* Technical Report, Eberhard-Karls-Universität Tübingen

[Tom95] **Tompkins, Robert (1995):** *Options Analysis: A State of the Art Guide to Options Pricing, Trading, and Portfolio Applications;* Irwin

[Wys00] **Wystup, Uwe (2000):** *Heston's Stochastic Volatility Model;* Working Paper

[WZ02] **Wu, Lixin; Zhang, Fan (2002):** *LIBOR Market Model: From Deterministic to Stochastic Volatility;* Working Paper

[Zuh02] **Zühlsdorff, Christian (2002):** *Extended Libor Market Models with Affine and Quadratic Volatility;* Discussion Paper, University of Bonn

Index